

COASTAL FLOOD IMPACT ASSESSMENT FOR SHAKTOOLIK, ALASKA

Keith C. Horen, Jessica E. Christian, and Nora M. Nieminski



DGGS staff surveying the remnants of the storm break berm in Shaktoolik, Alaska, following Typhoon Merbok in September, 2022.



Published by
STATE OF ALASKA
DEPARTMENT OF NATURAL RESOURCES
DIVISION OF GEOLOGICAL & GEOPHYSICAL SURVEYS
2025



COASTAL FLOOD IMPACT ASSESSMENT FOR SHAKTOOLIK, ALASKA

Keith C. Horen, Jessica E. Christian, and Nora M. Nieminski

Report of Investigation 2025-6

State of Alaska
Department of Natural Resources
Division of Geological & Geophysical Surveys

STATE OF ALASKA

Mike Dunleavy, Governor

DEPARTMENT OF NATURAL RESOURCES

John Boyle, Commissioner

DIVISION OF GEOLOGICAL & GEOPHYSICAL SURVEYS

Erin A. Campbell, State Geologist and Director

Publications produced by the Division of Geological & Geophysical Surveys (DGGS) are available for free download from the DGGS website (dggs.alaska.gov). Publications on hard-copy or digital media can be examined or purchased in the Fairbanks office:

Alaska Division of Geological & Geophysical Surveys
3354 College Rd., Fairbanks, Alaska 99709-3707
Phone: (907) 451-5010 Fax (907) 451-5050
dggspubs@alaska.gov | dggs.alaska.gov

DGGS publications are also available at:

Alaska State Library,
Historical Collections & Talking Book Center
395 Whittier Street
Juneau, Alaska 99811

Alaska Resource Library and Information Services (ARLIS)
3150 C Street, Suite 100
Anchorage, Alaska 99503

Suggested citation:

Horen, K.C., Christian, J.E., and Nieminski, N.M., 2025, Coastal flood impact assessment for Shaktoolik, Alaska: Alaska Division of Geological & Geophysical Surveys Report of Investigation 2025-6, 77 p. <https://doi.org/10.14509/31702>



Contents

Overview	1
Summary	1
Data	3
Digital Elevation Models and Orthoimagery	3
First-Floor Survey	3
Vertical Datums.....	3
Previous Studies	4
Flood Impact Categories.....	5
Historical Flood Record	9
Flood Event Summaries	16
Acknowledgments	34
References	34

Figures

Figure 1. Timeline of estimated dynamic still water level flood events and visual representation of flood height estimates and confidences for Shaktoolik, Alaska	14
Figure 2. Timeline of estimated still water level flood events and visual representation of flood height estimates and confidences for Shaktoolik, Alaska	15
Figure 3. Photographs showing debris line high water marks for a 1913 storm in Shaktoolik, Alaska.....	16
Figure 4. NOAA CO-OPS observed water levels for tide station 946 8691 in Shaktoolik, Alaska, from August 15, 2010, to August 18, 2010	27
Figure 5. Photographic evidence of still water level flood height in Shaktoolik, Alaska during the August 2019 flood event	31
Figure 6. Areas and maximum depths of overtopping accumulations flooding identified in the 2021 topobathy digital elevation model based on high water mark from the flood event on September 17, 2022, in Shaktoolik, Alaska	33
Figure 7. Before and after photographs of the berm in Shaktoolik, Alaska during the October 2024 flood event.....	33

Tables

Table 1. Summary of digital elevation models available for Shaktoolik, Alaska	3
Table 2. Summary of orthoimagery available for Shaktoolik, Alaska	3
Table 3. Local tidal datums for Shaktoolik, Alaska.....	4
Table 4. Summary of infrastructure heights and flood categories	5
Table 5. Summary of historical floods in Shaktoolik, Alaska, representing the dynamic still water level along the exposed coastal shore.....	10
Table 6. Summary of historical floods in Shaktoolik, Alaska, representing the still water level along the sheltered side of the community.....	12
Table 7. Summary of historical floods that could not be estimated in Shaktoolik, Alaska.....	13

Appendices

Appendix A: Shaktoolik, Alaska, first-floor heights.....	35
Appendix B: Re-analysis of previous flood history studies for Shaktoolik, Alaska	45

COASTAL FLOOD IMPACT ASSESSMENT FOR SHAKTOOLIK, ALASKA

Keith C. Horen¹, Jessica E. Christian², and Nora M. Nieminski¹

OVERVIEW

This Division of Geological & Geophysical Surveys (DGGS) report is an investigation of the historical flood record and provides an assessment of flood impacts for the community of Shaktoolik, Alaska. This community-specific report has three sections: data description, flood impact categorization, and historical flood record. Methods used to evaluate historical floods and delineate flood impact categories (minor, moderate, major) are defined by the National Weather Service (NWS) and described in detail by Horen and others (2024), an update from the methods described by Buzard and others (2021). Flood and infrastructure heights are relative to the local mean higher high water (MHHW) datum in feet (ft).

SUMMARY

The community of Shaktoolik, meaning “twig piles,” is currently located on a flat spit of mixed sand and gravel (Overbeck and others, 2020) approximately 200 ft (61 meters [m]) wide on the eastern coast of Norton Sound at the mouth of the Tagoomenik River, roughly 125 miles (201 kilometers [km]) east of Nome. The community has a history of moving due to storm impacts dating back to 1933, when the village relocated from upriver to the spit, settling about 1 miles (1.6 km) south of the current site. In 1967, the community relocated again, establishing the current village site. The 2015 Shaktoolik Multi-Jurisdictional Hazard Mitigation Plan (MJHMP; Native Village and City of Shaktoolik and LeMay Engineering & Consulting [Shaktoolik and LeMay], 2015) reported “the highest ground in the Shaktoolik area is approximately 14 feet above mean high tide”, or roughly



13.3 ft (4.06 m) MHHW, putting the community at high-risk of coastal and riverine flooding and erosion (Shaktoolik and LeMay, 2015). In a 2009 report by the Government Accountability Office (GAO), Shaktoolik was considered one of four communities immediately threatened by flooding and erosion (GAO, 2009).

A 2014 climate change adaptation plan (Johnson and Gray, 2014) recommended the construction of a vegetated berm just landward of the beach to “absorb some of the wave energy and reduce flood levels,” with the MJHMP (Shaktoolik and LeMay, 2015) noting, “...instead of a costly breakwater used to protect larger coastal communities, the plan suggests building a berm along the beach up to five feet high, using gravel, dirt, and native beach grass... [that] would run alongside and stabilize the tangled piles of driftwood deposited by past storms and would be a makeshift wave barrier.” The construction of the initial berm was completed in 2015 (Golder Associates Ltd., 2020) and, according to Dobson and others (2022), was “designed to help protect against a 20-year storm event.” Overbeck and others (2020) noted the “unconsolidated gravel berm” was significantly

¹Alaska Division of Geological & Geophysical Surveys, 3651 Penland Pkwy, Anchorage, Alaska 99508

²Alaska Division of Geological & Geophysical Surveys, 3354 College Rd., Fairbanks, Alaska 99709

susceptible to erosion, which they confirmed during a site visit following a storm in August of 2019; this finding was reiterated by Golder Associates Ltd. (2020). Since initial construction, the berm has required repeated maintenance, with KNOM Radio (2020) reporting on a grant from the Department of Housing and Urban Development (HUD) aimed at facilitating a new berm for Shaktoolik to replace the previous berm following storm damage in 2019; the article also included a photograph from Genevieve Rock showing heavy equipment working on the berm in 2017. Horen and others (2022) observed severe erosion of the berm in the wake of ex-tropical storm Merbok in September 2022, and photographs provided by Gloria Andrew showed the reconstructed berm was once again damaged during a storm in October 2024.

Semi-ephemeral due to the construction material, the earthen berm is the only mitigation structure protecting the community. Dobson and others (2022) asserted that the “twenty-year berm” did “not provide sufficient protection against large magnitude storms,” observing that a “winter storm in 2019 produced large waves that topped the berm and caused damage to critical infrastructure.” According to Dobson and others (2022), following the winter storm in 2019, the berm was redesigned “to withstand maximum storm surge water levels for a 50-year storm event,” which was reiterated by Hofstaedter (2019) who added that Bristol Engineering Services Company, LLC “designed the berm to... protect the community from waves that could come 3.5-4 feet above the elevation of the existing road.” Unfortunately, Horen and others (2022) found, despite any increases to the height and width of the berm prior to the Merbok storm event in 2022, the berm was impacted by severe erosion and substantial debris was carried over and deposited behind the berm by wave action during the event, posing an additional risk of damage to nearby infrastructure. These debris deposits are indicative of overtopping accumulations (OTA)

from wave runup cresting the berm and causing seawater to pool in the low-lying area behind.

The nature of flooding, especially flooding due to storm surge, will inherently vary between the exposed, coastal shoreline to the west of the community and the sheltered riverine environment to the east. To account for this difference, when possible, DGGs separately assessed the peak water height along both the exposed and sheltered sides of the community during flood events, estimating the dynamic still water level (DSWL) for the former and the still water level (SWL) for the latter, as described by Moritz and others (2016). The SWL includes storm surge and tides, while the DSWL also includes the portion of wave setup that contributes to a static, standing water height at the shoreface, though it is important to acknowledge the DSWL does not include any other hazards due to wave action such as runup or overtopping. Of the events estimated during our research, only the data available for the September 2022 storm displayed OTA flooding.

Six disaster declarations (2004, 2005, 2009, 2011, 2013, 2014) have been reported for flooding in Shaktoolik (Shaktoolik and LeMay, 2015). Based on the research done for this report, Shaktoolik experienced at least 48 storm surge flood events between 1913 and 2024 at either the old or new site, of which we estimated the still water heights of 34. There was not sufficient information to differentiate between DSWL, SWL, and runup extents for all events; in such cases we estimated only one flood height, which is presumed to represent the water height that would have been experienced on the sheltered side of the community unless otherwise noted. For the exposed coast, we estimated and categorized five flood events as minor, 28 as moderate, and one as major. For the sheltered coast, we estimated and categorized eight flood events as minor and 22 as moderate. The highest estimated flood occurred on September 17, 2022, reaching an estimated DSWL height of 11.9 ft (3.62 m) MHHW and an SWL height of 10.5 ft (3.21 m) MHHW.

DATA

DGGS used geospatial data to assess infrastructure impacts and estimate flood heights from various sources of evidence (e.g., photographs, personal accounts, official reports). We used Esri's ArcGIS Pro version 3.2.0 to process and map these geospatial data.

Digital Elevation Models and Orthoimagery

Accurate, high-resolution elevation models and orthoimagery are used to measure flood heights in the absence of high-water mark (HWM) data. Two digital elevation models (DEM; table 1) and two orthoimages (table 2) are available for Shaktoolik. Aerial imagery was collected in 2015 and used to create a digital surface model (DSM) and orthoimagery derived from photogrammetric structure from motion (SfM) processing (Overbeck and others, 2016). In 2019, DGGS collected

aerial imagery and attempted to create a DSM and orthoimagery derived from photogrammetric SfM processing; due to inconsistencies in the resulting DSM these data were not published, although the orthoimagery derived from these data remains useful for visual reference. The U.S. Army Corps of Engineers (USACE) collected topographic-bathymetric light detecting and ranging (topobathy lidar) data in 2021, from which a topobathy DEM (TBDEM) was created (Office of Coastal Management [OCM] Partners, 2024). All DEM and orthoimagery will be referenced in this report by the names assigned in tables 1 and 2.

First-Floor Survey

Bristol Engineering Services Company, LLC (2022) completed a field survey of the first-floor heights of occupied buildings in Shaktoolik in July 2022. These data were collected and reported in the North American Vertical Datum 1988 with GEOID12B applied (NAVD88 [GEOID 12B]) in U.S. survey feet (usft) (app. A). The reported vertical accuracy of these data is ± 0.2 ft (0.07 m). This survey will be referenced within this report as the 2022 first-floor survey. DGGS spatially joined these first-floor heights to building footprints digitized from the 2019 orthoimagery, identifying 92 as occupied buildings (i.e., residential, public, or commercial structures in which people live or work), 73 of which are residential.

Vertical Datums

Local tidal datums (table 3) for Shaktoolik are described by National Oceanic and Atmospheric Administration (NOAA) Center for Operational Oceanographic Products (CO-OPS) tide station 946 8691 available from <https://tidesandcurrents.noaa.gov/stationhome.html?id=9468691>. The NAVD88 (GEOID12B) transformation is based on the NOAA Online Positioning User Service (OPUS) shared solution for National Geodetic Survey vertical control monument 946 8691 A (PID: BBBZ37) available from <https://www.ngs.noaa.gov/OPUS/getDatasheet.jsp?PID=BBBZ37>, identified as the primary tidal bench mark for station 946 8691.

Table 1. Summary of digital elevation models available for Shaktoolik, Alaska.

	2015 DSM	2021 TBDEM
Collection date	2015-AUG-06	2021-MAY-31
Elevation type	Photogrammetric SfM	Topobathy Lidar
Vertical datum	NAVD88 (GEOID12A)	NAVD88 (GEOID12B)
Ground sample distance	0.3 ft (0.09 m)	3.0 ft (1.00 m)
Accuracy	0.4 ft (0.12 m)	0.7 ft (0.20 m)

Table 2. Summary of orthoimagery available for Shaktoolik, Alaska.

	2015 Orthoimagery	2019 Orthoimagery
Collection date	2015-AUG-06	2019-AUG-24
Ground sample distance	0.3 ft (0.09 m)	0.50 ft (0.15 m)

Table 3. Local tidal datums for Shaktoolik, Alaska (NOAA CO-OPS tide station 949 8691).

Tidal Datum	Abbreviation	ft MHHW	m MHHW	ft NAVD88 (GEOID12B)	m NAVD88 (GEOID12B)
Mean Higher High Water	MHHW	0.0	0.00	6.1	1.85
Mean High Water	MHW	-0.7	-0.21	5.4	1.65
Mean Tide Level	MTL	-1.9	-0.58	4.2	1.27
Mean Sea Level	MSL	-2.1	-0.63	4.0	0.22
Mean Low Water	MLW	-3.1	-0.95	3.0	0.90
Mean Lower Low Water	MLLW	-3.7	-1.14	2.3	0.71
North American Vertical Datum 1988 (GEOID12B)	NAVD88 (GEOID12B)	-6.1	-1.85	0.0	0.00

Previous Studies

Several previous flood history reports and estimation studies have been conducted for Shaktoolik (Sallenger, 1983; Chapman and others, 2009; USACE, 2011; Kinsman and DeRaps, 2012; Golder Associates Ltd., 2020; Rosales and others, 2021), although the primary focus of many of these studies was to analyze storm return period frequencies. Rosales and others (2021) attempted to estimate flooding by locating and mapping driftwood debris lines for the 2011, 2013, and 2019 storms, though they use a non-standard definition of “storm surge” that is analogous to runup extents, thus their reported “maximum storm surge” for these events is not indicative of either SWL or DSWL flooding. The Golder Associates Ltd. (2020) study relies heavily on the flood history compiled by USACE (2011), which was an update to a previous study by Chapman and others (2009) and a 2020 DGGS data request based on the 2011 USACE report. Additionally, a review of the USACE (2011) analysis was performed by Coastal Analytics, LLC (Kriebel, 2019), which identified several inconsistencies and potential flaws in the results presented by USACE (2011). Sallenger (1983) provides two beach profiles near Shaktoolik, one at the old village site and one at the new site, which included the heights of debris deposits from the 1974 storm event. The survey described by Sallenger (1983) was conducted

holding the observed sea level at the time of the survey as the basis for the vertical datum of their results, creating a minimum uncertainty of at least ± 1.9 ft (0.57 m) for any measurement taken. As is the case with Rosales and others (2021), Sallenger (1983) provides measurements of “combined storm surge and wave runup,” not SWL or DSWL, which Sallenger acknowledges and correctly describes.

For this risk assessment, we conducted our own review of these previous studies and came to the conclusion that, with the advent of the published local tidal datums for Shaktoolik that were not available to Sallenger (1983), Chapman and others (2009), and USACE (2011), and with a specific focus on estimating event flood heights rather than return intervals, it was possible to refine previous estimates for individual flood events with known surge heights to a greater degree of accuracy. During our review of the USACE (2011) report, we identified an incongruity between the “pre-1985” and “1985 to 2009” results that we believe is indicative of an overestimation of the storm surge and wave heights modeled for the older group of events. The pre-1985 events were reconstructed from a different historical weather dataset than the post-1984 events, the latter having been extracted from “continuous climatology data,” while the former came from “selected storm hindcast[s]” (Chapman and others, 2009). Without access to

either the original data inputs, or the model used, and after a thorough investigation of multiple confounding factors, we concluded the best course of action would be to forgo inclusion of these potentially dubious results in favor of the more reliable post-1984 estimates. A detailed description of our assessment of these previous studies, as well as an explanation of our estimation methodology related to the events covered in the USACE (2011) report can be found in appendix B, including the pre-1985 events.

FLOOD IMPACT CATEGORIES

Flood impact categories are used by the NWS to define and communicate flood risk to the public. These categories are designated as major, moderate, and minor (NWS, 2016). Definitions for these categories in the NWS guidance specific to Alaska are provided in the form of statements regarding flood impacts, some of which are more qualitative than quantitative (NWS, 2016). To ensure impact assessments are consistent and repeatable, DGGS developed a set of quantitative criteria for each category (Horen and others, 2024). A fourth category, extreme flooding, as defined by DGGS, is included in this report to delineate critical infrastructure situated at heights above the anticipated maximum based on the specifics of the local historical flood record, though flooding is still possible above this height (Horen and others, 2024).

Short definitions for each flood impact category are listed below and are explained in greater detail by Horen and others (2024). Table 4 provides a list of key infrastructure heights and the risk categories they fall within. Additional information about each piece of key infrastructure is detailed in the category blocks that follow table 4. All categories are based on the current infrastructure within the community; thus, they may not necessarily represent past conditions and may need to be updated as new infrastructure is built or old infrastructure is demolished. The map (sheet 1) that accompanies this report depicts the potential inundation extents for each flood impact category.

Minor Flooding: “Minimal or no property damage, but possibly some public threat” (NWS, 2016).

Moderate Flooding: “Some inundation of structures and roads... Some evacuations of people and/or transfer of property to higher elevations may be necessary” (NWS, 2016).

Major Flooding: “Extensive inundation of structures and roads. Significant evacuations of people and/or transfer of property to higher elevations are necessary” (NWS, 2016).

Extreme Flooding: Any flooding that reaches a height above the highest estimated flood height plus the confidence of that estimate. (Horen and others, 2024; NWS, 2018).

Table 4. Summary of infrastructure heights and flood categories. Gray = extreme, purple = major, red = moderate, yellow = minor. The extreme category represents infrastructure situated at heights above the highest estimated flood height with confidence included. Categories are based on current infrastructure conditions.

Feature	Height (ft MHHW)	Confidence (ft)	Height (m MHHW)	Confidence (m)
Clinic (evacuation center)	25.8	0.2	7.85	0.07
Fuel tank farm	24.2	0.3	7.37	0.09
AVEC power plant	22.9	0.2	6.98	0.07
AVEC fuel tanks	22.9	0.2	6.98	0.07
City office	22.6	0.2	6.89	0.07
National Guard armory	22.5	0.2	6.87	0.07

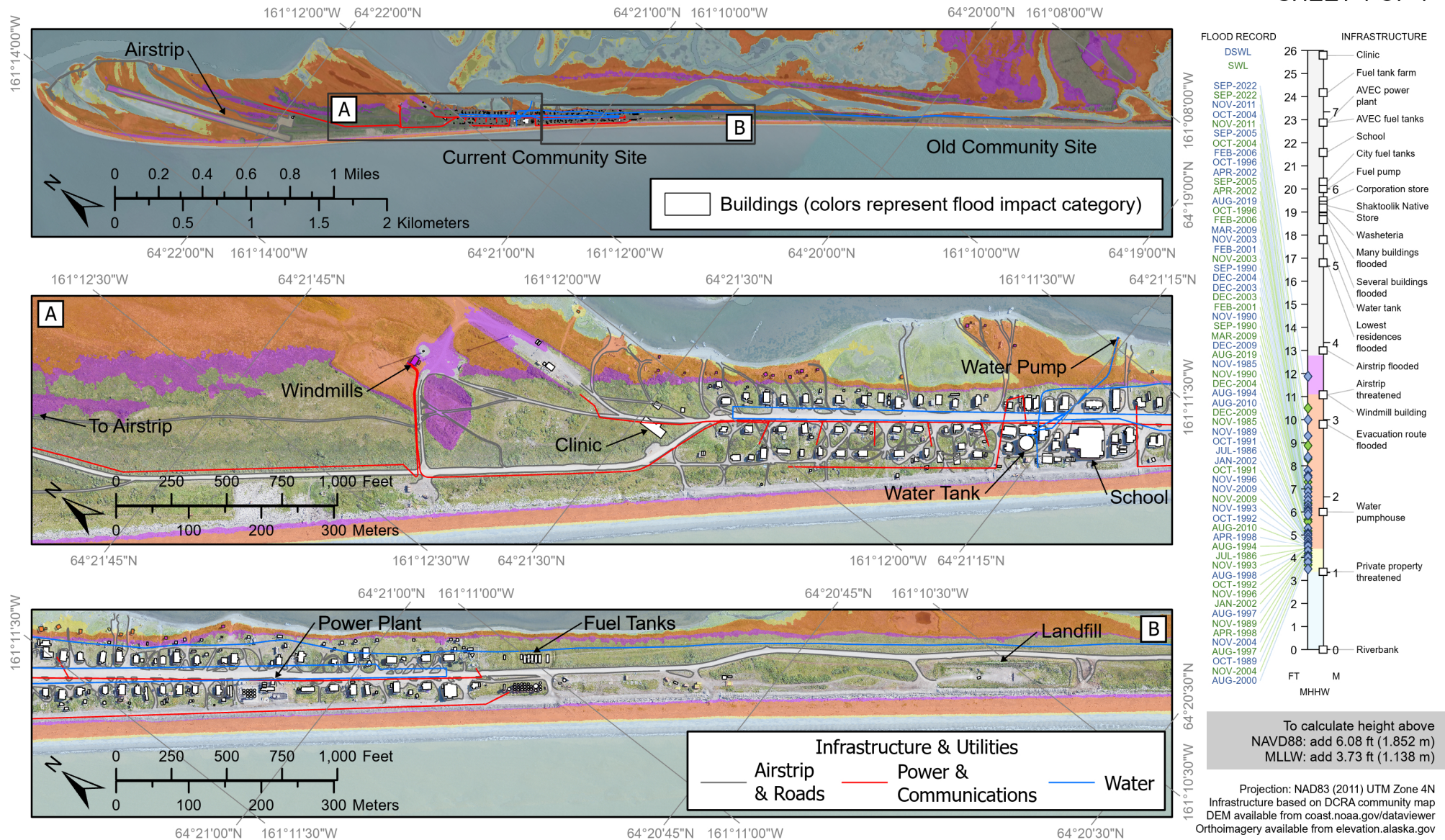
Table 4, continued. Summary of infrastructure heights and flood categories. Gray = extreme, purple = major, red = moderate, yellow = minor. The extreme category represents infrastructure situated at heights above the highest estimated flood height with confidence included. Categories are based on current infrastructure conditions.

Feature	Height (ft MHHW)	Confidence (ft)	Height (m MHHW)	Confidence (m)
School (secondary evacuation center)	21.6	0.2	6.59	0.07
Inupiat Assembly	20.6	0.2	6.27	0.07
City fuel tanks	20.3	0.2	6.20	0.07
Fuel pump	20.0	0.2	6.10	0.07
Corporation store	19.5	0.2	5.95	0.07
Village public safety office	19.4	0.2	5.90	0.07
Shaktoolik Native Store	19.3	0.2	5.88	0.07
GCI building	19.2	0.2	5.86	0.07
Washeteria / water treatment plant	19.2	0.2	5.86	0.07
Post Office	19.0	0.2	5.79	0.07
Many buildings flooded	18.8	0.2	5.73	0.07
IRA office	18.8	0.2	5.73	0.07
Several buildings flooded	18.7	0.2	5.71	0.07
Alascom building	18.4	0.2	5.61	0.07
Covenant Church	18.3	0.2	5.58	0.07
Water tank	17.8	0.2	5.41	0.07
Lowest residences flooded	16.8	0.2	5.11	0.07
Airstrip flooded	13.0	0.2	3.96	0.07
Extreme	12.8		3.89	
Windmill building	11.1	0.3	3.39	0.09
Major	11.1		3.39	
Airstrip threatened	11.1	0.3	3.38	0.09
Evacuation route flooded	9.8	0.3	2.98	0.09
Water pumphouse	6.0	0.2	1.82	0.08
Moderate	4.4		1.34	
Private property threatened	3.4	0.3	1.04	0.09
Minor	3.4		1.04	
Riverbank	0.0		0.00	

Coastal Flood Impact Map

Shaktoolik, Alaska

REPORT OF INVESTIGATION 2025-6
Horen, Christian, and Nieminski, 2025
SHEET 1 OF 1



STATE OF ALASKA
DEPARTMENT OF NATURAL RESOURCES
DIVISION OF GEOLOGICAL & GEOPHYSICAL SURVEYS

The State of Alaska makes no expressed or implied warranties (including warranties for merchantability and fitness) with respect to the character, functions, or capabilities of the electronic data or products, nor their appropriateness for any user's purposes. In no event will the State of Alaska be liable for any incidental, indirect, special, consequential, or other damages suffered by a user or any other person or entity, whether from the use of the electronic services or products, or any failure thereof or otherwise. In no event will the State of Alaska's liability to the Requestor or anyone else exceed the fee paid for the electronic service or product.

This work was made possible with National Fish and Wildlife Foundation's National Coastal Resilience Funding through a partnership with the Alaska Native Tribal Health Consortium.

Extreme Flooding: greater than 12.8 ft (3.89 m) MHHW**Clinic: 25.8 ± 0.2 ft (7.85 ± 0.07 m) MHHW**

As the public building with the highest first-floor height, the clinic has been identified as the most suitable flood evacuation point, though the building may not be large enough to shelter all residents.

Fuel tank farm: 24.2 ± 0.3 ft (7.37 ± 0.09 m) MHHW

This is the height of the protective berm surrounding the fuel tank farm. This tank farm is connected to the fuel pump.

AVEC power plant: 22.9 ± 0.2 ft (6.98 ± 0.07 m) MHHW

This is the first-floor height of the community's primary power source.

AVEC fuel tanks: 22.9 ± 0.2 ft (6.98 ± 0.07 m) MHHW

This is the height of the fuel tanks supplying the power plant.

City office: 22.6 ± 0.2 ft (6.89 ± 0.07 m) MHHW**National Guard armory: 12.7 ± 0.2 ft (3.88 ± 0.07 m) MHHW****School: 21.6 ± 0.2 ft (6.59 ± 0.07 m) MHHW**

As the largest public building with a first-floor height above the upper limit of the major flood category, the school has been identified as a secondary flood evacuation point in the event the primary evacuation location, the clinic, is unable to shelter all residents.

Inupiat Assembly: 20.6 ± 0.2 ft (6.27 ± 0.07 m) MHHW**City fuel tanks: 20.3 ± 0.2 ft (6.20 ± 0.07 m) MHHW****Fuel pump: 20.0 ± 0.2 ft (6.10 ± 0.07 m) MHHW**

This is the height of the primary fuel source.

Corporation store: 19.5 ± 0.2 ft (5.95 ± 0.07 m) MHHW**Village public safety office: 19.4 ± 0.2 ft (5.90 ± 0.07 m) MHHW**

This is the first-floor height of the lowest public safety office.

Shaktoolik Native store: 19.3 ± 0.2 ft (5.88 ± 0.07 m) MHHW**GCI building: 19.2 ± 0.2 ft (5.86 ± 0.07 m) MHHW**

This is the first-floor height of the GCI communications building.

Washeteria: 19.2 ± 0.2 ft (5.86 ± 0.07 m) MHHW

The washeteria provides resources such as laundry, showers, toilets, and is the community's water treatment facility.

Post Office: 19.0 ± 0.2 ft (5.79 ± 0.07 m) MHHW**Many buildings flooded 1.0 ft (0.30 m) or more: 18.8 ± 0.2 ft (5.73 ± 0.07 m) MHHW**

We consider "many" buildings to describe more than five occupied buildings.

IRA office: 18.8 ± 0.2 ft (5.73 ± 0.07 m) MHHW

This is the first-floor height of the lowest IRA office building.

Several buildings flooded less than 1.0 ft (0.30 m): 18.7 ± 0.2 ft (5.71 ± 0.07 m) MHHW

We consider "several" buildings to describe more than one, but less than six occupied buildings.

Alascom building: 18.4 ± 0.2 ft (5.61 ± 0.07 m) MHHW

This is the first-floor height of the Alascom communications building.

Covenant Church: 18.3 ± 0.2 ft (5.58 ± 0.07 m) MHHW

Water tank: 17.8 ± 0.2 ft (5.41 ± 0.07 m) MHHW

The water tank contains the community's fresh water supply.

Lowest residences flooded: 16.8 ± 0.2 ft (5.11 ± 0.07 m) MHHW

This is the height at which the lowest residences would experience flooding.

Airstrip flooded: 13.0 ± 0.2 ft (3.95 ± 0.07 m) MHHW

Measured from the 2021 TBDEM, at this height water would flood the airstrip across its full width.

Major Flooding: 11.1 to 12.8 ft (3.39 to 3.89 m) MHHW**Windmill building: 11.1 ± 0.3 ft (3.39 ± 0.09 m) MHHW**

Measured from the 2021 TBDEM, flood waters would reach the windmill power building at this height.

Moderate Flooding: 4.4 to 11.1 ft (1.34 to 3.39 m) MHHW**Airstrip threatened: 11.1 ± 0.3 ft (3.38 ± 0.09 m) MHHW**

Measured from the 2021 TBDEM, at this height water would reach any portion of the airstrip.

Evacuation route flooded: 9.8 ± 0.3 ft (2.98 ± 0.09 m) MHHW

Measured from the 2021 TBDEM, at this height the lowest point along the evacuation route road would be flooded to depth of 1.0 ft (0.30 m), the maximum depth for reasonably safe travel on flooded roads according to the NWS (2023).

Water pumphouse: 6.0 ± 0.2 ft (1.82 ± 0.08 m) MHHW

This is the first-floor height of the community's primary water source pumphouse.

Minor Flooding: 3.4 to 4.4 ft (1.04 to 1.34 m) MHHW**Private property threatened: 3.4 ± 0.3 ft (1.04 ± 0.09 m) MHHW**

Measured from the 2021 TBDEM, flood waters would reach the lowest private property at this height. Private property may include storage sheds, boats, fishing equipment, vehicles, and other property at ground level outside of occupied structures. From the 2019 orthoimagery, we identified 127 features meeting this description and extracted the average ground heights beneath each from the 2021 TBDEM.

HISTORICAL FLOOD RECORD

The historical flood record for Shaktoolik is listed in chronological order below, with estimated floods identified by impact category. This record was compiled from information available to the public through open sources or upon request. It is possible that additional, undocumented flood events have impacted the community. Historical information was used in conjunction with the best available, temporally relevant geospatial data to estimate flood heights where possible.

All estimate confidences were calculated following the methods developed by Horen and

others (2024). As described by Horen and others (2024), each estimate is accompanied by two confidence metrics, an estimate confidence based on the combined known potential errors and a time-based confidence based on the temporal relevance of the data used to estimate the given event. Temporal confidence values are noted with an asterisk (*) where the data used to estimate the flood event height were collected 20 years or more before or after the event: in these cases, the large temporal discontinuity may result in a value that could potentially exceed what the confidence model predicts (Horen and others, 2024).

For each flood event, a list and summarization of sources is included, as well as an explanation of the data used and steps performed during estimation, where relevant. Each flood height estimate is classified into a single flood impact category but estimate confidences may span more than one category. As previously noted, these categorizations are based on the disposition of the current infrastructure within the community and are not necessarily a reflection of the severity of the flooding experienced at the time of each event, especially for those events that occurred while the community was still situated at the old village site, though this is by design as it allows for the consistency needed for

further analysis, such as determining storm return intervals. Table 5 provides a complete list of our DSWL flood height estimates along the exposed coast, categorized and chronicled from highest to lowest flood height. Table 6 provides a complete list of our SWL estimates for the sheltered side of the community, also categorized and reported from highest to lowest. Table 7 includes the floods found during our research that we were unable to estimate, listed in chronological order. Figure 1 provides a timeline of the estimated DSWL flood events and a visual representation of the flood height estimates and confidences, with figure 2 providing the same for the estimated SWL flood events.

Table 5. Summary of historical floods in Shaktoolik, Alaska, representing the dynamic still water level along the exposed coastal shore. Flood categories are included for reference: purple = major, red = moderate, and yellow = minor.

Estimated Floods								
	Flood Date	Type	Height (ft MHHW)	Estimate Confidence (ft)	Temporal Confidence (ft)	Height (m MHHW)	Estimate Confidence (m)	Temporal Confidence (m)
Major	1970-SEP	Storm Surge	7.6	± 0.7	± 1.0*	2.33	± 0.21	± 0.30*
	2011-NOV-09	Storm Surge	10.0	± 0.9	± 0.0	3.04	± 0.27	± 0.00
	2004-OCT-19	Storm Surge	9.3	± 0.8	± 1.0*	2.83	± 0.26	± 0.30*
	2005-SEP-23	Storm Surge	8.4	± 0.9	± 1.0*	2.57	± 0.26	± 0.30*
	2006-FEB-09	Storm Surge	7.8	± 1.1	± 1.0*	2.36	± 0.32	± 0.30*
	1996-OCT-29	Storm Surge	7.6	± 0.8	± 1.0*	2.31	± 0.26	± 0.30*
Moderate	2002-APR-29	Storm Surge	7.5	± 0.8	± 1.0*	2.28	± 0.25	± 0.30*
	2019-AUG-03	Storm Surge	7.1	± 0.7	± 0.3	2.15	± 0.22	± 0.08
	2009-MAR-07	Storm Surge	6.9	± 1.1	± 1.0*	2.10	± 0.32	± 0.30*
	2003-NOV-26	Storm Surge	6.7	± 0.8	± 1.0*	2.05	± 0.25	± 0.30*
	2001-FEB-09	Storm Surge	6.5	± 0.8	± 1.0*	2.00	± 0.25	± 0.30*
	2004-DEC-26	Storm Surge	6.3	± 0.8	± 1.0*	1.93	± 0.26	± 0.30*
	1990-SEP-01	Storm Surge	6.3	± 0.8	± 1.0*	1.92	± 0.25	± 0.30*
	2003-DEC-22	Storm Surge	6.2	± 0.8	± 1.0*	1.89	± 0.26	± 0.30*
	1990-NOV-20	Storm Surge	6.1	± 0.8	± 1.0*	1.87	± 0.16	± 0.30*

Table 5, continued. Summary of historical floods in Shaktoolik, Alaska, representing the dynamic still water level along the exposed coastal shore. Flood categories are included for reference: purple = major, red = moderate, and yellow = minor.

Estimated Floods								
	Flood Date	Type	Height (ft MHHW)	Estimate Confidence (ft)	Temporal Confidence (ft)	Height (m MHHW)	Estimate Confidence (m)	Temporal Confidence (m)
Moderate	2009-DEC-05	Storm Surge	6.0	± 1.1	± 1.0*	1.81	± 0.32	± 0.30*
	1985-NOV-06	Storm Surge	5.9	± 1.1	± 1.0*	1.81	± 0.32	± 0.30*
	2010-AUG-16	Storm Surge	5.3	± 0.7	± 0.0	1.63	± 0.20	± 0.00
	1994-AUG-17	Storm Surge	5.3	± 0.8	± 1.0*	1.61	± 0.26	± 0.30*
	1991-OCT-24	Storm Surge	5.1	± 0.8	± 1.0*	1.56	± 0.25	± 0.30*
	1989-NOV-16	Storm Surge	5.1	± 0.9	± 1.0*	1.55	± 0.26	± 0.30*
	2002-JAN-14	Storm Surge	5.0	± 1.1	± 1.0*	1.52	± 0.32	± 0.30*
	1986-JUL-20	Storm Surge	5.0	± 0.8	± 1.0*	1.51	± 0.26	± 0.30*
	1996-NOV-15	Storm Surge	4.9	± 0.8	± 1.0*	1.50	± 0.26	± 0.30*
	2009-NOV-08	Storm Surge	4.8	± 0.8	± 1.0*	1.47	± 0.25	± 0.30*
	1993-NOV-17	Storm Surge	4.7	± 0.8	± 1.0*	1.45	± 0.25	± 0.30*
	1992-OCT-06	Storm Surge	4.6	± 0.9	± 1.0*	1.41	± 0.26	± 0.30*
	1960-SEP-27	Storm Surge	4.5	± 1.1	± 1.0*	1.38	± 0.32	± 0.30*
	1998-APR-28	Storm Surge	4.5	± 0.8	± 1.0*	1.36	± 0.26	± 0.30*
Minor	1998-AUG-17	Storm Surge	4.3	± 0.9	± 1.0*	1.33	± 0.26	± 0.30*
	1997-AUG-03	Storm Surge	4.1	± 0.8	± 1.0*	1.26	± 0.25	± 0.30*
	2004-NOV-19	Storm Surge	4.0	± 0.8	± 1.0*	1.21	± 0.25	± 0.30*
	1989-OCT-20	Storm Surge	3.8	± 0.8	± 1.0*	1.16	± 0.26	± 0.30*
	2000-AUG-29	Storm Surge	3.5	± 0.8	± 1.0*	1.07	± 0.26	± 0.30*

Table 6. Summary of historical floods in Shaktoolik, Alaska, representing the still water level along the sheltered side of the community. Flood categories are included for reference: purple = major, red = moderate, and yellow = minor.

Estimated Floods							
Flood Date	Type	Height (ft MHHW)	Estimate Confidence (ft)	Temporal Confidence (ft)	Height (m MHHW)	Estimate Confidence (m)	Temporal Confidence (m)
2022-SEP-17	Storm Surge	10.5	± 0.6	± 0.0	3.21	± 0.18	± 0.00
2011-NOV-09	Storm Surge	8.9	± 0.5	± 0.0	2.71	± 0.16	± 0.00
2004-OCT-20	Storm Surge	8.3	± 0.5	± 1.0*	2.54	± 0.16	± 0.30*
2005-SEP-25	Storm Surge	7.3	± 0.5	± 1.0*	2.23	± 0.16	± 0.30*
2002-APR-29	Storm Surge	7.3	± 0.5	± 1.0*	2.22	± 0.16	± 0.30*
1996-OCT-30	Storm Surge	7.1	± 0.5	± 1.0*	2.16	± 0.16	± 0.30*
2006-FEB-09	Storm Surge	7.0	± 0.5	± 1.0*	2.14	± 0.16	± 0.30*
2003-NOV-26	Storm Surge	6.4	± 0.5	± 1.0*	1.96	± 0.16	± 0.30*
2001-FEB-08	Storm Surge	6.2	± 0.5	± 1.0*	1.90	± 0.16	± 0.30*
2003-DEC-25	Storm Surge	6.2	± 0.5	± 1.0*	1.89	± 0.16	± 0.30*
2009-MAR-07	Storm Surge	6.1	± 0.5	± 1.0*	1.87	± 0.16	± 0.30*
1990-SEP-01	Storm Surge	6.1	± 0.5	± 1.0*	1.86	± 0.16	± 0.30*
2019-AUG-03	Storm Surge	6.0	± 0.2	± 0.3	1.82	± 0.06	± 0.08
1990-NOV-21	Storm Surge	5.7	± 0.5	± 1.0*	1.75	± 0.16	± 0.30*
2004-DEC-27	Storm Surge	5.6	± 0.5	± 1.0*	1.72	± 0.16	± 0.30*
2009-DEC-05	Storm Surge	5.2	± 0.5	± 1.0*	1.59	± 0.16	± 0.30*
1985-NOV-06	Storm Surge	5.2	± 0.5	± 1.0*	1.58	± 0.16	± 0.30*
1991-OCT-24	Storm Surge	5.0	± 0.5	± 1.0*	1.54	± 0.16	± 0.30*
2009-NOV-08	Storm Surge	4.8	± 0.5	± 1.0*	1.46	± 0.16	± 0.30*
2010-AUG-16	Storm Surge	4.6	± 0.0	± 0.0	1.42	± 0.01	± 0.00
1994-AUG-17	Storm Surge	4.5	± 0.5	± 1.0*	1.38	± 0.16	± 0.30*
1986-JUL-21	Storm Surge	4.4	± 0.5	± 1.0*	1.36	± 0.16	± 0.30*
1993-NOV-17	Storm Surge	4.4	± 0.5	± 1.0*	1.34	± 0.16	± 0.30*
1992-OCT-02	Storm Surge	4.3	± 0.5	± 1.0*	1.30	± 0.16	± 0.30*
1996-NOV-16	Storm Surge	4.3	± 0.5	± 1.0*	1.30	± 0.16	± 0.30*

Table 6, continued. Summary of historical floods in Shaktoolik, Alaska, representing the still water level along the sheltered side of the community. Flood categories are included for reference: purple = major, red = moderate, and yellow = minor.

Estimated Floods							
Flood Date	Type	Height (ft MHHW)	Estimate Confidence (ft)	Temporal Confidence (ft)	Height (m MHHW)	Estimate Confidence (m)	Temporal Confidence (m)
2002-JAN-14	Storm Surge	4.2	± 0.5	± 1.0*	1.29	± 0.16	± 0.30*
1998-APR-28	Storm Surge	4.1	± 0.5	± 1.0*	1.25	± 0.16	± 0.30*
1989-NOV-16	Storm Surge	4.1	± 0.5	± 1.0*	1.25	± 0.16	± 0.30*
1997-AUG-01	Storm Surge	3.9	± 0.5	± 1.0*	1.20	± 0.16	± 0.30*
2004-NOV-19	Storm Surge	3.7	± 0.5	± 1.0*	1.14	± 0.16	± 0.30*

Table 7. Summary of historical floods that could not be estimated in Shaktoolik, Alaska.

Floods Not Estimated	
Date	Type
1913	Storm Surge
1960-SEP-27	Storm Surge
1960-OCT-01	Storm Surge
1965-NOV-14	Storm Surge
1966-NOV-16	Storm Surge
1970-DEC-02	Storm Surge
1974-NOV-16	Storm Surge
1975-AUG-21	Storm Surge
1978-NOV-08	Storm Surge
1983-OCT-03	Storm Surge
2013-NOV-09	Storm Surge
2016-OCT-29	Storm Surge
2016-DEC-30	Storm Surge
2019-FEB	Storm Surge
2024-OCT-21	Storm Surge

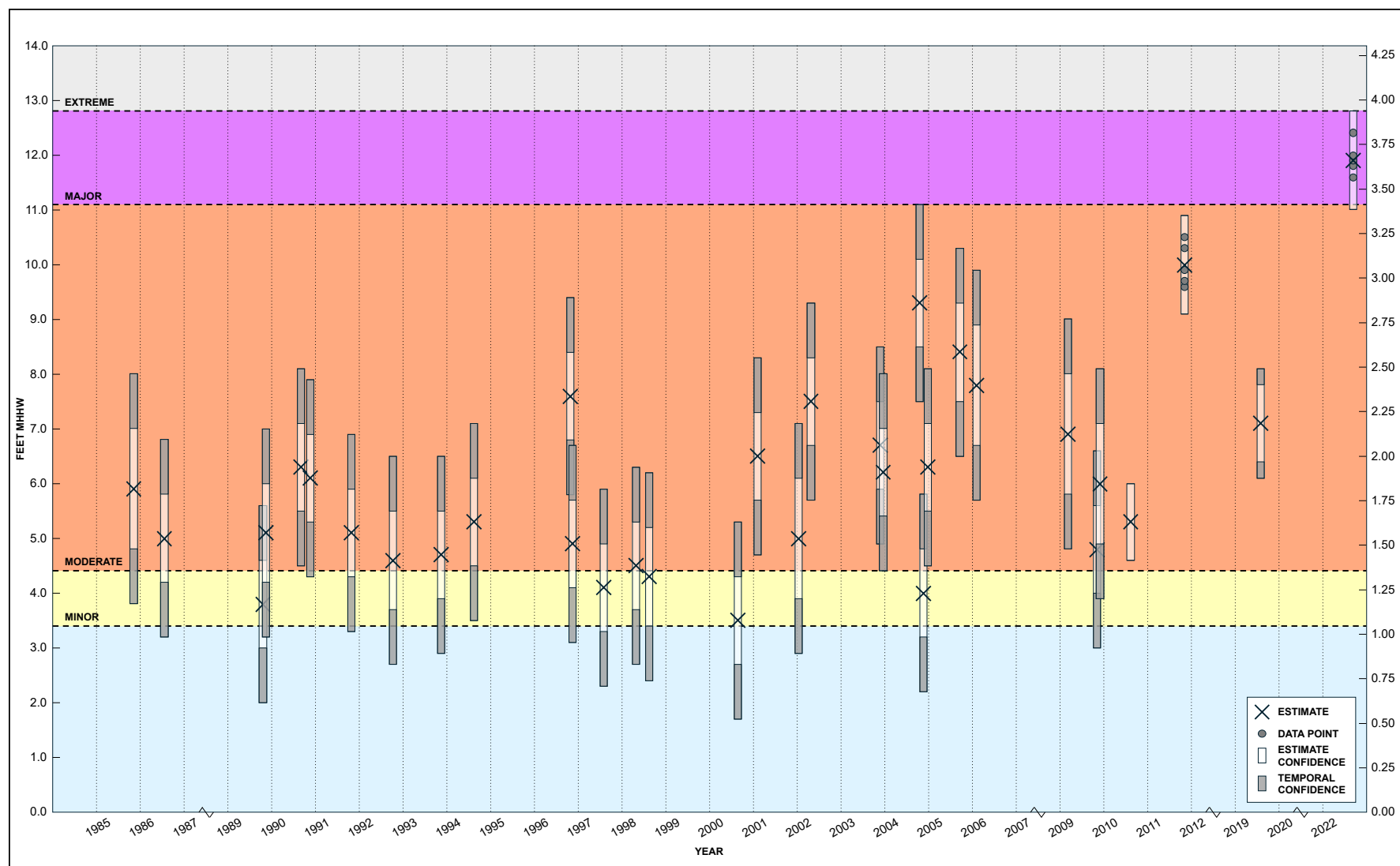


Figure 1. Timeline of estimated dynamic still water level flood events and visual representation of flood height estimates and confidences for Shaktolik, Alaska. Flood height estimates were calculated following the methods developed by Horen and others (2024) and, where applicable, the methods described in appendix B. Estimates are denoted by black X symbols. Data points used during estimation are represented by dark-gray dots. Estimate confidences are displayed as vertical, light-gray boxes. Temporal confidences are displayed as vertical, dark-gray boxes. Each flood height estimate may only be classified into a single flood impact category, but total estimate confidence may exceed the upper and lower bounds of the data used during estimation and may span more than one flood impact category.

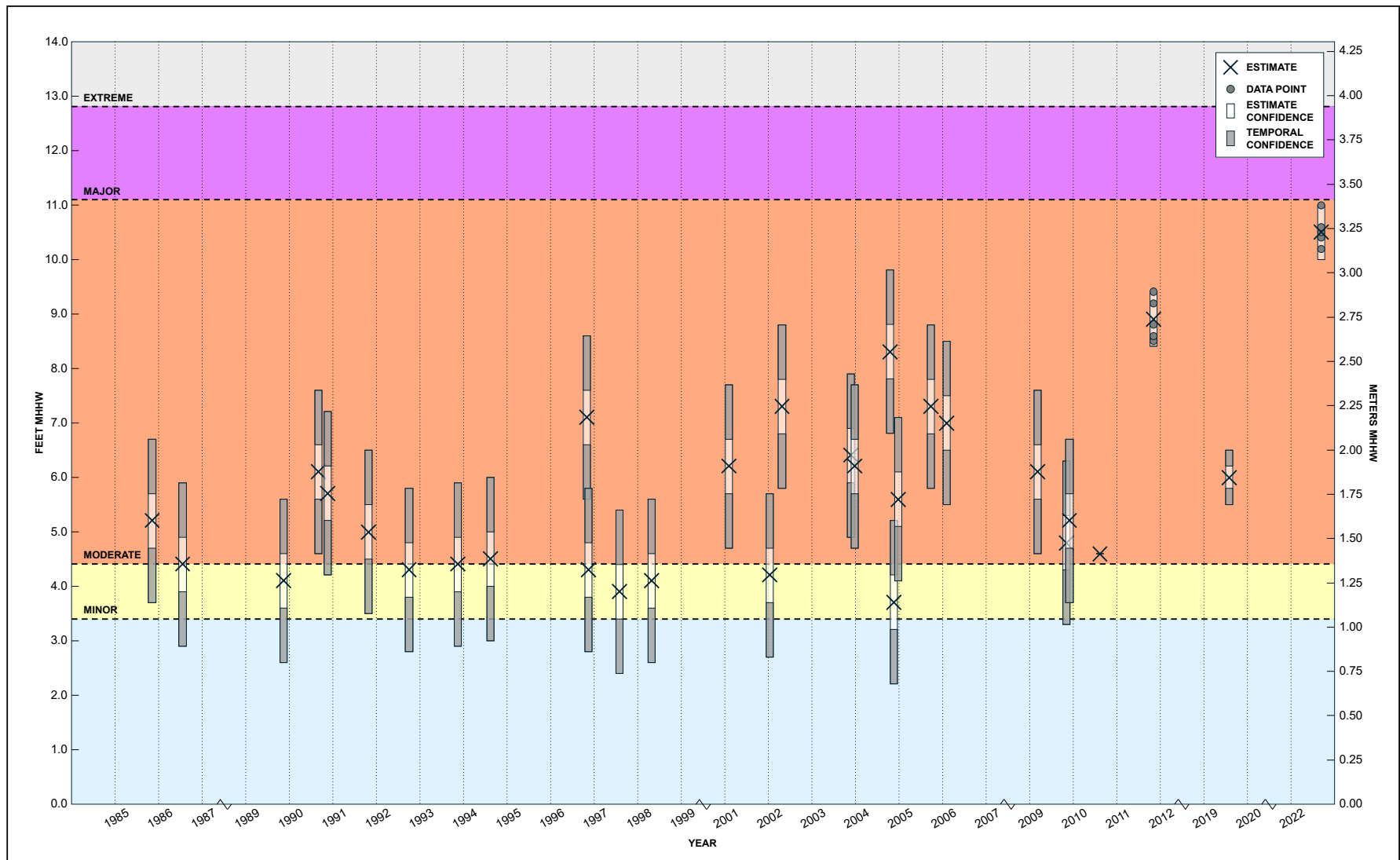


Figure 2. Timeline of estimated still water level flood events and visual representation of flood height estimates and confidences for Shaktoolik, Alaska. Flood height estimates were calculated following the methods developed by Horen and others (2024) and, where applicable, the methods described in appendix B. Estimates are denoted by black X symbols. Data points used during estimation are represented by dark-gray dots. Estimate confidences are displayed as vertical, light-gray boxes. Temporal confidences are displayed as vertical, dark-gray boxes. Each flood height estimate may only be classified into a single flood impact category, but total estimate confidence may exceed the upper and lower bounds of the data used during estimation and may span more than one flood impact category.

FLOOD EVENT SUMMARIES

Flood Date	Height (ft MHHW)	Estimate Confidence (ft)	Temporal Confidence (ft)	Height (m MHHW)	Estimate Confidence (m)	Temporal Confidence (m)	Category
1913	–	–	–	–	–	–	No flood height estimate

Several photographs of debris line HWM, dated “Aug 72” and labeled “1913 storm Shaktolik [sic]” were provided by USACE Alaska District floodplain management office (USACE, 1972; fig. 3).

A flood height could not be estimated for this event because we were unable to identify the locations depicted in the photographs.

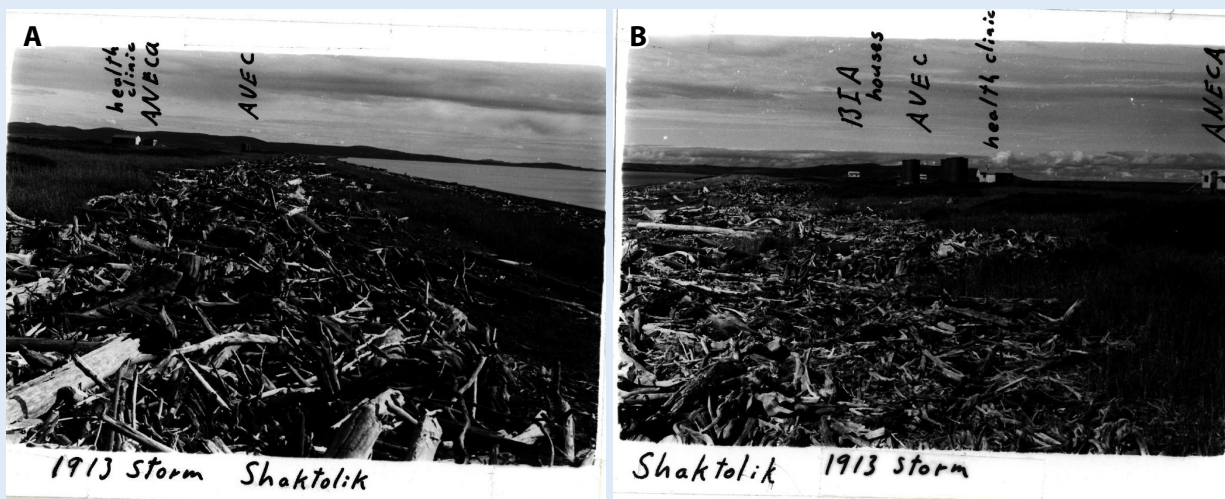


Figure 3. Photographs dated “Aug 72” showing debris line high water marks labeled as “1913 storm” in Shaktolik, Alaska (USACE, 1972).

Flood Date	Height (ft MHHW)	Estimate Confidence (ft)	Temporal Confidence (ft)	Height (m MHHW)	Estimate Confidence (m)	Temporal Confidence (m)	Category
1960-SEP-27	–	–	–	–	–	–	No flood height estimate

This flood event was simulated by USACE (2011). A full description of our processing approach, the data inputs used to generate our estimate, and a graphical depiction of our results are included in appendix B. This event was among those identified as having potentially overestimated storm surge and wave heights and has therefore been excluded from our estimates.

Flood Date	Height (ft MHHW)	Estimate Confidence (ft)	Temporal Confidence (ft)	Height (m MHHW)	Estimate Confidence (m)	Temporal Confidence (m)	Category
1960-OCT-01	–	–	–	–	–	–	No flood height estimate

This flood event was simulated by USACE (2011). A full description of our processing approach, the data inputs used to generate our estimate, and a graphical depiction of our results are included in appendix B. This event was among those identified as having potentially overestimated storm surge and wave heights and has therefore been excluded from our estimates.

Flood Date	Height (ft MHHW)	Estimate Confidence (ft)	Temporal Confidence (ft)	Height (m MHHW)	Estimate Confidence (m)	Temporal Confidence (m)	Category
1965-NOV-14	–	–	–	–	–	–	No flood height estimate

This flood event was simulated by USACE (2011). A full description of our processing approach, the data inputs used to generate our estimate, and a graphical depiction of our results are included in appendix B. This event was among those identified as having potentially overestimated storm surge and wave heights and has therefore been excluded from our estimates.

Flood Date	Height (ft MHHW)	Estimate Confidence (ft)	Temporal Confidence (ft)	Height (m MHHW)	Estimate Confidence (m)	Temporal Confidence (m)	Category
1966-NOV-16	–	–	–	–	–	–	No flood height estimate

This flood event was simulated by USACE (2011). A full description of our processing approach, the data inputs used to generate our estimate, and a graphical depiction of our results are included in appendix B. This event was among those identified as having potentially overestimated storm surge and wave heights and has therefore been excluded from our estimates.

Flood Date	Height (ft MHHW)	Estimate Confidence (ft)	Temporal Confidence (ft)	Height (m MHHW)	Estimate Confidence (m)	Temporal Confidence (m)	Category
1970-DEC-02	–	–	–	–	–	–	No flood height estimate

This flood event was simulated by USACE (2011). A full description of our processing approach, the data inputs used to generate our estimate, and a graphical depiction of our results are included in appendix B. This event was among those identified as having potentially overestimated storm surge and wave heights and has therefore been excluded from our estimates.

Flood Date	Height (ft MHHW)	Estimate Confidence (ft)	Temporal Confidence (ft)	Height (m MHHW)	Estimate Confidence (m)	Temporal Confidence (m)	Category
1974-NOV-16	–	–	–	–	–	–	No flood height estimate

This flood event was simulated by USACE (2011). A full description of our processing approach, the data inputs used to generate our estimate, and a graphical depiction of our results are included in appendix B. This event was among those identified as having potentially overestimated storm surge and wave heights and has therefore been excluded from our estimates.

Flood Date	Height (ft MHHW)	Estimate Confidence (ft)	Temporal Confidence (ft)	Height (m MHHW)	Estimate Confidence (m)	Temporal Confidence (m)	Category
1975-AUG-21	–	–	–	–	–	–	No flood height estimate

This flood event was simulated by USACE (2011). A full description of our processing approach, the data inputs used to generate our estimate, and a graphical depiction of our results are included in appendix B. This event was among those identified as having potentially overestimated storm surge and wave heights and has therefore been excluded from our estimates.

Flood Date	Height (ft MHHW)	Estimate Confidence (ft)	Temporal Confidence (ft)	Height (m MHHW)	Estimate Confidence (m)	Temporal Confidence (m)	Category	Flooding Type
1986-JUL-20	5.0	± 0.8	± 1.0*	1.51	± 0.26	± 0.30*	Moderate	DSWL
1986-JUL-21	4.4	± 0.5	± 1.0*	1.36	± 0.16	± 0.30*	Moderate	SWL

This flood event was simulated by USACE (2011). A full description of our processing approach, the data inputs used to generate our estimate, and a graphical depiction of our results are included in appendix B.

Flood Date	Height (ft MHHW)	Estimate Confidence (ft)	Temporal Confidence (ft)	Height (m MHHW)	Estimate Confidence (m)	Temporal Confidence (m)	Category	Flooding Type
1989-OCT-20	3.8	± 0.8	± 1.0*	1.16	± 0.26	± 0.30*	Minor	DSWL

This flood event was simulated by USACE (2011). A full description of our processing approach, the data inputs used to generate our estimate, and a graphical depiction of our results are included in appendix B.

Flood Date	Height (ft MHHW)	Estimate Confidence (ft)	Temporal Confidence (ft)	Height (m MHHW)	Estimate Confidence (m)	Temporal Confidence (m)	Category	Flooding Type
1989-NOV-16	5.1	± 0.9	± 1.0*	1.55	± 0.26	± 0.30*	Moderate	DSWL
	4.1	± 0.5	± 1.0*	1.25	± 0.16	± 0.30*	Minor	SWL

This flood event was simulated by USACE (2011). A full description of our processing approach, the data inputs used to generate our estimate, and a graphical depiction of our results are included in appendix B.

Flood Date	Height (ft MHHW)	Estimate Confidence (ft)	Temporal Confidence (ft)	Height (m MHHW)	Estimate Confidence (m)	Temporal Confidence (m)	Category	Flooding Type
1990-SEP-01	6.3	± 0.8	± 1.0*	1.92	± 0.25	± 0.30*	Moderate	DSWL
	6.1	± 0.5	± 1.0*	1.86	± 0.16	± 0.30*	Moderate	SWL

This flood event was simulated by USACE (2011). A full description of our processing approach, the data inputs used to generate our estimate, and a graphical depiction of our results are included in appendix B.

Flood Date	Height (ft MHHW)	Estimate Confidence (ft)	Temporal Confidence (ft)	Height (m MHHW)	Estimate Confidence (m)	Temporal Confidence (m)	Category	Flooding Type
1990-NOV-20	6.1	± 0.8	± 1.0*	1.87	± 0.25	± 0.30*	Moderate	DSWL
1990-NOV-21	5.7	± 0.5	± 1.0*	1.75	± 0.16	± 0.30*	Moderate	SWL

This flood event was simulated by USACE (2011). A full description of our processing approach, the data inputs used to generate our estimate, and a graphical depiction of our results are included in appendix B.

Flood Date	Height (ft MHHW)	Estimate Confidence (ft)	Temporal Confidence (ft)	Height (m MHHW)	Estimate Confidence (m)	Temporal Confidence (m)	Category	Flooding Type
1991-OCT-24	5.1	± 0.8	± 1.0*	1.56	± 0.25	± 0.30*	Moderate	DSWL
	5.0	± 0.5	± 1.0*	1.54	± 0.16	± 0.30*	Moderate	SWL

This flood event was simulated by USACE (2011). A full description of our processing approach, the data inputs used to generate our estimate, and a graphical depiction of our results are included in appendix B.

Flood Date	Height (ft MHHW)	Estimate Confidence (ft)	Temporal Confidence (ft)	Height (m MHHW)	Estimate Confidence (m)	Temporal Confidence (m)	Category	Flooding Type
1992-OCT-06	4.6	± 0.9	± 1.0*	1.41	± 0.26	± 0.30*	Moderate	DSWL
1992-OCT-02	4.3	± 0.5	± 1.0*	1.30	± 0.16	± 0.30*	Minor	SWL

This flood event was simulated by USACE (2011). A full description of our processing approach, the data inputs used to generate our estimate, and a graphical depiction of our results are included in appendix B.

Flood Date	Height (ft MHHW)	Estimate Confidence (ft)	Temporal Confidence (ft)	Height (m MHHW)	Estimate Confidence (m)	Temporal Confidence (m)	Category	Flooding Type
1993-NOV-17	4.7	± 0.8	± 1.0*	1.45	± 0.25	± 0.30*	Moderate	DSWL
	4.4	± 0.5	± 1.0*	1.34	± 0.16	± 0.30*	Minor	SWL

This flood event was simulated by USACE (2011). A full description of our processing approach, the data inputs used to generate our estimate, and a graphical depiction of our results are included in appendix B.

Flood Date	Height (ft MHHW)	Estimate Confidence (ft)	Temporal Confidence (ft)	Height (m MHHW)	Estimate Confidence (m)	Temporal Confidence (m)	Category	Flooding Type
1994-AUG-17	5.3	± 0.8	± 1.0*	1.61	± 0.26	± 0.30*	Moderate	DSWL
	4.5	± 0.5	± 1.0*	1.38	± 0.16	± 0.30*	Moderate	SWL

This flood event was simulated by USACE (2011). A full description of our processing approach, the data inputs used to generate our estimate, and a graphical depiction of our results are included in appendix B.

Flood Date	Height (ft MHHW)	Estimate Confidence (ft)	Temporal Confidence (ft)	Height (m MHHW)	Estimate Confidence (m)	Temporal Confidence (m)	Category	Flooding Type
1996-OCT-29	7.6	± 0.8	± 1.0*	2.31	± 0.26	± 0.30*	Moderate	DSWL
1996-OCT-30	7.1	± 0.5	± 1.0*	2.16	± 0.16	± 0.30*	Moderate	SWL

This flood event was simulated by USACE (2011). A full description of our processing approach, the data inputs used to generate our estimate, and a graphical depiction of our results are included in appendix B.

Flood Date	Height (ft MHHW)	Estimate Confidence (ft)	Temporal Confidence (ft)	Height (m MHHW)	Estimate Confidence (m)	Temporal Confidence (m)	Category	Flooding Type
1996-NOV-15	4.9	± 0.8	± 1.0*	1.50	± 0.26	± 0.30*	Moderate	DSWL
1996-NOV-16	4.3	± 0.5	± 1.0*	1.30	± 0.16	± 0.30*	Minor	SWL

This flood event was simulated by USACE (2011). A full description of our processing approach, the data inputs used to generate our estimate, and a graphical depiction of our results are included in appendix B.

Flood Date	Height (ft MHHW)	Estimate Confidence (ft)	Temporal Confidence (ft)	Height (m MHHW)	Estimate Confidence (m)	Temporal Confidence (m)	Category	Flooding Type
1997-AUG-03	4.1	± 0.8	± 1.0*	1.26	± 0.25	± 0.30*	Minor	DSWL
1997-AUG-01	3.9	± 0.5	± 1.0*	1.20	± 0.16	± 0.30*	Minor	SWL

This flood event was simulated by USACE (2011). A full description of our processing approach, the data inputs used to generate our estimate, and a graphical depiction of our results are included in appendix B.

Flood Date	Height (ft MHHW)	Estimate Confidence (ft)	Temporal Confidence (ft)	Height (m MHHW)	Estimate Confidence (m)	Temporal Confidence (m)	Category	Flooding Type
2004-NOV-19	4.0	± 0.8	± 1.0*	1.21	± 0.25	± 0.30*	Minor	DSWL
	3.7	± 0.5	± 1.0*	1.14	± 0.16	± 0.30*	Minor	SWL

This flood event was simulated by USACE (2011). A full description of our processing approach, the data inputs used to generate our estimate, and a graphical depiction of our results are included in appendix B.

Flood Date	Height (ft MHHW)	Estimate Confidence (ft)	Temporal Confidence (ft)	Height (m MHHW)	Estimate Confidence (m)	Temporal Confidence (m)	Category	Flooding Type
2005-SEP-23	8.4	± 0.9	± 1.0*	2.57	± 0.26	± 0.30*	Moderate	DSWL
2005-SEP-25	7.3	± 0.5	± 1.0*	2.23	± 0.16	± 0.30*	Moderate	SWL

This flood event was simulated by USACE (2011). A full description of our processing approach, the data inputs used to generate our estimate, and a graphical depiction of our results are included in appendix B.

Flood Date	Height (ft MHHW)	Estimate Confidence (ft)	Temporal Confidence (ft)	Height (m MHHW)	Estimate Confidence (m)	Temporal Confidence (m)	Category	Flooding Type
2006-FEB-09	7.8	± 1.1	± 1.0*	2.36	± 0.32	± 0.30*	Moderate	DSWL
	7.0	± 0.5	± 1.0*	2.14	± 0.16	± 0.30*	Moderate	SWL

This flood event was simulated by USACE (2011). A full description of our processing approach, the data inputs used to generate our estimate, and a graphical depiction of our results are included in appendix B.

Flood Date	Height (ft MHHW)	Estimate Confidence (ft)	Temporal Confidence (ft)	Height (m MHHW)	Estimate Confidence (m)	Temporal Confidence (m)	Category	Flooding Type
2009-MAR-07	6.9	± 1.1	± 1.0*	2.10	± 0.32	± 0.30*	Moderate	DSWL
	6.1	± 0.5	± 1.0*	1.87	± 0.16	± 0.30*	Moderate	SWL

This flood event was simulated by USACE (2011). A full description of our processing approach, the data inputs used to generate our estimate, and a graphical depiction of our results are included in appendix B.

Flood Date	Height (ft MHHW)	Estimate Confidence (ft)	Temporal Confidence (ft)	Height (m MHHW)	Estimate Confidence (m)	Temporal Confidence (m)	Category	Flooding Type
2009-NOV-08	4.8	± 0.8	± 1.0*	1.47	± 0.25	± 0.30*	Moderate	DSWL
	4.8	± 0.5	± 1.0*	1.46	± 0.16	± 0.30*	Moderate	SWL

This flood event was simulated by USACE (2011). A full description of our processing approach, the data inputs used to generate our estimate, and a graphical depiction of our results are included in appendix B.

Flood Date	Height (ft MHHW)	Estimate Confidence (ft)	Temporal Confidence (ft)	Height (m MHHW)	Estimate Confidence (m)	Temporal Confidence (m)	Category	Flooding Type
2009-DEC-05	6.0	± 1.1	± 1.0*	1.81	± 0.32	± 0.30*	Moderate	DSWL
	5.2	± 0.5	± 1.0*	1.59	± 0.16	± 0.30*	Moderate	SWL

This flood event was simulated by USACE (2011). A full description of our processing approach, the data inputs used to generate our estimate, and a graphical depiction of our results are included in appendix B.

Flood Date	Height (ft MHHW)	Estimate Confidence (ft)	Temporal Confidence (ft)	Height (m MHHW)	Estimate Confidence (m)	Temporal Confidence (m)	Category	Flooding Type
2010-AUG-16	5.3	± 0.7	± 0.0	1.63	± 0.20	± 0.00	Moderate	DSWL
	4.6	± 0.0	± 0.0	1.42	± 0.01	± 0.00	Moderate	SWL

During a water level sensor deployment aimed at establishing tidal datums at the Shaktoolik NOAA CO-OPS station, 946 8691, a period of high water was recorded (fig. 4). For our SWL estimate, we identified the peak water height from the data provided by NOAA and derived our uncertainty from the reported accuracy of the benchmarks used to establish tide station 946 8691.

To estimate the DSWL flooding for this event, we followed a similar methodology as outlined in appendix B, holding the SWL estimate as our tide and surge components of DSWL and calculating the average contribution of offshore significant wave height specified by Kriebel (1994) to account for the standing wave setup component. From the National Snow and Ice Data Center (NSIDC; Fetterer and others, 2017), we found there to be no sea ice off the coast of Shaktoolik during this storm event. The highest modeled significant wave height from the USACE (2024) Wave Information Study (WIS) data portal was 3.9 ft (1.19 m), contributing a standing wave setup of 0.7 ft (0.21 m) and establishing a DSWL estimate of 5.3 ft (1.63 m) MHHW.

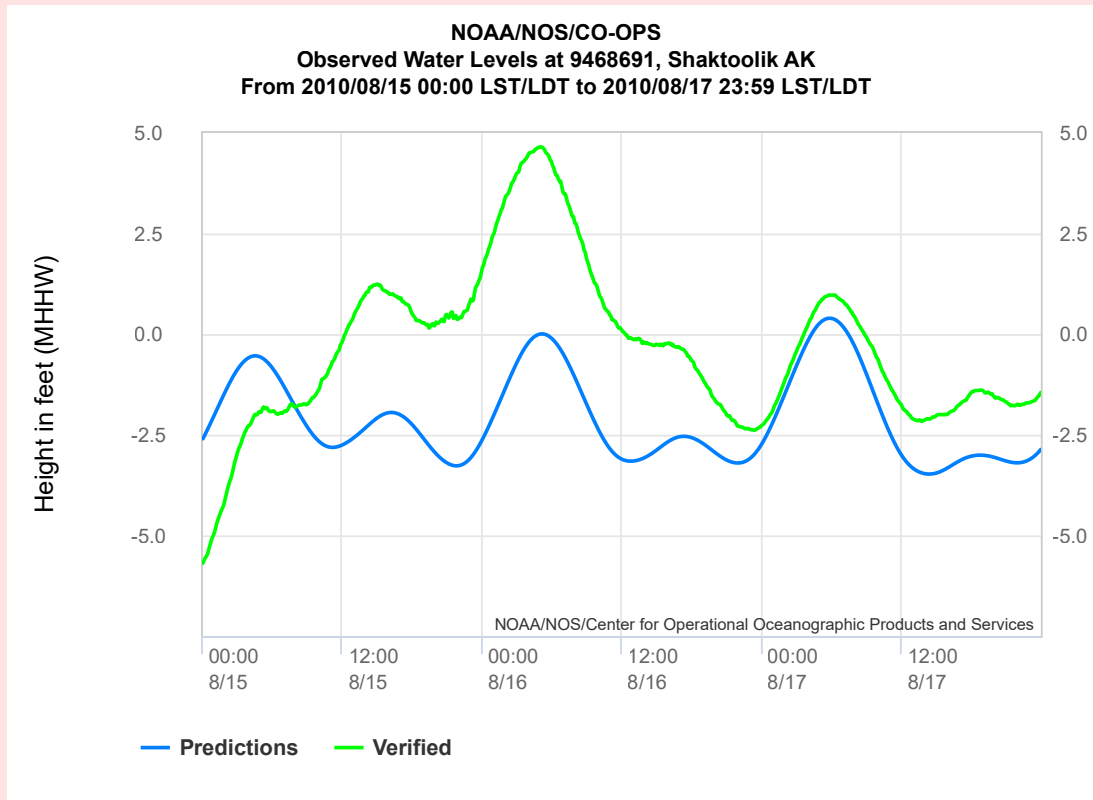


Figure 4. NOAA CO-OPS observed water levels for tide station 946 8691 in Shaktoolik, Alaska, from August 15, 2010, to August 18, 2010.

Flood Date	Height (ft MHHW)	Estimate Confidence (ft)	Temporal Confidence (ft)	Height (m MHHW)	Estimate Confidence (m)	Temporal Confidence (m)	Category	Flooding Type
2011-NOV-09	10.0	± 0.9	± 0.0	3.04	± 0.27	± 0.00	Moderate	DSWL
	8.9	± 0.5	± 0.0	2.71	± 0.16	± 0.00	Moderate	SWL

In early November 2011, an extra-tropical cyclone impacted Western Alaska and Norton Sound. In the immediate wake of the storm, DGGS deployed a team to collect HWM data and accounts in several communities, including Shaktoolik (Kinsman and DeRaps, 2012). At least 23 flood-related points were collected in and around the community, with five of these identified as strong indicators of the maximum still water height, described as “storm tide (surge + tide...)” by Kinsman and DeRaps (2012). An average of these five heights was calculated to estimate an SWL flood height of 8.9 ft (2.71 m) MHHW.

To estimate the DSWL flooding for this event, we followed a similar methodology as outlined in appendix B, holding the SWL estimate as our tide and surge components of DSWL and calculating the average contribution of offshore significant wave height specified by Kriebel (1994) to account for the standing wave setup component. From the NSIDC, we found there to be 34.0 percent sea ice concentration index (Fetterer and others, 2017) off the coast of Shaktoolik during this storm event, prompting us to apply a damping factor as described by Montiel and others (2018) to the highest modeled significant wave height, 7.1 ft (2.17 m), gathered from the USACE (2024) WIS data portal, thus calculating a wave setup contribution of 1.1 ft (0.33 m) and establishing a DSWL estimate of 10.0 ft (3.04 m) MHHW.

Flood Date	Height (ft MHHW)	Estimate Confidence (ft)	Temporal Confidence (ft)	Height (m MHHW)	Estimate Confidence (m)	Temporal Confidence (m)	Category
2013-NOV-09	–	–	–	–	–	–	No flood height estimate

The National Centers for Environmental Information (NCEI; 2013) reported “shoreline erosion occurred... washing out the fuel tank farm protection berm and the city landfill protection berm” in Shaktoolik, noting “the community evacuation road was washed out.”

A flood height could not be estimated for this event because a specific water height could not be identified from the information provided.

Flood Date	Height (ft MHHW)	Estimate Confidence (ft)	Temporal Confidence (ft)	Height (m MHHW)	Estimate Confidence (m)	Temporal Confidence (m)	Category
2016-OCT-29	–	–	–	–	–	–	No flood height estimate

For this event, Golder Associates Ltd. (2020) provided an estimate of 6.3 ft (1.92 m), claiming to have estimated the still water height in Shaktoolik for this event using “the reported SWL at Golovin and the measured SWL at Unalakleet.” We found that Buzard and Overbeck (2021) reported the flood height in Golovin for this event at 6.3 ± 0.7 ft (1.92 ± 0.21 m) MHHW, citing an estimate from Overbeck (2017), although the latter provided an SWL of 5.6 ft (1.70 m) MHHW and a “marine total water level (MTWL...)” of 6.4 ft (1.96 m) MHHW, which included “wave setup, wave setdown, wave groups, wave runup, and wash” (Overbeck, 2017). From the Unalakleet NOAA CO-OPS tide station 946 8333, we found that the peak water height during this event was recorded as 4.8 ft (1.48 m) MHHW. Based on the evidence available, it appears Golder Associates Ltd. (2020) may have simply transposed the estimated water height from Golovin for this event.

A flood height could not be estimated for this event because of the ambiguous provenance and dubious methodology of the Golder Associates Ltd. (2020) estimate, and more importantly, because there was no specific water height information reported for Shaktoolik.

Flood Date	Height (ft MHHW)	Estimate Confidence (ft)	Temporal Confidence (ft)	Height (m MHHW)	Estimate Confidence (m)	Temporal Confidence (m)	Category
2016-DEC-30	–	–	–	–	–	–	No flood height estimate

For this event, Golder Associates Ltd. (2020) provided an estimate of 7.0 ft (2.13 m), claiming to have estimated the still water height in Shaktoolik for this event using “the reported SWL at Golovin and the measured SWL at Unalakleet.” We found that Buzard and Overbeck (2021), reported the flood height in Golovin for this event at 7.0 ± 1.2 ft (2.13 ± 0.37 m) MHHW. From the Unalakleet NOAA CO-OPS tide station 946 8333, we found that the peak water height during this event was recorded as 6.6 ft (2.01 m) MHHW. Based on the evidence available, it appears Golder Associates Ltd. (2020) may have simply transposed the estimated water height from Golovin for this event.

A flood height could not be estimated for this event because of the ambiguous provenance and dubious methodology of the Golder Associates Ltd. (2020) estimate, and more importantly, because there was no specific water height information reported for Shaktoolik.

Flood Date	Height (ft MHHW)	Estimate Confidence (ft)	Temporal Confidence (ft)	Height (m MHHW)	Estimate Confidence (m)	Temporal Confidence (m)	Category
2019-FEB	–	–	–	–	–	–	No flood height estimate

In a list of “historical coastal flood events,” Golder Associates Ltd. (2020) included an estimate of 9.4 ft (2.87 m) MHHW for an event that occurred in February 2019, but did not provide any observations or explanation for their estimate. NCEI (2019a) indicated a low pressure system “moved rapidly northward through the western Bering Sea” on February 11, though neither Shaktoolik nor Norton Sound were mentioned. Dobson and others (2022) characterized this event as “a lower [than 20-year] magnitude winter storm” that “produced large waves that topped the berm and caused damage to critical infrastructure.”

A flood height could not be estimated for this event because of the ambiguous provenance and dubious methodology of the Golder Associates Ltd. (2020) estimate, and more importantly, because there was no specific water height information reported for Shaktoolik.

Flood Date	Height (ft MHHW)	Estimate Confidence (ft)	Temporal Confidence (ft)	Height (m MHHW)	Estimate Confidence (m)	Temporal Confidence (m)	Category	Flooding Type
2019-AUG-03	7.1	± 0.7	± 0.3	2.15	± 0.22	± 0.08	Moderate	DSWL
	6.0	± 0.2	± 0.3	1.82	± 0.07	± 0.08	Moderate	SWL

NCEI (2019b) reported “in Shaktoolik, water surrounded the village, much of the normally dry tundra was inundated, but erosion of the evacuation route out of town was the biggest impact.” Tribal coordinator, Sophia Katchatag, provided DGGS with a photograph of the flood waters, in which a flood staff is visible on a power pole near the pump house (fig. 5). During a visit in July 2024, DGGS collected a GPS point at the base of this power pole. From the photograph, the water height corresponds to roughly 2.5 ft (0.76 m) on the flood staff, which we added to the ground height at the base of the power pole to form our SWL flood height estimate.

To estimate the DSWL flooding for this event, we followed a similar methodology as outlined in appendix B, holding the SWL estimate as our tide and surge components of DSWL and calculating the average contribution of offshore significant wave height specified by Kriebel (1994) to account for the standing wave setup component. From the NSIDC (Fetterer and others, 2017), we found there to be no sea ice off the coast of Shaktoolik during this storm event. The highest modeled significant wave height from the USACE (2024) WIS data portal was 6.3 ft (1.91 m), contributing a standing wave setup of 1.1 ft (0.33 m) and establishing a DSWL estimate of 7.1 ft (2.15 m) MHHW.



Figure 5. Photographic evidence of still water level flood height in Shaktoolik, Alaska during the August 2019 flood event (credit: Sophia Katchatag).

Flood Date	Height (ft MHHW)	Estimate Confidence (ft)	Temporal Confidence (ft)	Height (m MHHW)	Estimate Confidence (m)	Temporal Confidence (m)	Category	Flooding Type
2022-SEP-17	11.9	± 0.9	± 0.0	3.62	± 0.28	± 0.00	Major	DSWL
	10.5	± 0.6	± 0.0	3.21	± 0.18	± 0.00	Moderate	SWL

NCEI (2022) reported the remnants of Typhoon Merbok reached the eastern coast of Norton Sound on September 17, 2022, with an estimate “that water levels peaked at 12 feet above Mean Higher High Water Saturday afternoon but remained elevated into Sunday afternoon” in Shaktoolik. NCEI (2022) detailed several impacts from this storm, including “moderate flooding and erosion... in parts of the village,” and damage to roads and the shoreline berm due to “storm surge and wave runup,” with debris pushed “onto the west end of the runway” damaging the runway lights.

DGGS deployed a team to Shaktoolik on September 22, 2022, to collect HWM data following this storm event (Horen and others, 2022). The team photographed and measured 59 HWM points, recording the GNSS position, type of high-water feature, height above ground (if applicable), and description of each mark (Horen and others, 2022). For this assessment, we grouped these HWM based on location, evidence type, and type of flooding. During this event, Shaktoolik experienced three types of flooding, SWL flooding along the riverine side of the community, DSWL flooding north of the berm along the exposed coastline, and accumulation flooding in the lee of the berm due to overtopping. The DGGS team also documented severe erosional damage to the berm as a result of this storm event (Horen and others, 2022).

To estimate the SWL flooding, we identified five wash line HWM and one present-at-the-peak HWM (Horen and others, 2022) along the riverine side of the community, all together averaging 10.5 ft (3.21 m) MHHW.

To estimate the DSWL flooding for this event, we first identified HWM data (Horen and others, 2022) along the exposed shore of the community, focusing on areas shoreward of or without protection from the berm, finding only one location with HWM between the north end of the berm and the south end of the airstrip. These HWM averaging 15.2 ft (4.63 m) MHHW, but because the SWL represents the tide and surge components of the water level, in order for there to be nearly 5.0 ft (1.52 m) of wave setup contribution to the DSWL, we would expect to see offshore wave heights reaching upward of 25.0 ft (7.62 m) in accordance with the observations of Kriebel (1994). We investigated this possibility by querying the USACE (2024) WIS data portal for the modeled wave heights during the Merbok event, finding that the highest modeled significant wave height was 8.7 ft (2.65 m). Following a similar methodology as outlined in appendix B, we held the SWL estimate as our tide and surge components of DSWL and calculated the average contribution of offshore significant wave height specified by Kriebel (1994) to account for a standing wave setup component of 1.3 ft (0.41 m) after finding there to be a sea ice concentration index of 23.2 percent (Fetterer and others, 2017) and applying a damping factor as described by Montiel and others (2018), thus establishing a DSWL estimate of 11.9 ft (3.62 m) MHHW. The upper limit of this estimate's confidence forms the basis for the threshold between the major and extreme impact categories.

As an additional note, Horen and others (2022) observed evidence of OTA flooding during this event, which we believe is directly related to the severity of this storm and the structure of the berm itself. Analyzing the heights and distribution of these HWM, we found five distinct areas of OTA flooding behind the berm, separated by instances of higher ground, or in the case of the two southernmost areas, by a gap in the berm (fig. 6). These HWM also displayed a general reduction in ground height along the reach of the berm, ranging from the highest, 18.4 ft (5.61 m) MHHW, near the landfill at the southern end of the community, to the lowest, 16.1 ft (4.90 m) MHHW, near the northernmost stretch of the berm. As this type of flooding is distinct from both DSWL and SWL, displays a ground height dependency, and likely resulted from a type of flood protection failure, we believe it is more appropriate to provide water depths for these areas rather than flood heights (fig. 6). There may be areas in the lee of the berm that experienced greater water depths than were identified in our analysis due to the limitations of the data available to us. A further 22 HWM were identified as OTA flood indicators around the south end of the airstrip. However, because this flooding occurred in uninhabited and unutilized locations, we have not estimated the water depths in this area.

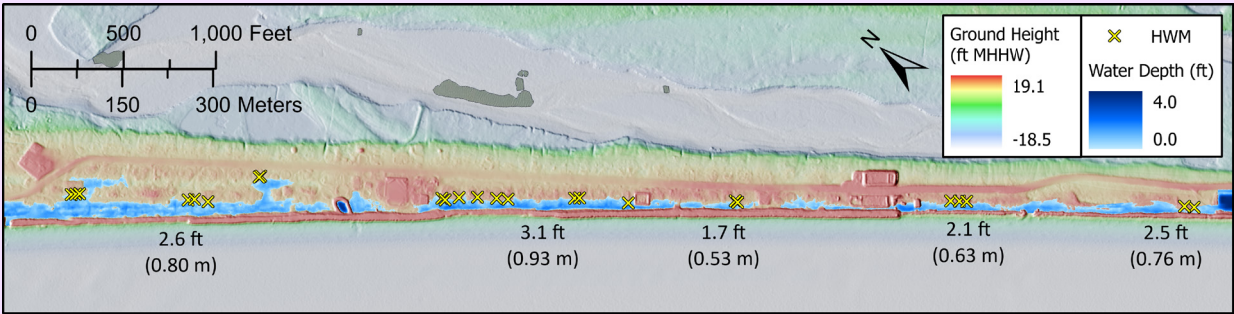


Figure 6. Areas and maximum depths of overtopping accumulations flooding identified in the 2021 topobathy digital elevation model based on high water mark from the flood event on September 17, 2022, in Shaktoolik, Alaska.

Flood Date	Height (ft MHHW)	Estimate Confidence (ft)	Temporal Confidence (ft)	Height (m MHHW)	Estimate Confidence (m)	Temporal Confidence (m)	Category
2024-OCT-21	–	–	–	–	–	–	No flood height estimate

In October 2024 a powerful storm struck the west coast of Alaska causing coastal flooding, erosion, and infrastructure damage. The Alaska Department of Transportation & Public Facilities (DOT&PF; 2024) issued warnings and detailed impacts for communities along the west coast, including Shaktoolik. NCEI (2024) reported a coastal flood event occurred October 20–22, 2024, noting “officials reported a loss of an unknown amount of shoreline protection berm” in Shaktoolik. Before and after photographs of the berm were provided to DGGs by Gloria Andrew (fig. 7).

A flood height could not be estimated for this event because a specific water height could not be identified from the information provided.



Figure 7. Before and after photographs of the berm in Shaktoolik, Alaska during the October 2024 flood event (credit: Gloria Andrew).

ACKNOWLEDGMENTS

We thank the Native Village and City of Shaktoolik for supporting this work, made possible with the National Fish and Wildlife Foundation's National Coastal Resilience Funding through our partners at the Alaska Native Tribal Health Consortium. The views and conclusions contained in this document are those of the authors and should not be interpreted as representing the opinions or policies of the Alaska Division of Geological & Geophysical Surveys, the U.S. Government, the National Fish and Wildlife Foundation, or the National Fish and Wildlife Foundation's funding sources. Mention of trade names or commercial products does not constitute endorsement by the Alaska Division of Geological & Geophysical Surveys, the U.S. Government, the National Fish and Wildlife Foundation, or the National Fish and Wildlife Foundation's funding sources.

REFERENCES

- Alaska Department of Transportation and Public Facilities (DOT&PF), 2024, 2024 Storms, Western Alaska Storm Situation Report. <https://dot.alaska.gov/2024storms/#:~:text=A%20powerful%20storm%20struck%20Alaska%27s,damage%20and%20coordinating%20recovery%20efforts>.
- Bristol Engineering Services Company, LLC, 2022, Shaktoolik community finished floor elevations: Bristol project No. 32210041, 6 p.
- Buzard, R.M., and Overbeck, J.R., 2021, Coastal flood impact assessments for Alaska communities: Golovin: Alaska Division of Geological & Geophysical Surveys Report of Investigation 2021-1E, 32 p. <https://doi.org/10.14509/30855>
- Buzard, R.M., Overbeck, J.R., Chriest, Jonathan, Endres, K.L., and Plumb, E.W., 2021, Coastal flood impact assessments for Alaska communities: Alaska Division of Geological & Geophysical Surveys Report of Investigation 2021-1, 16 p. <https://doi.org/10.14509/30573>
- Chapman, R.S., Kim, Sung-Chan, and Mark, D.J., 2009, Storm-induced water level prediction study for the western coast of Alaska: United States Army Corps of Engineers, 102 p.
- Dobson, Greg, Johnson, Ian, Orlando, Jessica, Kowal, Virginia, Rhodes, Kim, Byler, Kristen, and Lussier, Bridget, 2022, Alaska coastal resilience assessment: National Fish and Wildlife Foundation, 105 p. <https://www.nfwf.org/sites/default/files/2022-04/alaska-coastal-resilience-assessment.pdf>
- Fetterer, F., Knowles, K., Meier, W. N., Savoie, M., and Windnagel, A. K., 2017, Sea Ice Index (G02135, Version 3): National Snow and Ice Data Center. <https://doi.org/10.7265/N5K072F8>
- Golder Associates Ltd., 2020, Climate change vulnerability and risk assessment - Shaktoolik, Alaska: Golder Associates Ltd., 134 p.
- HDR and RIM First People, 2016, Shaktoolik strategic management plan: Alaska Department of Commerce, Community, and Economic Development, 107 p.
- Hofstaedter, Emily, 2019, Shaktoolik reinforces protective berm, but it may not be enough to keep stormwater away: Alaska Public Media, accessed June 27, 2025, <https://alaskapublic.org/news/2019-12-11/shaktoolik-reinforces-protective-berm-but-it-may-not-be-enough-to-keep-storms-at-bay>.
- Horen, K.C., Poisson, A.C., Christian, J.E., and Nieminski, N.M., 2024, Methods for evaluating coastal flood impacts in Alaska communities: Alaska Division of Geological & Geophysical Surveys Miscellaneous Publication 177, 13 p. <https://doi.org/10.14509/31279>
- Horen, K.C., Poisson, A.C., Siemsen, Z.J., Donohue, J.M., Widmer, K.L., Adams, J.D., and Overbeck, J.R., 2022, Storm impact survey data for selected Alaska coastal communities in response to extra-tropical cyclone Merbok, September 2022: Alaska Division of Geological & Geophysical Surveys Raw Data File 2022-14, 8 p. <https://doi.org/10.14509/30909>
- Johnson, Terry, and Gray, Glenn, 2014, Shaktoolik, Alaska: Climate change adaptation for an at-risk community: National Oceanic and Atmospheric Administration Alaska Sea Grant Program Adaption Plan, 41 p.

- Kinsman, N.E.M., and DeRaps, M.R., 2012, Coastal hazard field investigations in response to the November 2011 Bering Sea storm, Norton Sound, Alaska: Alaska Division of Geological & Geophysical Surveys Report of Investigation 2012-2 v. 1.1, 51 p., 1 sheet <https://doi.org/10.14509/24484>
- KNOM Radio Mission, 2020, New berm for Shaktoolik, several other projects to be developed with HUD funds, accessed June 27, 2025, <https://web.archive.org/web/20230208064021/https://knom.org/2020/06/18/new-berm-for-shaktoolik-several-other-projects-to-be-developed-with-hud-funds/>.
- Kriebel, D.L., 1994, Swash zone wave characteristics from SUPERTANK, 24th International Conference on Coastal Engineering, Kobe, Japan, p. 2,207–2,221.
- 2019, Review of the USACE report on Shaktoolik water levels: Coastal Analytics, LLC, 17 p.
- Montiel, Fabien, Squire, V.A., Doble, Martin, Thomson, J.M., and Wadhams, Peter, 2018, Attenuation and directional spreading of ocean waves during a storm event in the autumn Beaufort Sea marginal ice zone: *Journal of Geophysical Research: Oceans*, v. 123, no. 8, p. 5,912–5,932. <https://doi.org/10.1029/2018JC013763>
- Moritz, Heidi, White, Kathleen, and Gouldby, Ben, 2016, An updated USACE approach to the evaluation of coastal total water levels for present and future flood risk analysis: United States Army Corps of Engineers, 9 p. <https://doi.org/10.1051/e3sconf/20160701012>
- National Centers for Environmental Information (NCEI), 2013, Storm events database: National Oceanic and Atmospheric Administration, 1 p. <https://www.ncdc.noaa.gov/stormevents/eventdetails.jsp?id=485202>
- 2019a, Storm events database: National Oceanic and Atmospheric Administration, 1 p. <https://www.ncdc.noaa.gov/stormevents/eventdetails.jsp?id=805361>
- 2019b, Storm events database: National Oceanic and Atmospheric Administration, 1 p. <https://www.ncdc.noaa.gov/stormevents/eventdetails.jsp?id=852822>
- 2022, Storm events database: National Oceanic and Atmospheric Administration, 1 p. <https://www.ncdc.noaa.gov/stormevents/eventdetails.jsp?id=1058046>
- 2024, Storm events database: National Oceanic and Atmospheric Administration, 1 p. <https://www.ncdc.noaa.gov/stormevents/eventdetails.jsp?id=1220721>
- National Weather Service (NWS), 2016, High water level terminology, accessed May 8, 2024, <https://www.weather.gov/aprfc/terminology>.
- 2018, Coastal flood categories: National Weather Service Eastern Region supplement 01-2018, 9 p. https://www.weather.gov/media/directives/010_pdfs/pd01001003a012018curr.pdf
- 2023, Flood safety: During a flood, accessed May 8, 2024, <https://www.weather.gov/safety/flood-during>.
- Native Village & City of Shaktoolik, and LeMay Engineering & Consulting (Shaktoolik and LeMay), 2015, City of Shaktoolik/Shaktoolik Tribal Council, Alaska—Multi-Jurisdictional Hazard Mitigation Plan: Federal Emergency Management Agency, 122 p.
- Office of Coastal Management (OCM) Partners, 2024, 2021 USACE NCMP topobathy lidar DEM: Alaska <https://www.fisheries.noaa.gov/inport/item/73829/>
- Overbeck, J.R., 2017, Storm water level feature extraction from digital elevation models using intra-storm photographs: Alaska Division of Geological & Geophysical Surveys Report of Investigation 2017-6, 10 p. <https://doi.org/10.14509/29730>
- Overbeck, J.R., Buzard, R.M., Turner, M.M., Miller, K.Y., and Glenn, R.J.T., 2020, Shoreline change at Alaska coastal communities: Alaska Division of Geological & Geophysical Surveys Report of Investigation 2020-10, 35 p., 43 sheets <https://doi.org/10.14509/30552>
- Overbeck, J.R., Hendricks, M.D., and Kinsman, N.E.M., 2016, Photogrammetric digital surface models and orthoimagery for 26 coastal communities of western Alaska: Alaska Division of Geological & Geophysical Surveys Raw Data File 2016-1, 3 p. <https://doi.org/10.14509/29548>

- Rosales, Jon, Cady, Carol, Juday, Glenn, Alix, Claire, Morimoto, Miho, Chapman, Jessica, Casserly, Dakota, and Katchatag, Sophia, 2021, Storm surge proxies in a data-poor landscape: a practical monitoring method for under-surveyed and -studied communities vulnerable to climate change: *Climate Change*, vol. 164, no. 22, 17 p. <https://doi.org/10.1007/s10584-021-02995-4>
- Sallenger, A.H., Jr., 1983, Measurements of debris-line elevations and beach profiles following a major storm: northern Bering Sea coast of Alaska: United States Geological Survey Open-File Report 83-394, 12 p. <https://pubs.usgs.gov/of/1983/0394/report.pdf>
- United States Army Corps of Engineers (USACE), 1972, Shaktoolik flood data—Shaktoolik (new townsite): U.S. Army Corps of Engineers Alaska District, 3 p.
- 2011, Shaktoolik coastal flooding analysis, 73 p.
- 2024, Wave information study data portal: U.S. Army Corps of Engineers Research and Development Center, Coastal & Hydraulics Laboratory. <https://wisportal.erdc.dren.mil/>
- United States Government Accountability Office (GAO), 2009, Report to congressional requestors—Alaska Native villages, limited progress has been made on relocating villages threatened by flooding and erosion: U.S. General Accountability Office Report GAO-040895T, 53 p.

APPENDIX A: SHAKTOOLIK, ALASKA, FIRST-FLOOR HEIGHTS

Betts, Tanner

From: opus <opus@ngs.noaa.gov>
Sent: Tuesday, August 30, 2022 8:19 AM
To: Betts, Tanner
Subject: OPUS solution : log0729b.tps OP1661876273419

[External Email]

FILE: log0729b.tps OP1661876273419

NGS OPUS SOLUTION REPORT =====

All computed coordinate accuracies are listed as peak-to-peak values.
 For additional information: <https://www.ngs.noaa.gov/OPUS/about.jsp#accuracy>

USER: tbetts@bristol-companies.com DATE: August 30, 2022
 RINEX FILE: log0210b.22o TIME: 16:18:37 UTC

SOFTWARE: page5 2008.25
<https://linkprotect.cudasvc.com/url?a=https%3a%2f%2fmaster295.pl&c=E,1,ZLcPjxLnPnnADbCgXJ8iZW2Bd6Sfn4Q1Kd4kXzKkZe-4m1qVTE0cdRkt959nWG7U5PxViCcAWUcjellx561u2o77btbb67eMBe3IABhZiq91iD5toiEcsj8,&typo=1> 160321
 START: 2022/07/29 01:41:00
 EPHEMERIS: igs22205.eph [precise] STOP: 2022/07/29 10:31:30
 NAV FILE: brdc2100.22n OBS USED: 26510 / 26856 : 99%
 ANT NAME: TPSGR5 NONE # FIXED AMB: 93 / 94 : 99%
 ARP HEIGHT: 1.356 OVERALL RMS: 0.016(m)

REF FRAME: NAD_83(2011)(EPOCH:2010.0000) ITRF2014 (EPOCH:2022.5733)

X:	-2620057.493(m)	0.008(m)	-2620058.710(m)	0.008(m)
Y:	-891880.907(m)	0.003(m)	-891879.911(m)	0.003(m)
Z:	5727093.854(m)	0.010(m)	5727094.153(m)	0.010(m)

LAT:	64 21 27.54709	0.008(m)	64 21 27.52708	0.008(m)
E LON:	198 47 55.80802	0.004(m)	198 47 55.70851	0.004(m)
W LON:	161 12 4.19198	0.004(m)	161 12 4.29149	0.004(m)
EL HGT:	13.921(m)	0.011(m)	14.550(m)	0.011(m)
ORTHO HGT:	6.666(m)	0.354(m)	[NAVD88 (Computed using GEOID12B)]	

UTM COORDINATES STATE PLANE COORDINATES

UTM (Zone 04) SPC (5007 AK 7)

Northing (Y) [meters]	7138709.863	1153936.259
Easting (X) [meters]	393730.885	538583.383
Convergence [degrees]	-1.98456111	0.72016944

Point Scale 0.99973828 0.99991822
 Combined Factor 0.99973610 0.99991604

US NATIONAL GRID DESIGNATOR: 4WCS9373138710(NAD 83)

BASE STATIONS USED

PID	DESIGNATION	LATITUDE	LONGITUDE	DISTANCE(m)
DL7647 AC31	BALD_HEAD_AK2006	CORS ARP	N643816.725 W1621420.758	58864.2
DL6684 AC07	BUCKLAND__AK2007	CORS ARP	N655740.665 W1611711.716	178839.9
DL6423 AB11	NOME_ANVILAK2006	CORS ARP	N643352.198 W1652224.358	202065.7

NEAREST NGS PUBLISHED CONTROL POINT

UW3681 SHAKTOLIK N642158.304 W1611312.624 1322.9

This position and the above vector components were computed without any knowledge by the National Geodetic Survey regarding the equipment or field operating procedures used.

Betts, Tanner

From: opus <opus@ngs.noaa.gov>
Sent: Tuesday, August 30, 2022 9:02 AM
To: Betts, Tanner
Subject: OPUS solution : log0729q.tps OP1661878837183

[External Email]

FILE: log0729q.tps OP1661878837183

NGS OPUS SOLUTION REPORT
 =====

All computed coordinate accuracies are listed as peak-to-peak values.
 For additional information: <https://www.ngs.noaa.gov/OPUS/about.jsp#accuracy>

USER: tbetts@bristol-companies.com DATE: August 30, 2022
 RINEX FILE: log0210q.22o TIME: 17:01:29 UTC

SOFTWARE: page5 2008.25
https://linkprotect.cudasvc.com/url?a=https%3a%2f%2fmaster252.pl&c=E,1,_qCk4sZso7TQvCy3u3ON_VZ8hOqTThH3B2yUQaosxWRVUnnw8V422iP9OTfacfZ6dgDanopZJENoFbi_6zkZiLBCqvjjm6afjsPXPXXPHBd4pM1Z_jgQ6YSqNvO9&typo=1
 160321 START: 2022/07/29 16:23:00
 EPHEMERIS: igs22205.eph [precise] STOP: 2022/07/29 23:27:00
 NAV FILE: brdc2100.22n OBS USED: 21624 / 21761 : 99%
 ANT NAME: TPSGR5 NONE # FIXED AMB: 76 / 76 : 100%
 ARP HEIGHT: 1.356 OVERALL RMS: 0.018(m)

REF FRAME: NAD_83(2011)(EPOCH:2010.0000) ITRF2014 (EPOCH:2022.5749)

X: -2620057.488(m) 0.012(m)	-2620058.705(m) 0.012(m)
Y: -891880.916(m) 0.010(m)	-891879.920(m) 0.010(m)
Z: 5727093.864(m) 0.006(m)	5727094.163(m) 0.006(m)

LAT: 64 21 27.54727 0.009(m)	64 21 27.52726 0.009(m)
E LON: 198 47 55.80877 0.014(m)	198 47 55.70927 0.014(m)
W LON: 161 12 4.19123 0.014(m)	161 12 4.29073 0.014(m)
EL HGT: 13.929(m) 0.004(m)	14.559(m) 0.004(m)
ORTHO HGT: 6.674(m) 0.354(m) [NAVD88 (Computed using GEOID12B)]	

UTM COORDINATES STATE PLANE COORDINATES

UTM (Zone 04) SPC (5007 AK 7)

Northing (Y) [meters]	7138709.868	1153936.265
Easting (X) [meters]	393730.896	538583.393
Convergence [degrees]	-1.98456111	0.72016944

Point Scale 0.99973828 0.99991822
 Combined Factor 0.99973610 0.99991604

US NATIONAL GRID DESIGNATOR: 4WCS9373138710(NAD 83)

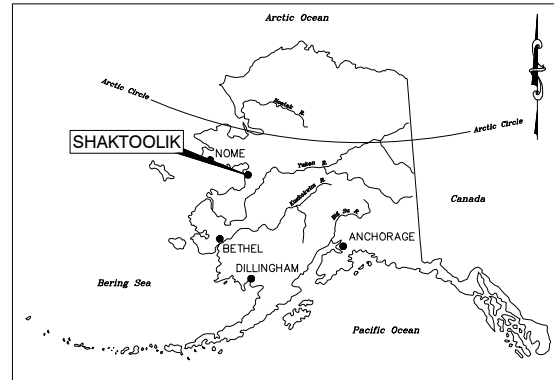
BASE STATIONS USED

PID	DESIGNATION	LATITUDE	LONGITUDE	DISTANCE(m)
DL6429 AB17	UNALAKLEETAK2008 CORS ARP	N635310.903	W1604140.939	58044.4
DR5468 AT01	STMICHAEL_AK2018 CORS ARP	N632902.580	W1620022.950	105093.0
DL6423 AB11	NOME_ANVILAK2006 CORS ARP	N643352.198	W1652224.358	202065.7

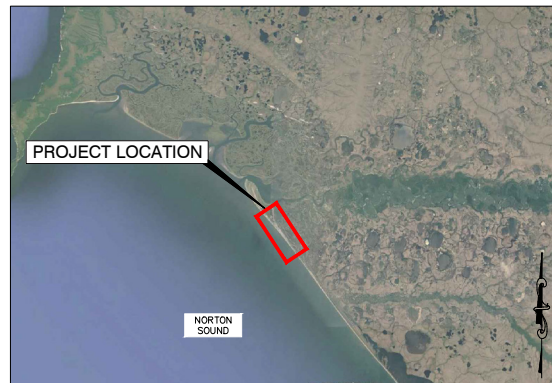
NEAREST NGS PUBLISHED CONTROL POINT

UW3681	SHAKTOLIK	N642158.304	W1611312.624	1322.9
--------	-----------	-------------	--------------	--------

This position and the above vector components were computed without any knowledge by the National Geodetic Survey regarding the equipment or field operating procedures used.



LOCATION MAP
NTS



VICINITY MAP
NTS
IMAGE SOURCE: GOOGLE EARTH 2016

SHAKTOOLIK COMMUNITY FINISHED FLOOR ELEVATIONS

BRISTOL PROJECT NO. 32210041

LEGEND	
	EXISTING
EDGE OF WATER	----
MEAN HIGH WATER	-----
OVERHEAD TELEPHONE	---o---
WATER LINE	---W---
PROPERTY LINE	---P---
BUILDING/STRUCTURE	---B---
PROPERTY LINES	---X---
FENCE	---F---
GROUND CONTOUR (MAJOR)	---20---
GROUND CONTOUR (MINOR)	---10---

INDEX OF SHEETS	
SHEET NO.	TITLE
FIG 1	TITLE SHEET
FIG 2	FINISHED FLOOR ELEVATIONS TABULAR
FIG 3	KEY MAP
FIG 4	FINISHED FLOOR ELEVATIONS PLAN VIEW
FIG 5	FINISHED FLOOR ELEVATIONS PLAN VIEW
FIG 6	FINISHED FLOOR ELEVATIONS PLAN VIEW

NOTES:

- IN JULY 2022 BRISTOL INFRASTRUCTURE DESIGN SERVICES COLLECTED FINISH FLOOR ELEVATION DATA FOR 106 STRUCTURES IN SHAKTOOLIK. HORIZONTAL DATUM: NAD 83 STATE PLANE ZONE 7 VERTICAL DATUM: NAVD 88 GEOID 12B
- LOT AND BLOCK NUMBER AND GENERAL DESCRIPTION WERE RECORDED FOR EACH BUILDING SURVEYED.
- LINEWORK FOR STRUCTURES, LOT LINES, AND TOPOGRAPHY WERE GENERATED USING THE 2004 PUBLIC DCRA COMMUNITY PROFILE MAPS.
- SATELLITE IMAGERY WAS TAKEN IN SEPTEMBER 2022 AFTER TYPHON MERBOK HIT THE WEST COAST OF ALASKA. IMAGERY WAS COLLECTED TO AID IN RESPONSE AND RECOVERY EFFORTS BY STATE, FEDERAL, AND UNIVERSITY PARTNERS WITH HELICOPTERS, UAS, FIXED WING PLANES AND SATELLITES. IMAGERY WAS RECEIVED FROM THE ALASKA DIVISION OF GEOLOGICAL & GEOPHYSICAL SURVEYS (DGGS).

User: TMARTIN Jan 20, 2023 - 11:34am
Drawing: C:\Users\TMARTIN\OneDrive - BRISTOL INDUSTRIES, LLC\32210041 SHK TOI2 HUD CAISO DESIGN FF SURVEY 2022\A040\32170001_A1-42.DWG - Layout: A1
Path: C:\Users\TMARTIN\OneDrive - BRISTOL INDUSTRIES, LLC\32210041 SHK TOI2 HUD CAISO DESIGN FF SURVEY 2022\A040\32170001_A1-42.DWG - Images: SHK A040\32170001_A1-42.DWG

REVISIONS					
NO.	DATE	BY	DESCRIPTION	NO.	DATE

Bristol
ENGINEERING
SERVICES COMPANY, LLC
111 W. 10th Avenue, Third Floor
Anchorage, AK 99501
Phone (907) 955-2013 Fax (907) 955-4713
License Number: AE00287

NATIVE VILLAGE OF SHAKTOOLIK
P.O. BOX 100
SHAKTOOLIK, ALASKA 99771
Phone (907) 955-3701
Fax (907) 955-2352

SHAKTOOLIK, ALASKA				SHEET NO.	
TITLE SHEET				Figure A1	
SCALE: SHOWN	DESIGNED: --	CHECKED: IPP	DRAWN: T.M.	DATE: JAN 2023	SHEET 1 OF 6

User: TMARTIN Jan 20, 2023 - 11:34am
Drawing: C:\USERS\TMARTIN\ONE DRIVE - BRISTOL INDUSTRIES, LLC\222 0041 - SHK TO 2 HUD CA 50 DESIGN FF SURVEY 2022\A040\32170001_A1-42.DWG - Layout: A2
Path: C:\USERS\TMARTIN\ONE DRIVE - BRISTOL INDUSTRIES, LLC\222 0041 - SHK TO 2 HUD CA 50 DESIGN FF SURVEY 2022\A040\32170001_A1-42.DWG - Images: SHK TO 2 HUD CA 50 DESIGN FF SURVEY 2022\A040\32170001_A1-42.DWG

No.	Lot/Block	Description	Finish Floor Elevation
1	Shaktoolik Clinic Site	TRD Clinic	31.83
2	Shaktoolik Clinic Site	TRD CLINIC GARAGE	25.98
3	L1B1	Green House, Brown Roof	25.05
4	L4B1	Turquoise	26.85
5	L2B1	Purple House	24.93
6	L6B1	VPSO, White, Brown Roof	27.32
7	L1B2	Blue House	25.23
8	L7B1	Tan House	27.3
9	L3B2	Purple House, Tin Roof	25.53
10	L3B1	Abandoned	22.58
11	L9B1	Tan, Blue Roof	27.63
12	L6B2	Orange House, Tin Roof	25.47
13	L5B1	Abandoned	25.22
14	L2B2		25.81
15	L5B2	Abandoned/plywood Tin roof	26.02
16	L9B2	Red Barn	25.35
17	L6B3	Green	26.43
18	L4B2	Tan House, Red Roof	25.38
19	L7B2	Blue House, Tin Roof	24.42
20	L2B3	Blue House, Tin Roof	25.85
21	L1B3	Grey, Tin Roof	24.34
22	L5B3	Purple Grey	27.28
23	L3B3	Blue, Tin Roof	23.88
24	L4B3	Green House, Tin Roof	25.84
25	L7B3	Red House	27.7
26	L2B4	Green, Tin Roof	25.91
27	L4B4	Turquoise	25.26
28	L1B4	Blue House, Tin roof	27.84
29	L3B4	Purple, Tin Roof	25.08
30	L7B4	Red Brown	27.11
31	L1B5	Blue	23.69
32	L5B4		25.13
33	L9B4		28.49
34	L6B5		28
35	L3B5		24.75
36	L1B6		24.48
37	L2B5		25.26
38	L4B5		25.11
39	L2B5	Red Garage	24.57
40	L5B5	Pink	26.4
41	L2B6		24.37
42	Tract H		25.99
43	L6B4		29.79
44	Parcel A	School	27.71
45	Parcel A	Truck Shop/ Blue	25.36
46	Parcel A	Principle home/ Blue	26.41
47	Parcel A	School Duplex/Yellow Red Roof	28.06
48	L3C B6	Postoffice	25.08
49	L3B B6	Old Clinic/ VPSO	25.44
50	L3B B6	VPSO Arctic Entry	25.52
51	L3A B6	IRA BUILDING Green	25.58
52	L3A B6	IRA BUILDING YELLOW	24.86
53	Parcel A	Washeteria	25.3

No.	Lot/Block	Description	Finish Floor Elevation
54	Parcel A	School Triplex	27.29
55	Parcel A	Water Tank	23.84
56	L6B6	Grey House, Brown Roof	25.2
57	L4A-1 B6	Shaktoolik Native Store	25.36
58	L5B B6	Old Clinic	28.68
59	L1B7	Blue House, Grey Roof	26.14
60	L5A B6	Fuel Tanks	26.4
61	L5A B6	Purple	25.66
62	L3D2 B6	Duplex	26.32
63	Parcel A	Garage Yellow Building	25.31
64	L3B7	Grey House, Tin Roof	23.89
65	L4B7	Sophia, Green House, Tin Roof	26.68
66	-	NOT USED	-
67	L2B7	Yellow House, Red	26.66
68	L5B7	Grey, Blue Roof	26.63
69	L6B7	Tan, Green Roof	28.17
70	L1B8	Blue House, Tin Roof	23.87
71	L3B8	Yellow, Tin Roof	24.49
72	L2B8	Brown House, Tin Roof	26.7
73	L4B8	Green House, Tin Roof	26.12
74	L6B8	Tan, Red Roof	27.97
75	L5B8	Tan, Red Roof	25.91
76	L1B9	Purple House, Tin Roof	23.83
77	L2B9	Light Blue House, Tin Roof	26.88
78	L3B9	Light Blue House, Tin Roof, Church	23.94
79	L4B9	Light Blue house, Tin Roof	26.8
80	L6B9	Tan House, Green Roof	27.75
81	L2B10	Orange House, Tin Roof	26.33
82	L5B9	Tan, Brown Roof	25.45
83	L1B10	Tan House, Tin Roof	24.32
84	L4B10	Purple House, Tin Roof	26.43
85	L3B10	Blue House, Red Roof	23.57
86	L5B10	Yellow House, Brown Roof	25.86
87	L2B11	Grey Building/Avec Tanks	28.97
88	L3B11	Blue House, Tin Roof	24.47
89	L5B11	Green, Tin Roof	23.52
90	L2B12	Army National Guard	28.61
91	L4B12	Pink, Red House	27.9
92	L6B12	Tan House, Green Roof	27.84
93	L3B12	Turquoise, Tin Roof	24.64
94	L2B13	Red House, Red Roof	26.75
95	L5B12	Tan House, Brown Roof	26.57
96	L1B13	Tan House, Green Roof	25.53
97	L3B13	Tan House, Blue Roof	28
98	L1B14	Blue House, Brown Roof	25.56
99	L3B14		25.39
100	L2B14	Purple House, Grey Roof	27.29
101	L4B13	Grey House, Blue Roof	30.49
102	TBM15		26.21
103	L4B14	Shaktoolik Native Store	25.6
104	Tract Q1	Fuel Storage	25.59
105	Tract O	GCI TOWER	25.31
106	Tract Q1	Gas pump	26.1

REVISIONS					
NO.	DATE	BY	DESCRIPTION	NO.	DATE

Project No. 3220033

Bristol

ENGINEERING SERVICES COMPANY, LLC

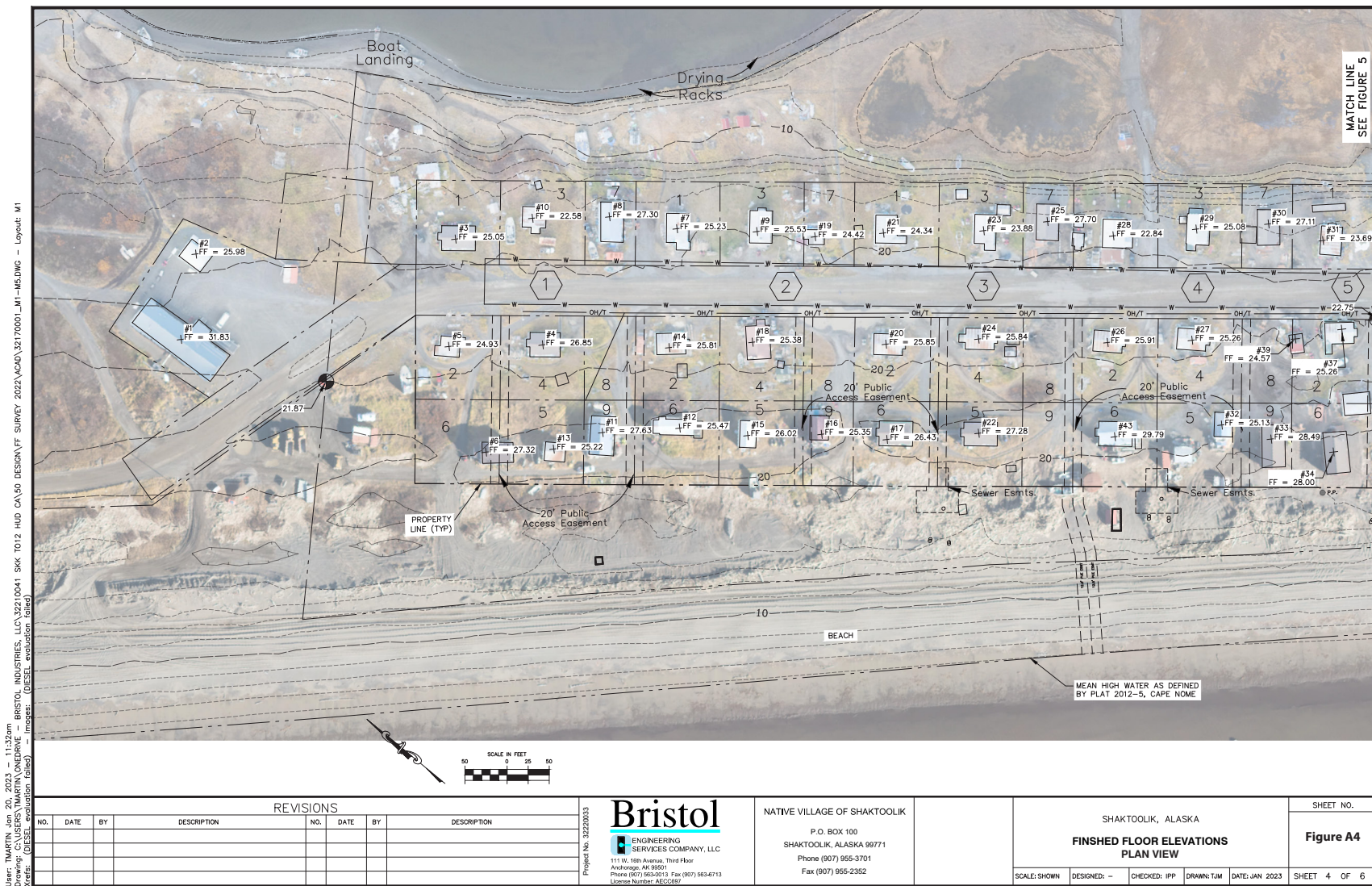
111 W. 18th Avenue, Third Floor
Anchorage, AK 99501
Phone (907) 955-2013 Fax (907) 953-4713
License Number: AEUCB97

NATIVE VILLAGE OF SHAKTOOLIK

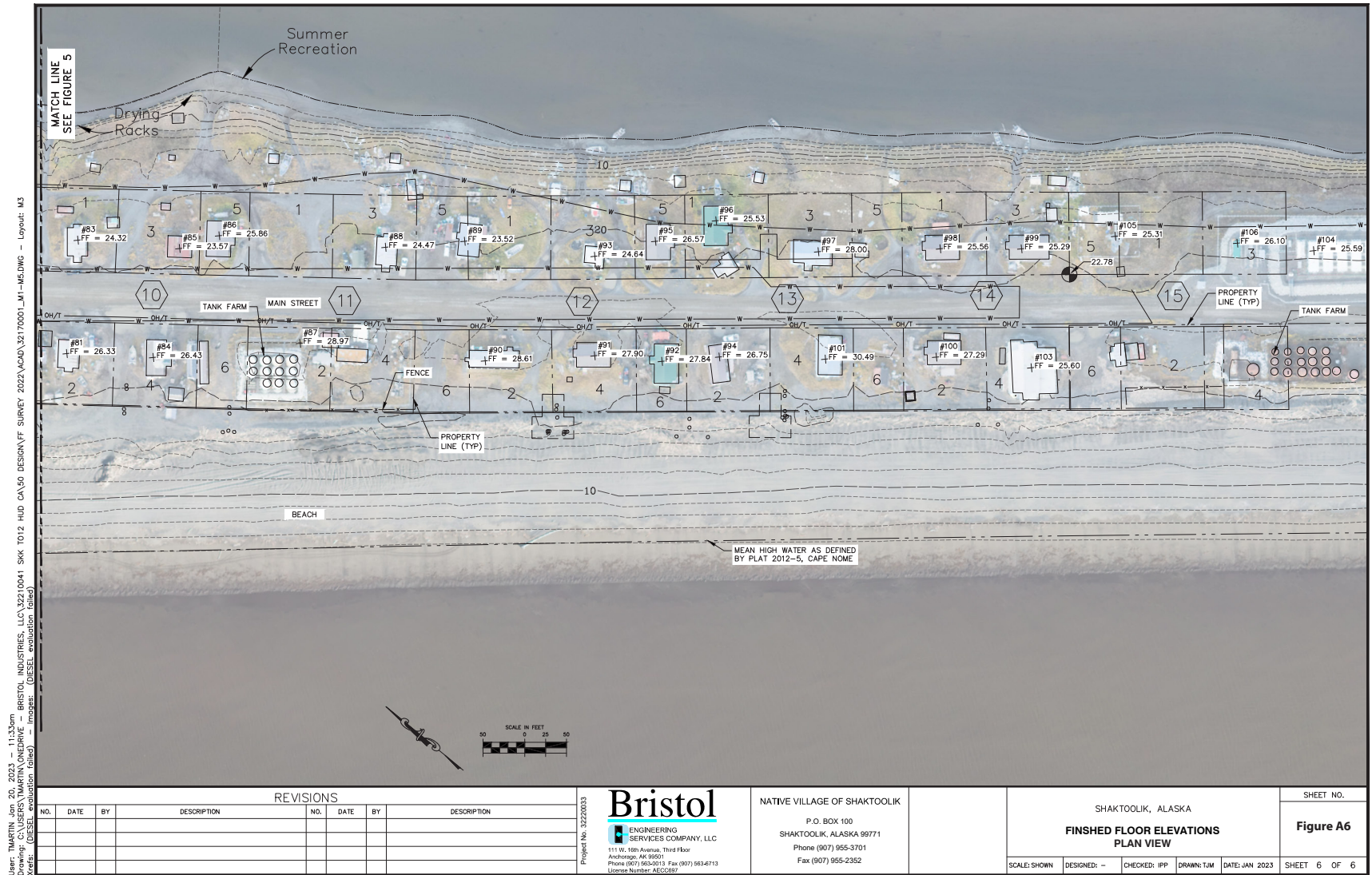
P.O. BOX 100
SHAKTOOLIK, ALASKA 99771
Phone (907) 955-3701
Fax (907) 955-2352

SHAKTOOLIK, ALASKA					SHEET NO.
FINISHED FLOOR ELEVATIONS TABULAR					Figure A2
SCALE: SHOWN	DESIGNED: --	CHECKED: JPP	DRAWN: TJM	DATE: JAN 2023	SHEET 2 OF 6









User: TMARTIN Jan 20, 2023 - 11:33am
Drawing: C:\USERS\TMARTIN\ONE DRIVE - BRISTOL INDUSTRIES, LLC\322 0041 SKK TO 12 HUD CA\50 DESIGN\FF SURVEY 2023\A04\3270001_M1-M5.DWG - Layout: M3
Notes: (CHECK ELEVATION) - (CHECK ELEVATION) - (CHECK ELEVATION)

APPENDIX B: RE-ANALYSIS OF PREVIOUS FLOOD HISTORY STUDIES FOR SHAKTOOLIK, ALASKA

ASSESSMENT OF PREVIOUS STUDIES

A Climate Change Vulnerability and Risk Assessment, published in 2020 by Golder Associates Ltd., details a flood history for Shaktoolik from 1960 to 2019. These values were reportedly obtained from various sources, including a coastal flooding analysis (USACE, 2011), which was an update to a previous study (Chapman and others, 2009), as well as a 2020 data request to DGGS that was largely based on the 2011 USACE report. A review of the USACE analysis was conducted by Coastal Analytics, LLC (Kriebel, 2019) that identified several inconsistencies and potential flaws in the results presented by USACE (2011). The USACE (2011) report describes “storm water level” as the combination of “astronomical tide,... storm surge,... and wave setup...” but Kriebel (2019) notes the USACE (2011) “schematic illustration of wave effects” figure does not include wave setup as a component of “storm water level,” instead including it as a component of “wave runup elevation,” though Kriebel (2019) indicates that USACE (2011) “dramatically overstates the wave setup” in their calculations.

Additionally, Kriebel (2019) points out that a value of 1.97 ft (0.60 m) was added to the surge estimates provided by USACE (2011) to adjust these results from “MTL to MLLW,” despite USACE (2011) reporting that they applied “a preliminary [datum] adjustment of 1.95 ft.” The NOAA CO-OPS Bench Mark Sheet for tide station 946 8691, lists publication date for the local tidal datums at Shaktoolik as January 6, 2011, so it can be reasonably assumed that the datum conversions USACE (2011) used during their study were not based on the finalized datums provided by NOAA, and in fact, USACE (2011) states “the original [empirical simulation technique

(EST)] estimates... used the tide range at Unalakleet (2.20 ft) to adjust the MTL simulation results to MLLW, whereas the more recent estimates used tide measurements at Shaktoolik...” To find the “peak water elevation,” which USACE (2011) defines as “...the peak combined storm surge and mean high tide water level estimate” for each of the top 10 events, Kriebel (2019) found these estimates “are based on the further assumption that all storms occur at a high tide of +1.89 ft.” From tide station 946 8691, this value would appear to align with the MHHW datum conversion from MTL, which would indicate that USACE (2011) may have misidentified from which datum they were deriving their assumed high tide value.

There is potential ambiguity in the USACE (2011) report and the study it updates (Chapman and others, 2009) regarding the datums applied to simulations, results, and estimates. Chapman and others (2009) never explicitly state in which vertical datum their simulations were performed, though as noted previously, the indication that maximum surge estimates were converted from MTL to MLLW before the EST performed during return period analysis implies that MTL was likely the vertical basis for these simulations, as Kriebel (2019) asserts. Both USACE (2011) and Chapman and others (2009) provide input and output data in a variety of datums and units throughout their reports, including in MSL, MTL, and local station datum in meters; MLLW in feet; and MSL in feet in the case of significant wave heights collected from USACE’s Wave Information Studies (WIS) database and the maximum surge heights listed for the “[t]op 10 surge events between 1954 and 2004” for Shaktoolik, though out of the 17 locations investigated, this datum only appears to be used for Shaktoolik and only to report maximum surge heights. These maximum surge values match the metric values found in the full 56 simulated

events provided by USACE (2011) in a table without a datum label and a graph where they are plotted against a vertical axis labeled “Water Level (m above MTL).”

Both USACE (2011) and Kriebel (2019), while not explicitly stating their assumptions, appear to hold the maximum surge values to be in the MTL datum, the latter providing some insight by positing that the simulations were “run without tides using a fixed initial water level corresponding to mid tide.” To test this assumption, we compared the Shaktoolik surge events to those of the nearest community, Unalakleet, using the datum conversion values associated with NOAA CO-OPS tide station 946 8333 (available from tidesandcurrents.noaa.gov/stationhome.html?id=9468333) as indicated by USACE (2011). We found the results for these two locations to be within a maximum agreement of ± 0.5 ft (0.15 m) when converting from MSL to MLLW and ± 0.6 ft (0.19 m) when converting from MTL to MLLW. While this simple check provides some confidence that the datum used to report the maximum surge results for Shaktoolik in Chapman and others (2009) was likely purposefully, if inexplicably, inconsistent with the selection of the MLLW datum used for all other results in that study, it ultimately does not clarify whether the reported datum should have been MSL or MTL. Due to this ambiguity, we have decided to assume these data were provided in the MTL datum but will include the difference between MSL and MTL at tide station 946 8333, ± 0.1 ft (0.04 m), as a component of uncertainty for our estimates.

Finally, during their runup analysis, USACE (2011) provides “peak wave height” values for the top 10 events, defined as “the average of the highest one percent of waves,” which they “found to best match the ‘on the ground’ accounts of each storm” based on HWM evidence provided by residents of the community. For clarity, USACE (2011) points out, “[m]aximum runup elevations indicate waves pushing debris up the beach slope and receding, not standing water at the location.” Golder (2020)

states their flood history consists of “the estimated Still Water Level (SWL) for each flood event, which is the water level reached by a coastal flood event before wave effects are considered,” yet of the nine events estimated by Golder (2020) that appear in the USACE (2011) report, six are an exact match with, and two fall within ± 0.6 ft (0.19 m) of the “peak wave height” values provided by USACE (2011). This is perhaps by coincidence, as Golder (2020) describes a different methodology for producing their estimates from that used by USACE (2011), though both reports apply to each estimate an assumed coincident tide height equal to the local MHHW offset from their preferred datum.

ESTIMATION METHODS

In order to more accurately estimate and better account for uncertainty in the potential flood events identified by Chapman and others (2009) and USACE (2011), DGGS conducted our own modeling effort, taking into account the predictable tides, modeled wave information, and real-world sea ice data available for the time periods during which these events occurred according to the list provided by USACE (2011).

In an appendix, USACE (2011) provided the start dates for, duration of, and maximum storm surge heights (presumably in the MTL datum) for 56 events between 1960 and 2009 that were simulated using the ADvanced CIRCulation (ADCIRC) model, though it should be noted that one of these events was listed with a start date month of “0” and the February 4, 2006 event appears in the list three times with different maximum surge heights. Using this list of now 53 events as our starting point, DGGS gathered additional data from several sources, including the USACE WIS for wave height and wave period hindcasts from July 18, 1986 to November 14, 2009 (USACE, 2024), NOAA CO-OPS for tide predictions from September 21, 1960 to December 11, 2009, NSIDC for sea ice concentration data from October 30, 1978 to December 11, 2009 (Fetterer and others, 2024), as well as nautical charts (NOAA, 2004) and the

2021 topographic-bathymetric digital elevation model (TBDEM; Office of Coastal Management [OCM] Partners, 2024) for on- and off-shore elevation data. Additionally, USACE (2011) provided wave heights for several pre-1985 events, listing the 11 highest wave heights corresponding to their list of events between 1960 and 2009, allowing us to establish a limited wave height range between 0.0 and 8.5 ft (2.58 m) for events during this period with wave height data appearing in neither the USACE (2011) report, nor the WIS (USACE, 2024) database.

Wave Information

As previously noted, USACE (2011) listed the 11 highest wave heights occurring during their study period, including several pre-1985 events that do not appear in the WIS database (USACE, 2024). This not only provided us with wave heights for the listed events, but it also allowed us to set a value and range for missing wave data at a wave height of 4.2 ± 4.2 ft (1.29 ± 1.29 m), though this is a relatively large uncertainty for events with missing wave information. Additionally, all pre-1985 events and any, more recent event lacking wave data, would also lack information about the wave period. Under this limited input constraint, the wave height provided by USACE (2011), or the missing data constant wave height was applied at all timesteps for the duration of the event time-frame, essentially acting as a continuous vertical offset to the calculated water height derived from other inputs.

For post-1985 events that have both wave height and period data, it is possible, in conjunction with water depths along a transect from the wave buoy to the shore, to calculate the celerity of these wave and thus the timing of their arrival at the shore, with the caveat that we simplified our approach by assuming a constant wave direction perpendicular to the shore. To perform this calculation, we applied the celerity equations described by Sorensen (2006) along a 29,194.00 m transect composed of depth values extracted at each meter

from a depth surface derived from nautical chart number 16200 (NOAA, 2004) and the 2021 TBDEM. The specific nautical chart used in the creation of our merged surface, the depths of which are listed in fathoms and feet to the nearest foot and are based on a lead-line survey performed in 1900 (NCEI, 2024), was selected because it was the highest resolution chart published within temporal proximity to Chapman and others (2009), wherein they describe applying updates based on recent nautical charts to the ADCIRC grid used in simulating the events listed in USACE (2011). For each wave, and at each meter-interval along our transect, we applied the following celerity equations:

$$L_t = \frac{gT_t^2}{2\pi} \quad (1)$$

$$\frac{d_x}{L_t} \geq 0.50 \quad C_x = \frac{gT_t}{2\pi} \quad (2)$$

$$0.50 > \frac{d_x}{L_t} > 0.05 \quad C_x = \frac{gT_t}{2\pi} \tanh \frac{2\pi d_x}{L_t} \quad (3)$$

$$\frac{d_x}{L_t} \leq 0.05 \quad C_x = \sqrt{gd_x} \quad (4)$$

where L is the deep-water wavelength for the given wave in meters at initial date and time t , g is the acceleration due to gravity constant (9.80665 m/s^2), T is the wave period of the given wave in seconds, d is the depth in meters at distance x in meters along the transect from the point of origin (the buoy), and C is the celerity in m/s. By dividing one by the celerity at each meter-interval we can determine the amount of time in seconds it takes the wave to transition to the next interval and by adding these accumulated times to the initial time we can establish the time at which the given wave will reach the shore.

Additionally, along the exposed shore, according to Kriebel (1994), we should expect to see an increase in water height due to the standing wave component of wave setup. Kriebel (1994), through observation, identified this standing wave height at 15 to 20 percent of the offshore significant wave height, regardless of wave steepness or beach slope. In our analysis this is quantified by retaining

17.5 ± 2.5 percent of the offshore significant wave height as a component of DSWL as described by Moritz and others (2016), though this aspect would not be present on the sheltered, river side of the community, which would represent the SWL. We found it important to estimate both the DSWL and SWL whenever possible because the former could result in increased impacts in areas along the shore that are at or below the water height or where mitigation measures may be lacking.

Tide Predictions

Since the original Chapman and others (2009) and USACE (2011) storm surge simulations were performed without tidal forcing included, previous studies (Chapman and others, 2009; USACE, 2011; Kriebel, 2019; Golder, 2020) assumed the peak surge of all events must coincide with a maximum tide equal to the MHHW offset from their preferred vertical datum, with the exception of Kriebel (2019) who assumed a maximum tide equal to the MHW offset. We feel this is an unnecessary assumption, given that it is possible to predict the tides during any of these events by applying the harmonic constituents published for the Shaktoolik tide station 946 8691, amplitude reduction factor (node f) and equilibrium arguments from their respective tables in the Manual of Harmonic Analysis and Prediction of Tides (Schureman, 2001) or its supplement (Zetler, 1982), to the tide prediction formula (Schureman, 2001):

$$h_t = \sum fA \cos(\omega\Delta t + (V_0 + u) - \kappa) \quad (5)$$

where h is the tide height in meters at universal coordinate time (UTC) date and time t , f is the factor for reducing the mean amplitude A of all constituents to the year of the prediction, ω is the angular speed in degrees per hour of the rate change in the phase of a given constituent, Δt is the time in hours from the beginning of the year of the prediction, $(V_0 + u)$ is the equilibrium argument for the year of the prediction, and κ is the phase lag of the observed tidal constituent relative to the theoretical equilibrium tide. We predicted all tides to a six-minute

interval, with events lacking wave information tied to this interval and events with wave information tied to the six-minute interval nearest to the time at which a wave reached the shore.

Sea Ice Concentration

The presence of sea ice creates a damping effect on wave heights through attenuation (Liu and others, 1991; Kohout and others, 2014; Montiel and others, 2018). While the precise relationship between sea ice concentration and wave height decay has not been fully described, it is generally assumed to be exponential in nature, though both Kohout and others (2014) and Montiel and others (2018) found larger waves (significant wave height > 3.00 m) do not follow this initial assumption. For our analysis we selected the empirical attenuation model presented by Montiel and others (2018) because, while their study was in general agreement with Kohout and other (2014) regarding the linear nature of large wave attenuation, the data used by Montiel and others (2018) were collected in the arctic and included uncertainties for the derived attenuation coefficients. Using the same buoy-to-shore transect used in our wave celerity calculation, from Montiel and other (2018) we utilized the following attenuation formulas:

$$H = H_s - x(5.74 \times 10^{-6} \pm 5.42 \times 10^{-7}) \quad (6)$$

$$H = H_s e^{-x(4.48 \times 10^{-6} \pm 4.51 \times 10^{-7})} \quad (7)$$

(where H_s is the offshore significant wave height in meters, H is the attenuated wave height at the shore in meters, and x is the distance in meters along the transect from the point of origin (the buoy).

Sea ice concentration data are available for the northern polar region as raster datasets from NSIDC, covering every other day beginning in October 1978 and every day beginning in August 1987 at a resolution of roughly 25 km² (Fetterer, 2017) and averaged monthly spanning back to the year 1850 at a 1/4-degree resolution (Walsh and others, 2019). The coarse spatial and temporal resolution of the pre-1978 sea ice data, as well as poor

precision, precluded us from including these data in our estimates. From the satellite-derived sea ice data we identified the raster pixel representing the water immediately offshore near Shaktoolik and extracted the concentration value from that pixel for each day during each of the event timeframes provided by USACE (2011) for which there were data available, substituting an average concentration from the day before and after any day that fell within the temporal range of the NSIDC dataset but for which an image was unavailable. We then established three attenuation conditions based on sea ice concentration, applying no attenuation for days with no ice present, applying the Montiel and others (2018) attenuation formulas for days with a concentration greater than zero but less than 90 percent, and assuming full attenuation (i.e., no wave action) for days with 90 percent or greater sea ice concentration.

ANALYSIS OF RESULTS

As a part of our investigation of the USACE (2011) study we performed an analysis of our results (fig. B1) prior to finalizing our findings. Through this process, we identified a potential overestimation for the “pre-1985” events, which indicated an inconsistency in the overall trend seen within these data. While the USACE (2011) storm surge estimates were generally consistent with a Weibull distribution as discussed by Chapman (2009), which should be expected of a wind-related phenomena and thus might not induce concerns regarding the reasonableness of these results, the temporal distribution of these estimates and how they relate to each other must also be considered. With attention to the temporal context of the USACE (2011) results, as is evident in figure 1, it was clearly necessary we better understand the constituent inputs from which Chapman (2009) and USACE (2011) derived their storm surge estimates.

The weather data used by Chapman and others (2009) was compiled from “surface meteorological data, including composite wind, pressure, and ice-concentration fields... generated

by blending point-source meteorological station data into QuicksCAT satellite data and background wind fields from the National Centers for Environmental Prediction—National Center for Atmospheric Research (NCEP-NCAR)” (Erikson and others, 2015). This would only be true of the “continuous climatology records from 1985 to 2004” (Chapman and others, 2009), subsequently extended to 2009 in USACE (2011), but could not be true of the earlier weather data because satellite information would only have become available beginning in 1978 and the WIS (USACE, 2024) data for the Alaska region only dates back to 1985. Thus, it can be inferred that, while the pre-1985 hindcasts were likely derived from the NCEP-NCAR reanalysis and other sources of the highest reliability available at the time, these data could not have been informed or corrected by satellite or other data of comparable quality to those available for the more recent events.

In the absence of the original data used by USACE (2011) for their surge simulations, we looked to the Iowa Environmental Mesonet (IEM) Automated Surface Observation System (ASOS) and Automated Weather Observation System (AWOS) network for historical wind and pressure readings (IEM, 2024), these data likely being among the “point-source meteorological station data” described by Erikson and others (2015). The nearest weather stations to Shaktoolik with sufficient temporal coverage are Unalakleet (PAUN) and Nome (PAOM). For our investigation, we downloaded the available wind speed and atmospheric pressure readings between January 1, 1960, and December 31, 2010, consolidated these by month, and extracted the monthly maximum wind speeds and minimum atmospheric pressures. Based on the USACE (2011) modeled surge results, we would expect to see appreciable differences in the primary contributing factors of storm surge, wind speed and atmospheric pressure, when comparing the pre-1985 and post-1984 data. Though we did see larger variance in the pre-1985 data, we found no significant indicators in the data, the general

range of the data, or the long-term trends of the data (figs. B2–B5) that would reflect the heightened storm surges modeled in the earlier USACE (2011) results.

From Sorensen’s formulas for “simplified analysis of storm surge” (2006), it is clear that, in addition to wind speed and direction, the largest factors contributing to storm surge setup come from depth and distance, the latter of which can be interpreted as fetch length, which is, in part, a function of the duration of sustained, elevated wind speeds. Thus, it is conceivable, despite a lack of noticeable changes in maximum wind speeds, the pre-1985 models might be indicative of an abrupt change in storm durations. To test this theory, using the start and end dates of the storms provided by USACE (2011), we downloaded the recorded wind speeds during each storm event from the Alaska ASOS/AWOS network (IEM, 2024), and calculated for each the total duration during which wind speeds exceeding the USACE (2011) provided 15 meter per second (m/s) storm identification criteria (fig. B6). With the exception of the 1965 storm event, the remaining pre-1985 events were of similar duration as the post-1984 events, again suggesting we should not see any significant difference in the magnitude of the surge estimates regardless of the time period during which they occurred.

As indicated by Chapman (2009), sea ice concentration was taken into account during their study, acting on their modeled wind drag coefficients. In the Chapman (2009) model, sea ice concentration influenced storm surge results

directly and would therefore be separate from and unaffected by the wave damping we calculated for our DSWL estimates. For this reason, as shown in figure 1, we focused on our SWL estimates when comparing the pre-1985 and post-1984 results. Nonetheless, as a contributing factor to the surge model described by Chapman (2009), it was necessary for us to also investigate sea ice trends off the coast of Shaktoolik during both time periods. We first collected ice concentration estimates from the monthly, gridded concentration data provided by Walsh and others (2019), which included the data compiled by Walsh and Johnson (1979) as described by Chapman (2009) and covering the time period 1960 to 1979 (fig. B7). Comparing these data to the satellite-derived sea ice concentration data described in the eponymic section above (fig. B8) strongly suggests the local, offshore ice conditions have not changed to a degree sufficient to account for the heightened pre-1985 results from USACE (2011), despite the significant spatial and temporal resolution, as well as precision, difference between these two datasets.

Taken together, the available weather and sea ice data indicate a level of consistency throughout the entire study period that is in contradiction with the pre-1985 USACE (2011) results. Without the mean or capacity to reconstruct the modeling methods used by Chapman (2009), an endeavor that would be greatly hampered without access to the original input data, we believe it to be most appropriate for us to exclude the pre-1985 estimates from our final flood impact assessment and categorization.

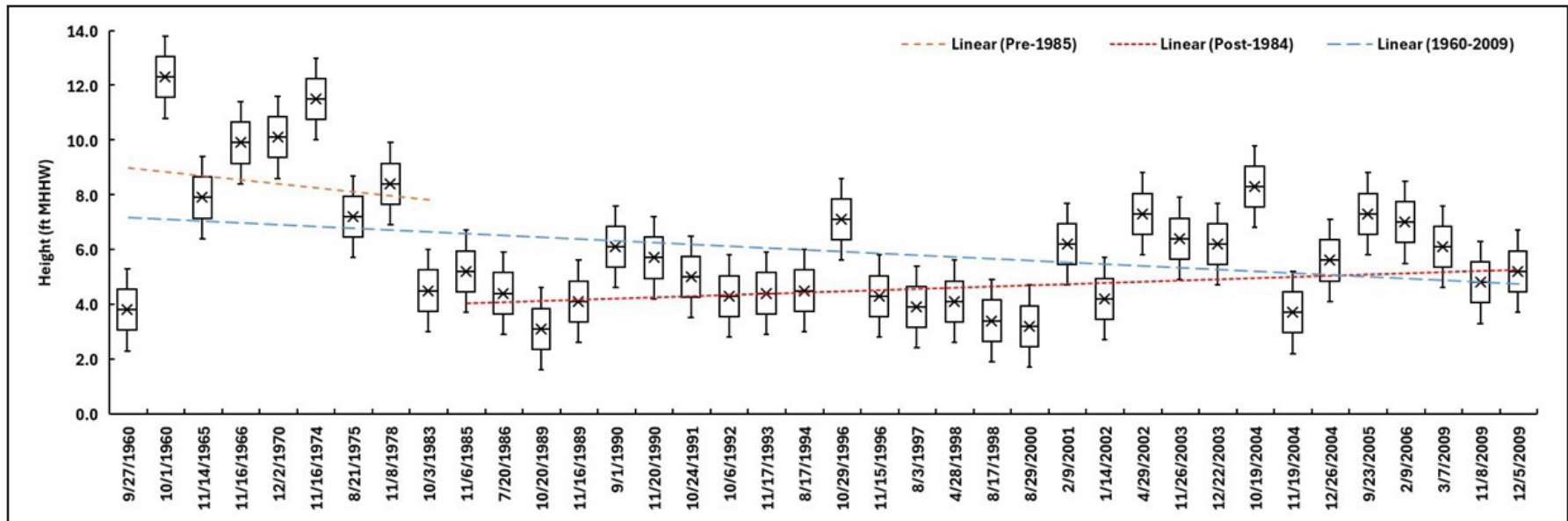


Figure B1. Timeline of estimated SWL flood events and visual representation of flood height estimates and confidences for Shaktoolik, Alaska, based on surge heights modeled by USACE (2011), including linear trend lines for the overall, pre-1985, and post-1984 results.

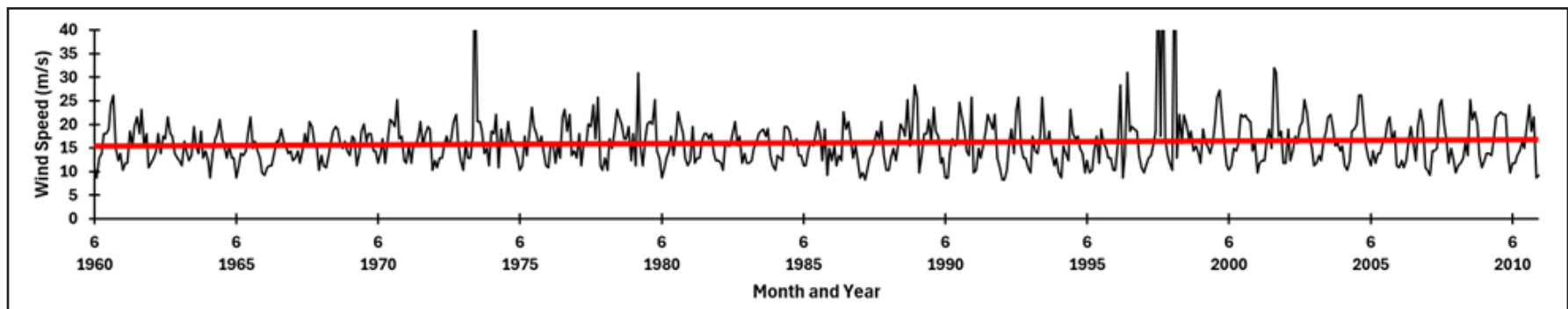


Figure B2. Timeline of monthly maximum wind speeds in Unalakleet, Alaska from 1960 to 2010, compiled from Alaska ASOS/AWOS network station PAUN (IEM, 2024).

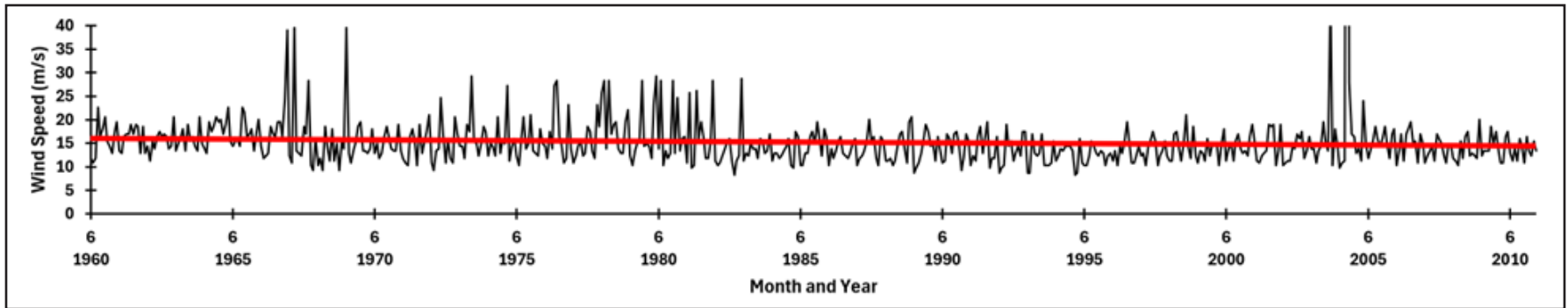


Figure B3. Timeline of monthly maximum wind speeds in Nome, Alaska from 1960 to 2010, compiled from Alaska ASOS/AWOS network station PAOM (IEM, 2024).

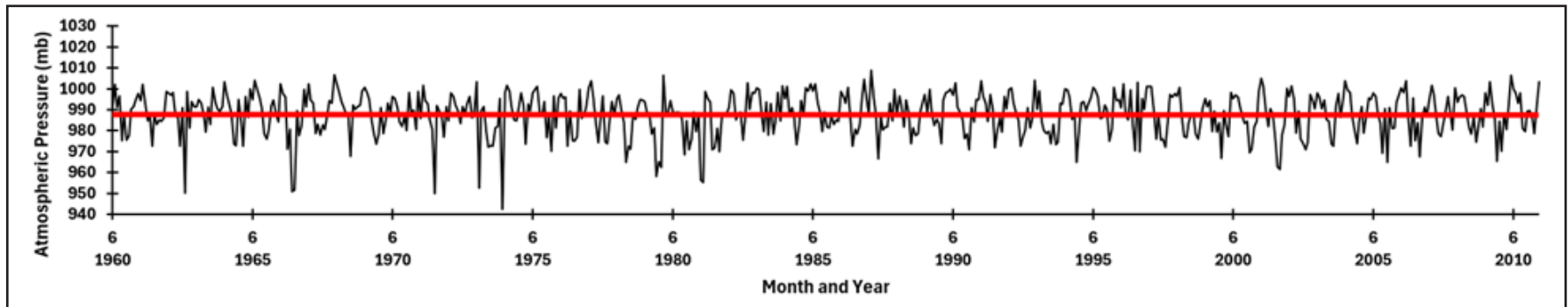


Figure B4. Timeline of monthly minimum atmospheric pressure in Unalakleet, Alaska from 1960 to 2010, compiled from Alaska ASOS/AWOS network station PAUN (IEM, 2024).

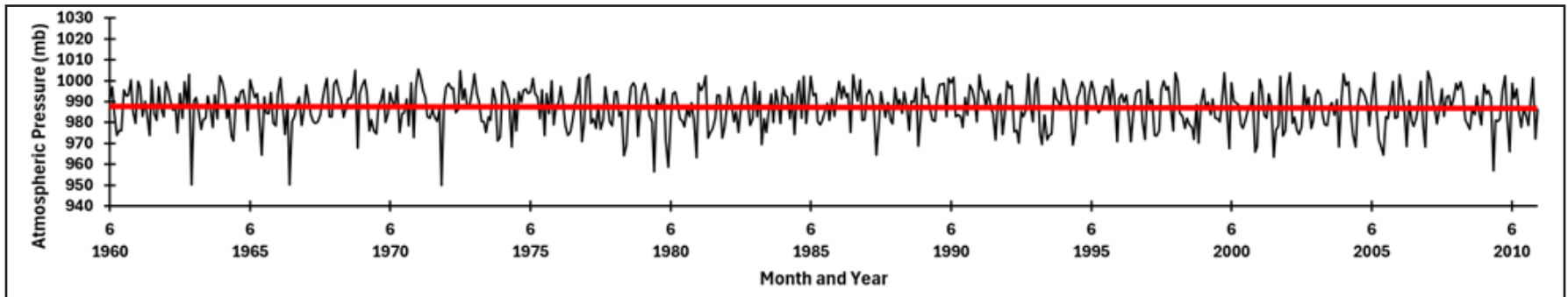


Figure B5. Timeline of monthly minimum atmospheric pressure in Nome, Alaska from 1960 to 2010, compiled from Alaska ASOS/AWOS network station PAOM (IEM, 2024).

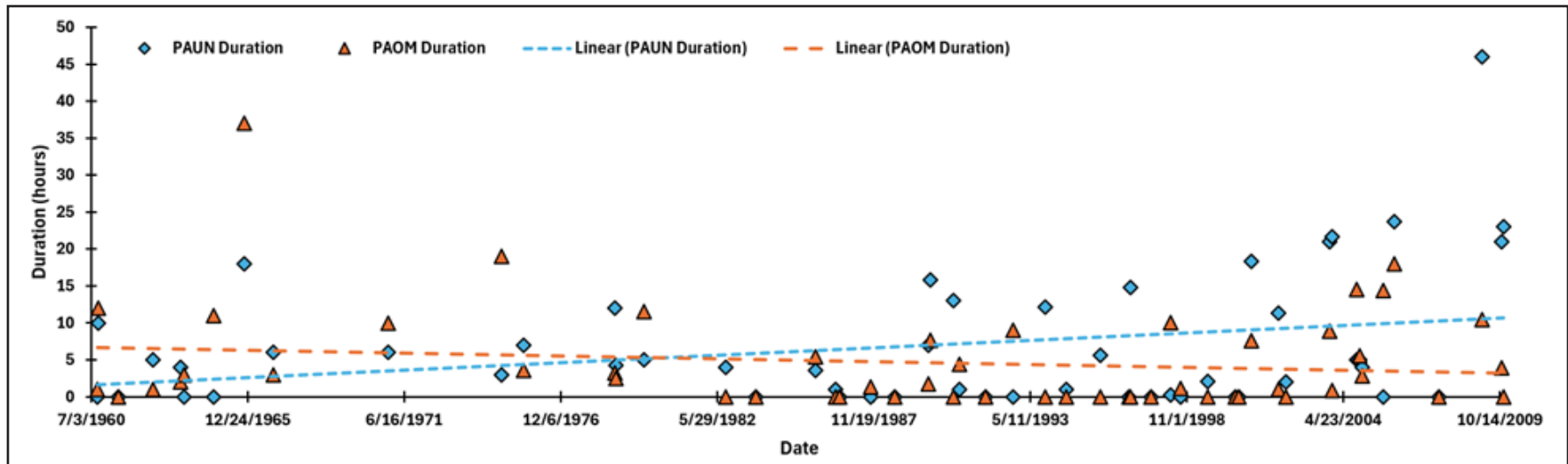


Figure B6. Timeline of storm events identified by USACE (2011) by duration in hours of wind speeds in excess of 15 m/s in Nome (blue diamonds) and Unalakleet (orange triangles), Alaska, compiled from Alaska ASOS/AWOS network stations PAOM and PAUN (IEM, 2024).

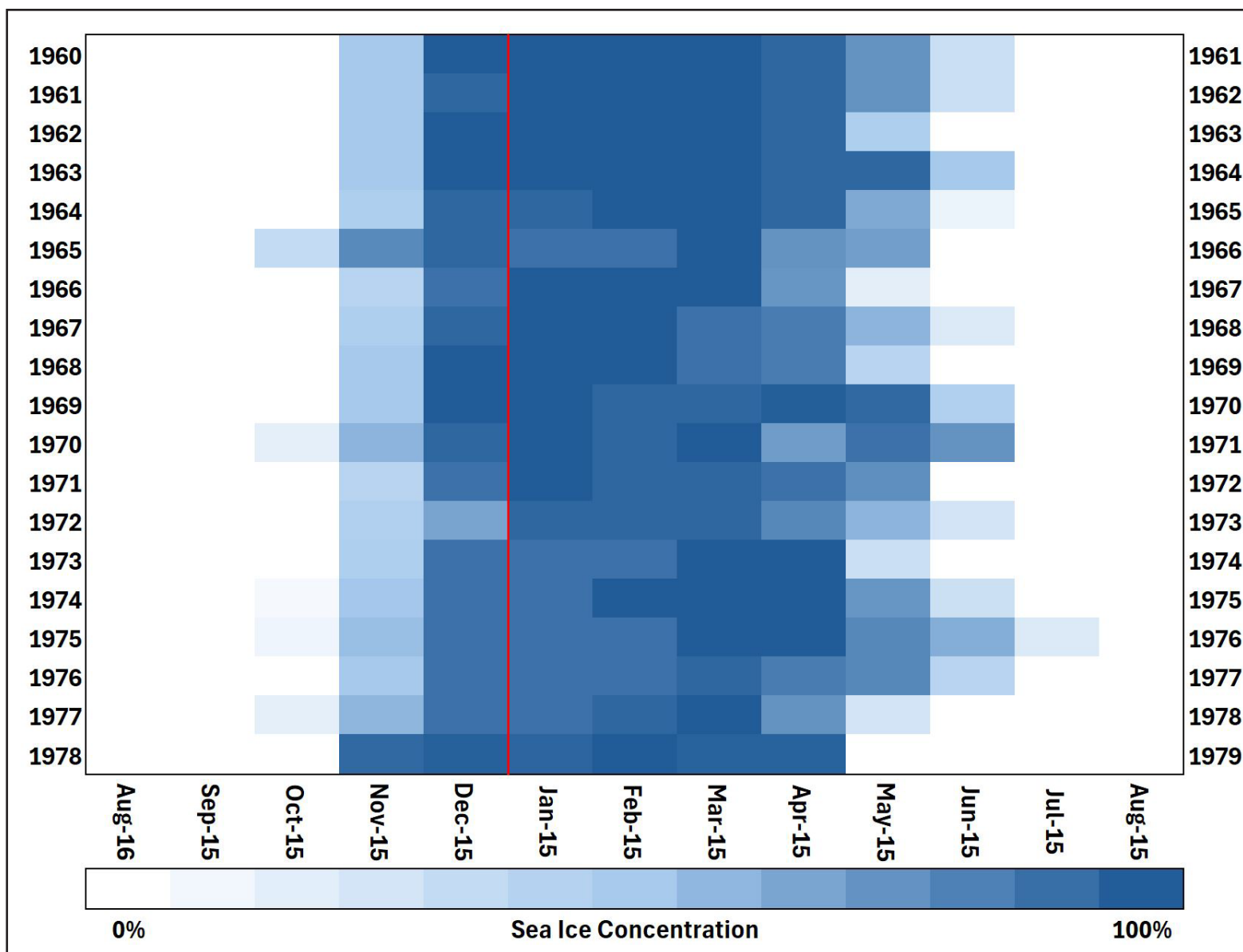


Figure B7. Timeline of sea ice concentration off the coast of Shaktolik, Alaska, 1960 to 1979, compiled from NSIDC data (Walsh and others, 2019), red line indicates change of year.

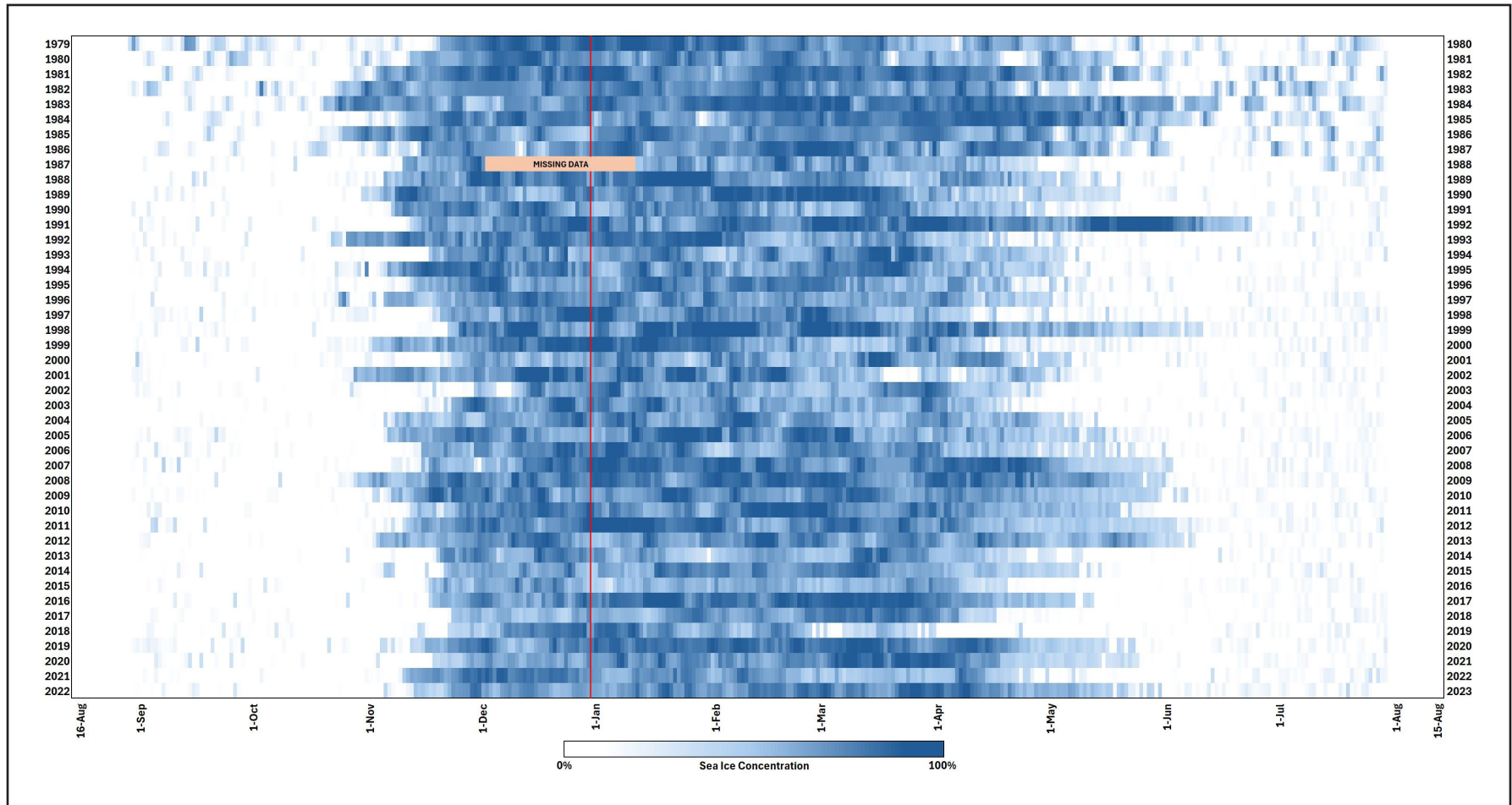


Figure B8. Timeline of sea ice concentration off the coast of Shaktoolik, Alaska, 1979 to 2023, compiled from NSIDC data (Fetterer and others, 2024), red line indicates change of year.

FINAL RESULTS

For each event, we have established two estimates following the delineation described by Moritz and others (2016), with a DSWL to reflect the flooding that would have been experienced on the exposed coast to the west of the community and an SWL to capture the flooding the sheltered riverbank to the east; the primary difference being the inclusion of the standing wave height at the shore due to setup as quantified by Kriebel (1994). Since we lacked the means to identify the exact timing of the peak surge for any given event, we decided to adopt a similar approach as those taken in previous studies, selecting the highest water height during each event for our estimate, though refined significantly by the inclusion of predicted

tides and, where available, the timing of waves. While DGGS processed all 53 unique and identifiable events listed by USACE (2011), we have only included charts for the events with at least one estimated water height above the minimum cutoff for the minor flood category.

Since the original surge simulations were generated using a bathymetric surface collected, in part, from the nautical charts available for the area off the coast of Shaktoolik (NOAA, 2004), those having been derived from a lead-line survey performed in the year 1900 (NCEI, 2024), all estimates warrant the maximum temporal uncertainty of ± 1.0 ft (0.30 m). The following results are listed in chronological order by the date of the estimated maximum flood height for each event.

1960-SEP-27

DSWL 4.5 ± 1.1 ft (1.38 ± 0.32 m) MHHW
SWL 3.8 ± 0.5 ft (1.16 ± 0.16 m) MHHW

Surge Height (MHHW)

3.8 ft (1.15 m)

Peak Wave Height

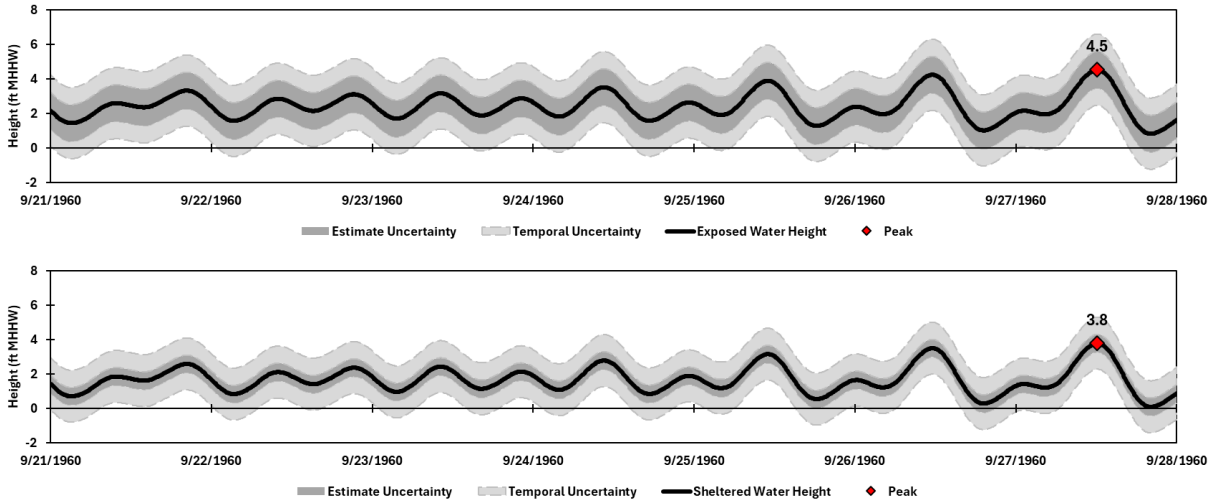
4.2 ft (1.29 m)

Not provided (default)

Sea Ice Concentration

0.0 %

Unavailable



*Estimate not used in flood categorization determinations.

1960-OCT-01

DSWL 14.3 ± 0.9 ft (4.35 ± 0.27 m) MHHW
SWL 12.3 ± 0.5 ft (3.76 ± 0.16 m) MHHW

Surge Height (MHHW)

12.4 ft (3.77 m)

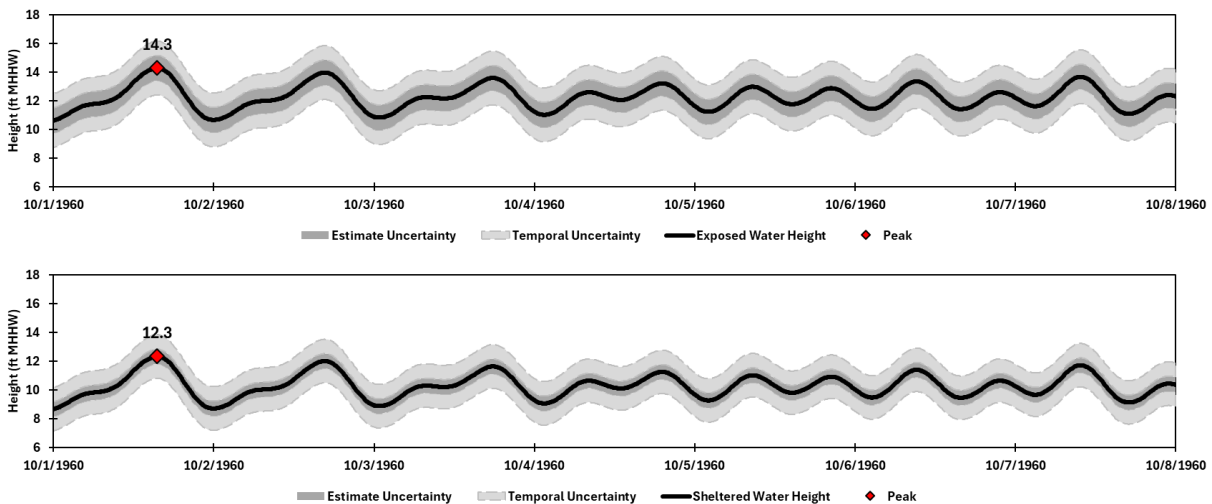
Peak Wave Height

11.2 ft (3.41 m)

Sea Ice Concentration

0.0 %

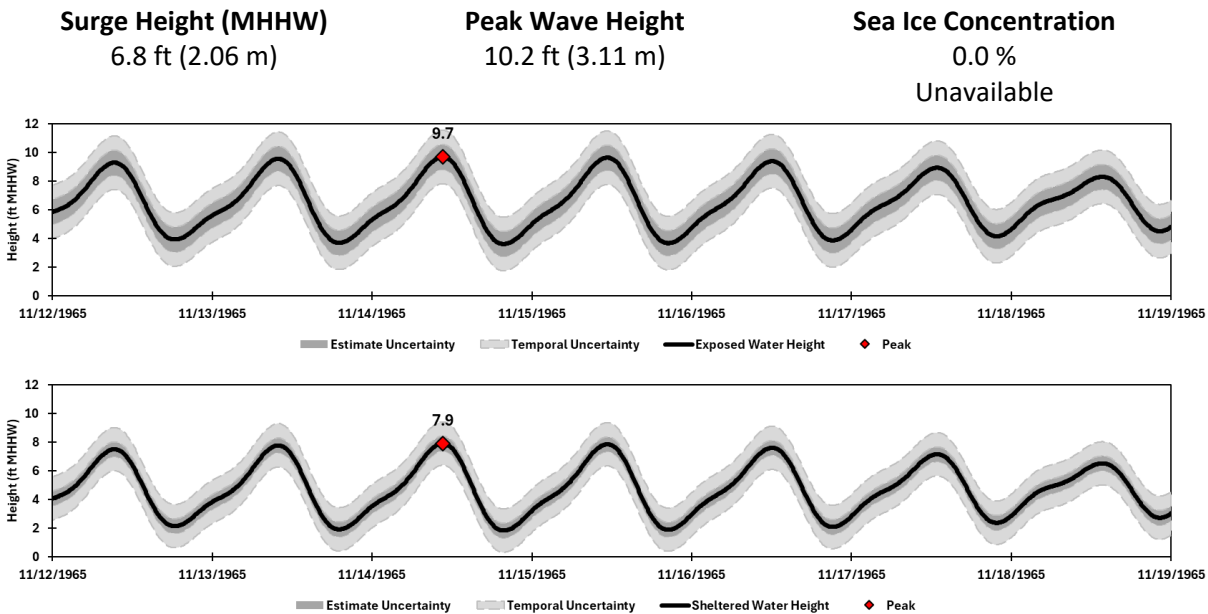
Unavailable



*Estimate not used in flood categorization determinations.

1965-NOV-14

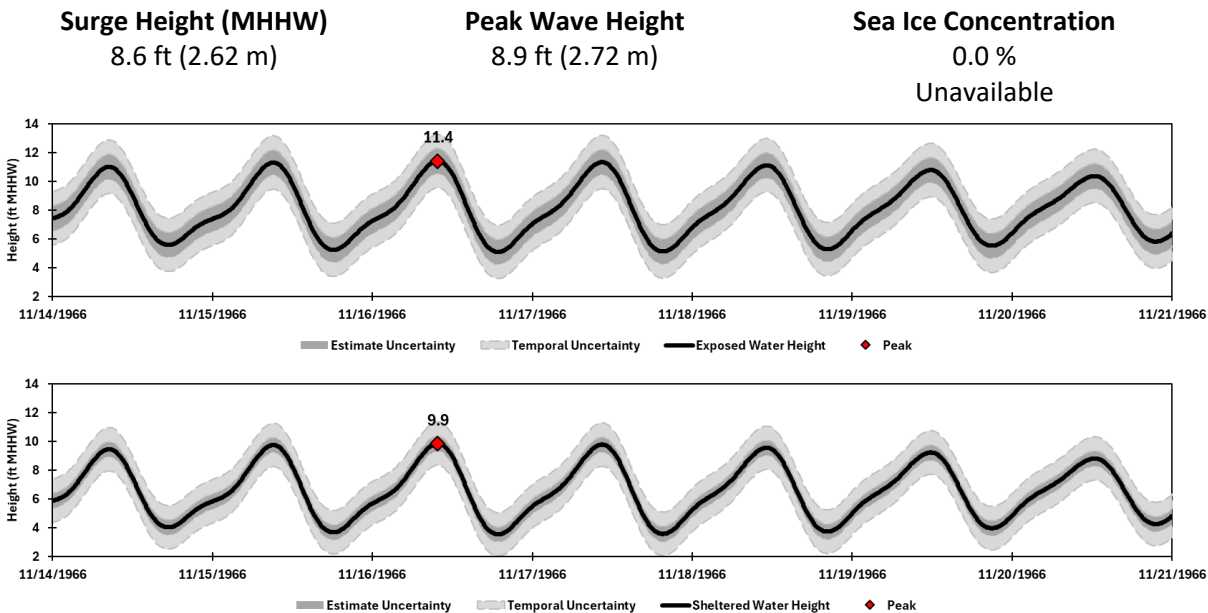
DSWL 9.7 ± 0.9 ft (2.95 ± 0.27 m) MHHW
SWL 7.9 ± 0.5 ft (2.41 ± 0.16 m) MHHW



*Estimate not used in flood categorization determinations.

1966-NOV-16

DSWL 11.4 ± 0.9 ft (3.48 ± 0.26 m) MHHW
SWL 9.9 ± 0.5 ft (3.01 ± 0.16 m) MHHW



*Estimate not used in flood categorization determinations.

1970-DEC-02**DSWL** 11.7 ± 0.9 ft (3.56 ± 0.26 m) MHHW**SWL** 10.1 ± 0.5 ft (3.09 ± 0.16 m) MHHW**Surge Height (MHHW)**

8.8 ft (2.69 m)

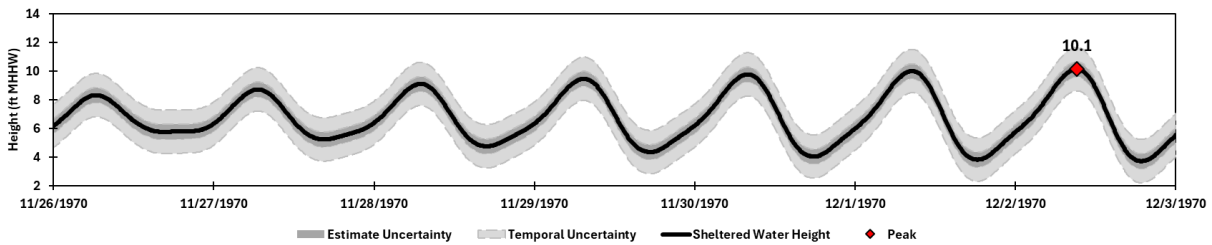
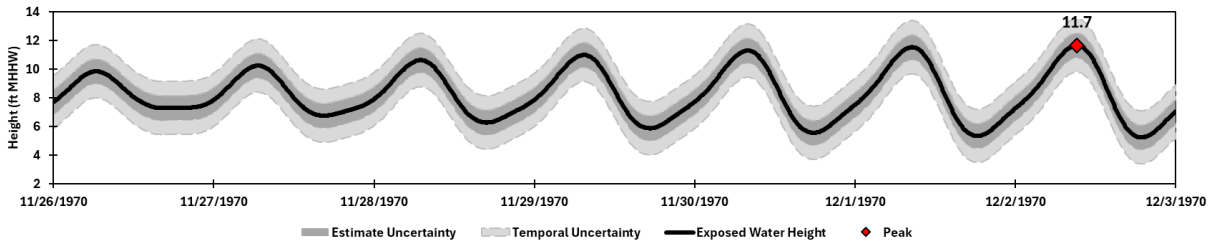
Peak Wave Height

8.7 ft (2.65 m)

Sea Ice Concentration

0.0 %

Unavailable



*Estimate not used in flood categorization determinations.

1974-NOV-16**DSWL** 12.2 ± 1.1 ft (3.73 ± 0.32 m) MHHW**SWL** 11.5 ± 0.5 ft (3.51 ± 0.16 m) MHHW**Surge Height (MHHW)**

10.6 ft (3.22 m)

Peak Wave Height

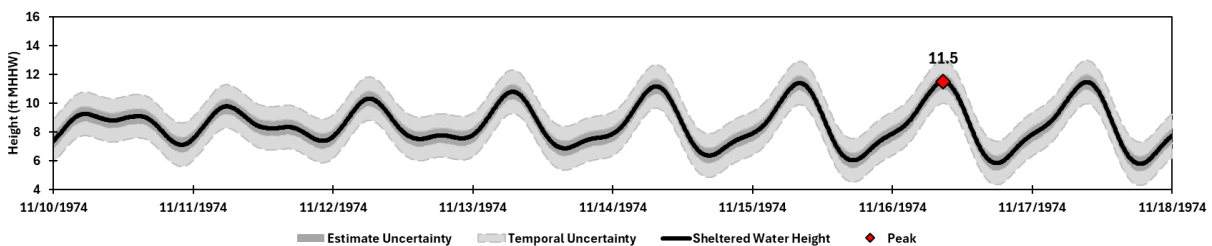
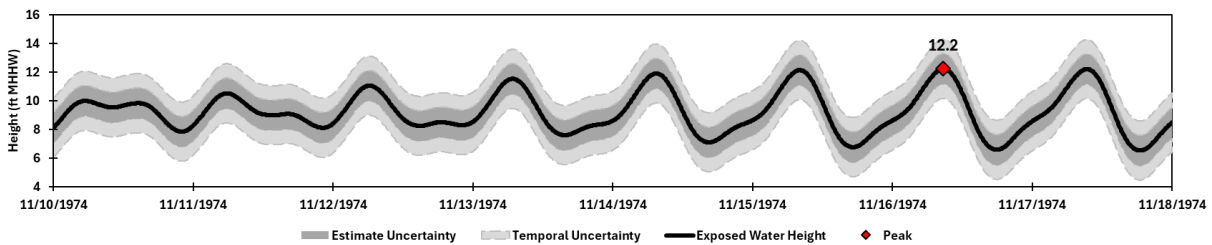
4.2 ft (1.29 m)

Not provided (default)

Sea Ice Concentration

0.0 %

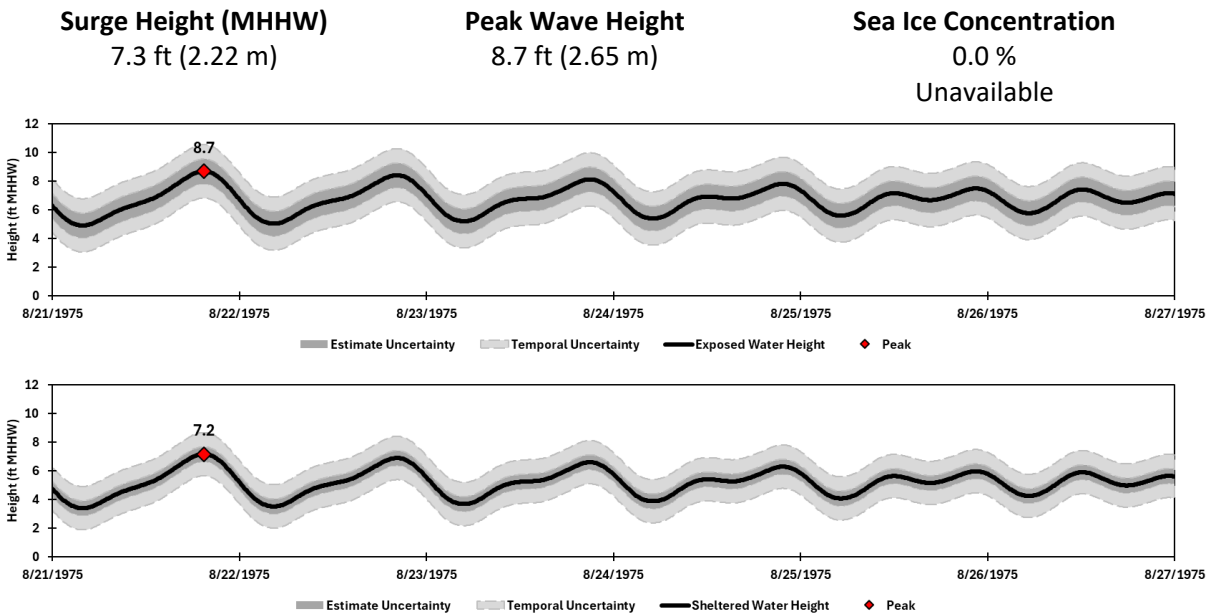
Unavailable



*Estimate not used in flood categorization determinations.

1975-AUG-21

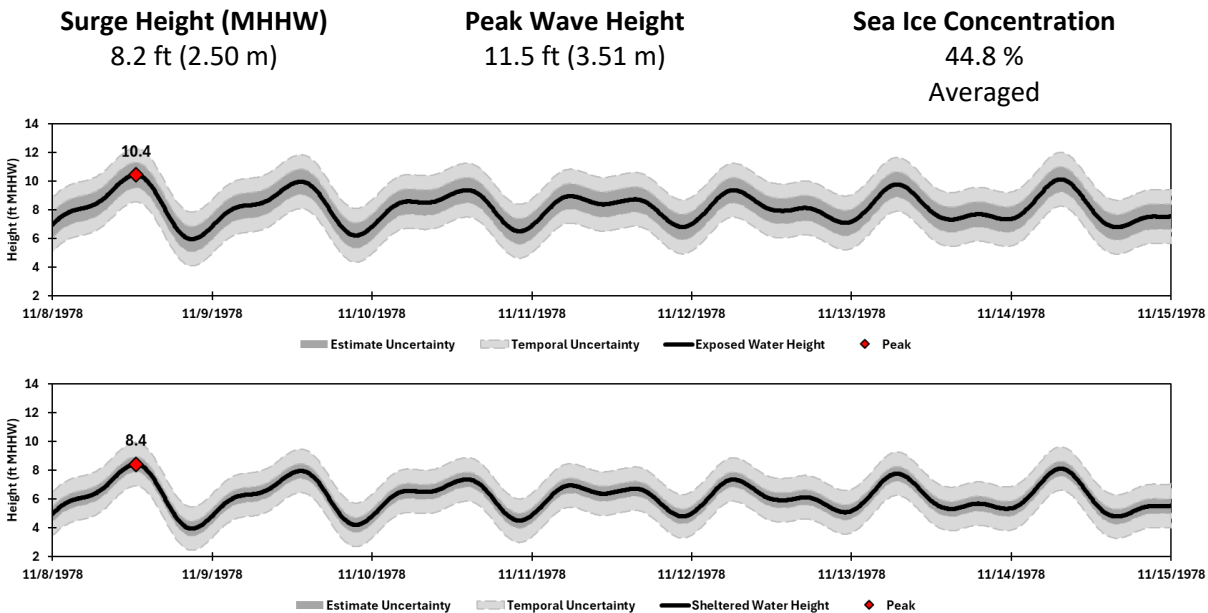
DSWL 8.7 ± 0.9 ft (2.65 ± 0.26 m) MHHW
SWL 7.2 ± 0.5 ft (2.18 ± 0.16 m) MHHW



*Estimate not used in flood categorization determinations.

1978-NOV-08

DSWL 10.4 ± 0.9 ft (3.18 ± 0.27 m) MHHW
SWL 8.4 ± 0.5 ft (2.57 ± 0.16 m) MHHW



*Estimate not used in flood categorization determinations.

1983-OCT-03

DSWL **5.2 ± 1.1 ft (1.59 ± 0.32 m) MHHW**
SWL **4.5 ± 0.5 ft (1.36 ± 0.16 m) MHHW**

Surge Height (MHHW)

4.1 ft (1.26 m)

Peak Wave Height

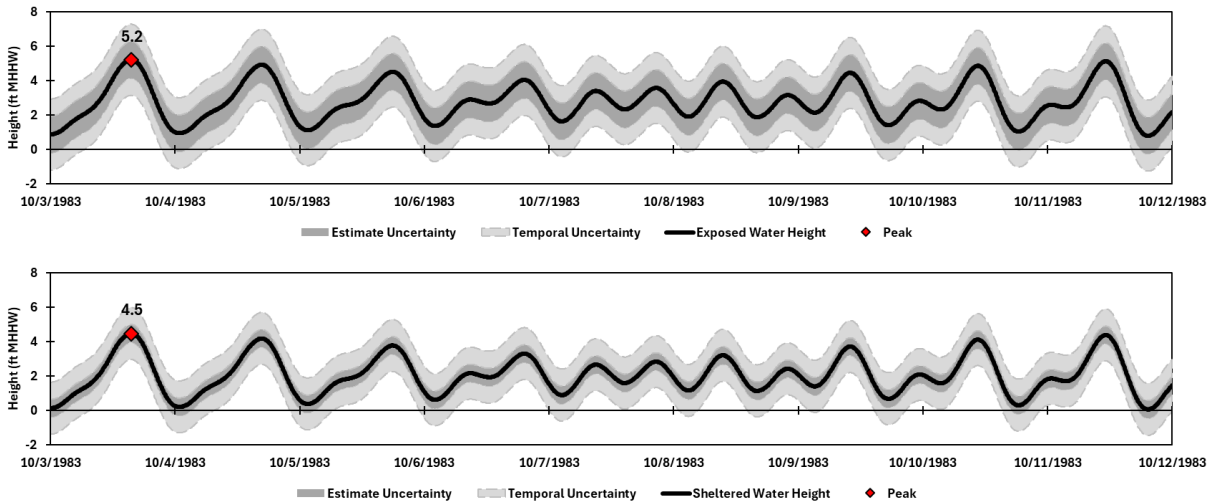
4.2 ft (1.29 m)

Not provided (default)

Sea Ice Concentration

7.2 %

Averaged



*Estimate not used in flood categorization determinations.

1985-NOV-06

DSWL **5.9 ± 1.1 ft (1.81 ± 0.32 m) MHHW**
SWL **5.2 ± 0.5 ft (1.58 ± 0.16 m) MHHW**

Surge Height (MHHW)

4.9 ft (1.49 m)

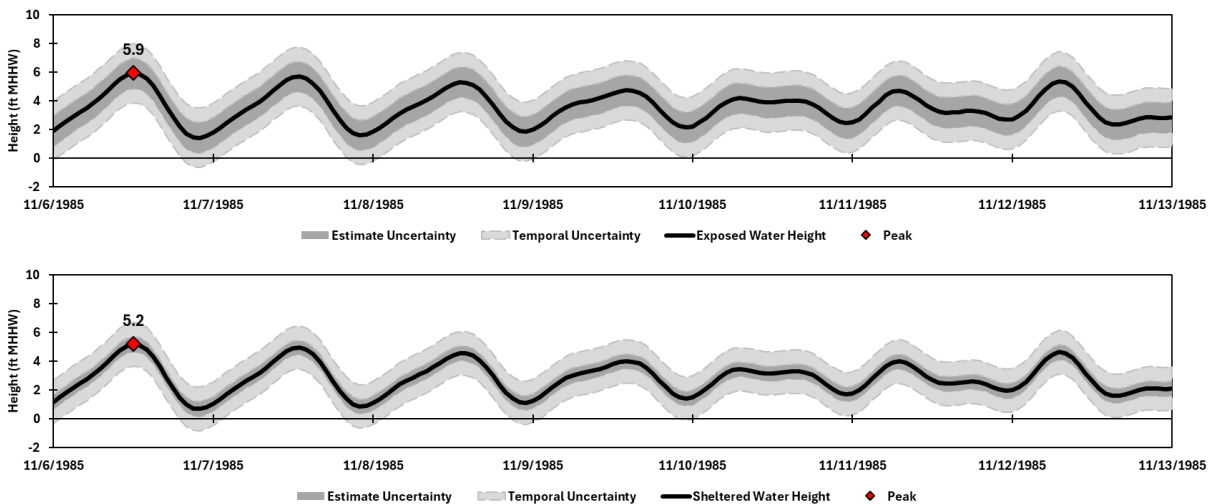
Peak Wave Height

4.2 ft (1.29 m)

Not available (default)

Sea Ice Concentration

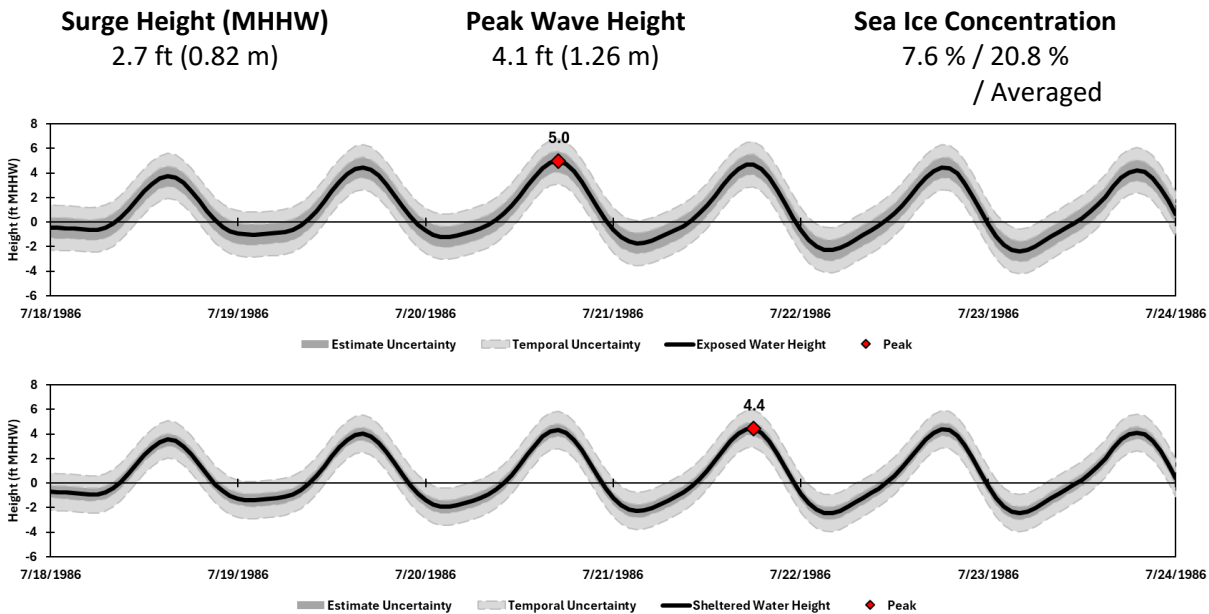
70.0 %



1986-JUL-20
1986-JUL-21

DSWL
SWL

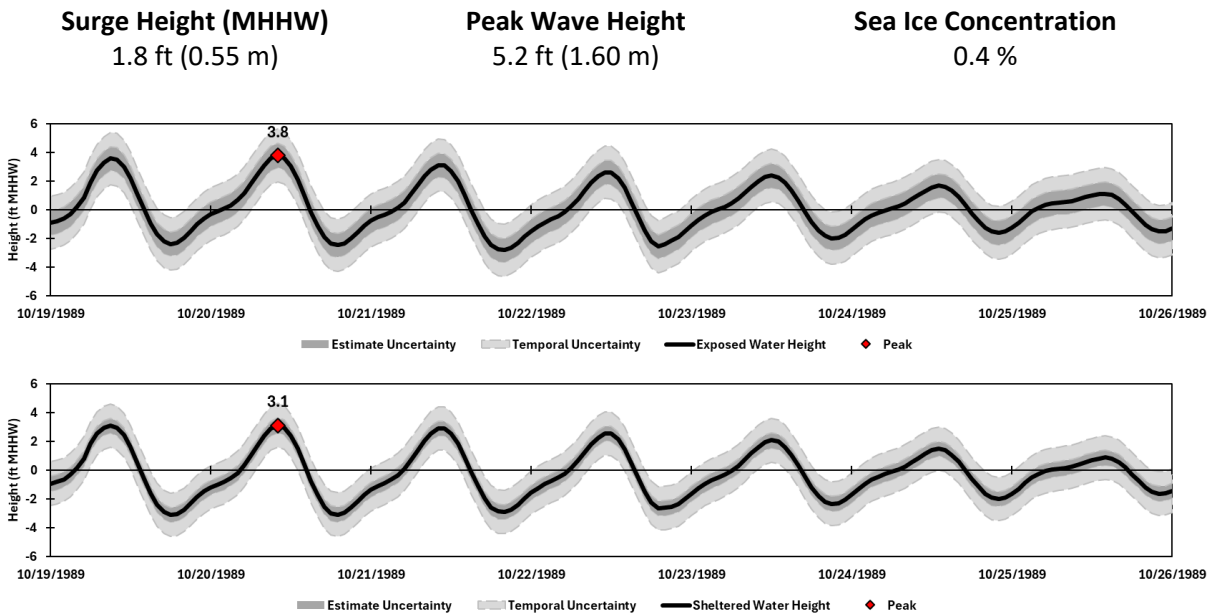
5.0 ± 0.8 ft (1.51 ± 0.26 m) MHHW
4.4 ± 0.5 ft (1.36 ± 0.16 m) MHHW

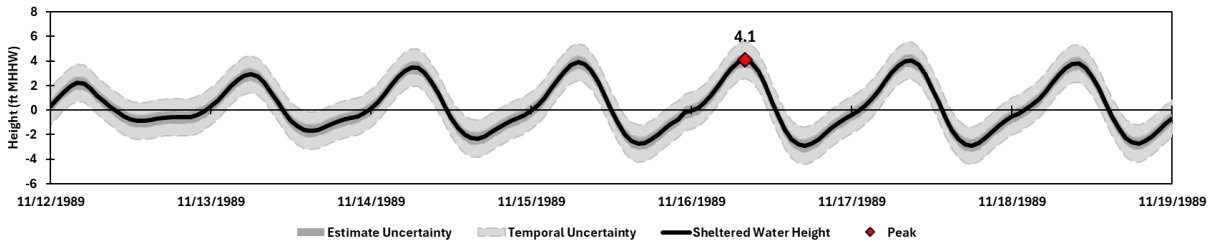
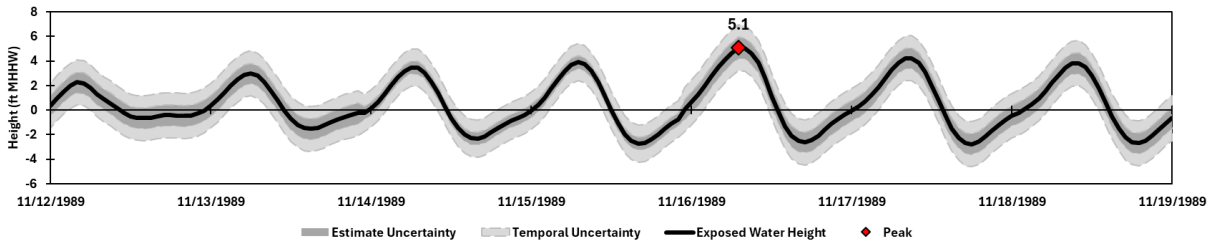
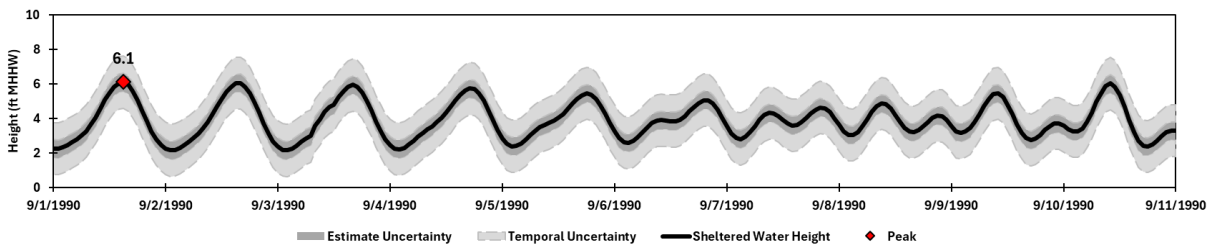
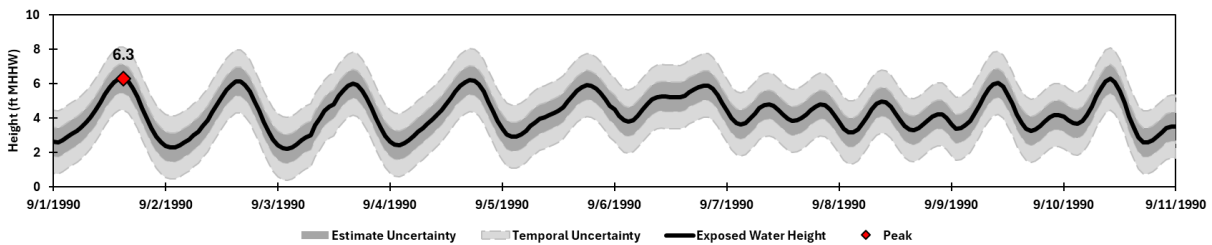


1989-OCT-20

DSWL
SWL

3.8 ± 0.8 ft (1.16 ± 0.26 m) MHHW
3.1 ± 0.5 ft (0.95 ± 0.16 m) MHHW



1989-NOV-16**DSWL** **5.1 ± 0.9 ft (1.55 ± 0.26 m) MHHW****SWL** **4.1 ± 0.5 ft (1.25 ± 0.16 m) MHHW****Surge Height (MHHW)****2.4 ft (0.73 m)****Peak Wave Height****8.7 ft (2.65 m)****Sea Ice Concentration****78.8 %****1990-SEP-01****DSWL** **6.3 ± 0.8 ft (1.92 ± 0.25 m) MHHW****SWL** **6.1 ± 0.5 ft (1.86 ± 0.16 m) MHHW****Surge Height (MHHW)****6.0 ft (1.82 m)****Peak Wave Height****4.9 ft (1.48 m)****Sea Ice Concentration****20.0 %**

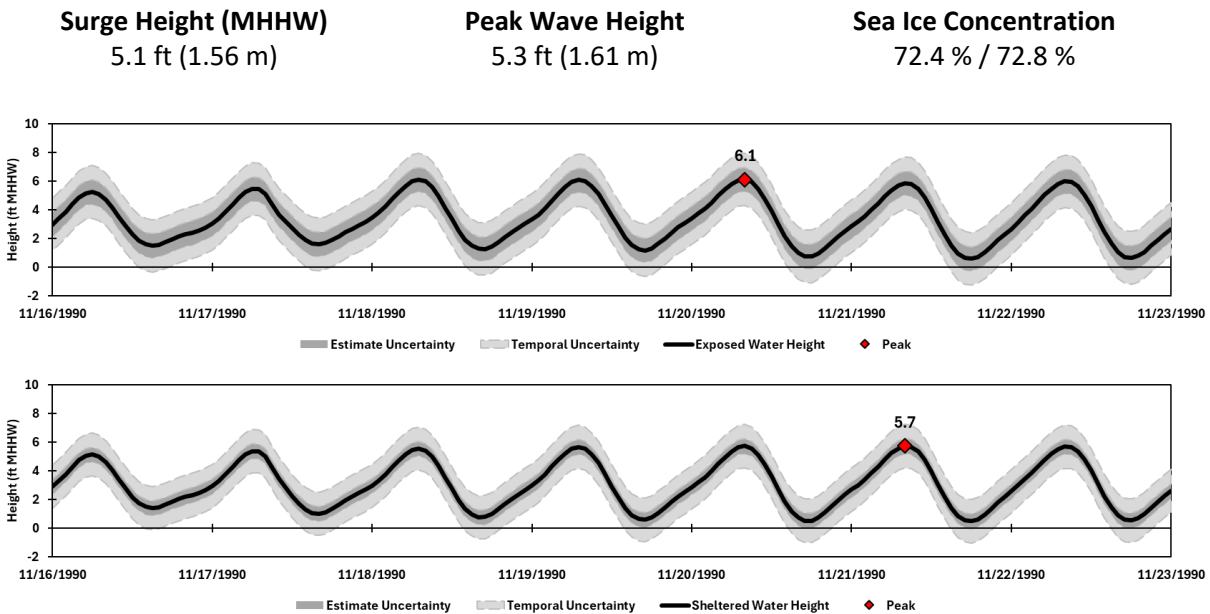
1990-NOV-20
1990-NOV-21

DSWL

SWL

6.1 ± 0.8 ft (1.87 ± 0.25 m) MHHW

5.7 ± 0.5 ft (1.75 ± 0.16 m) MHHW



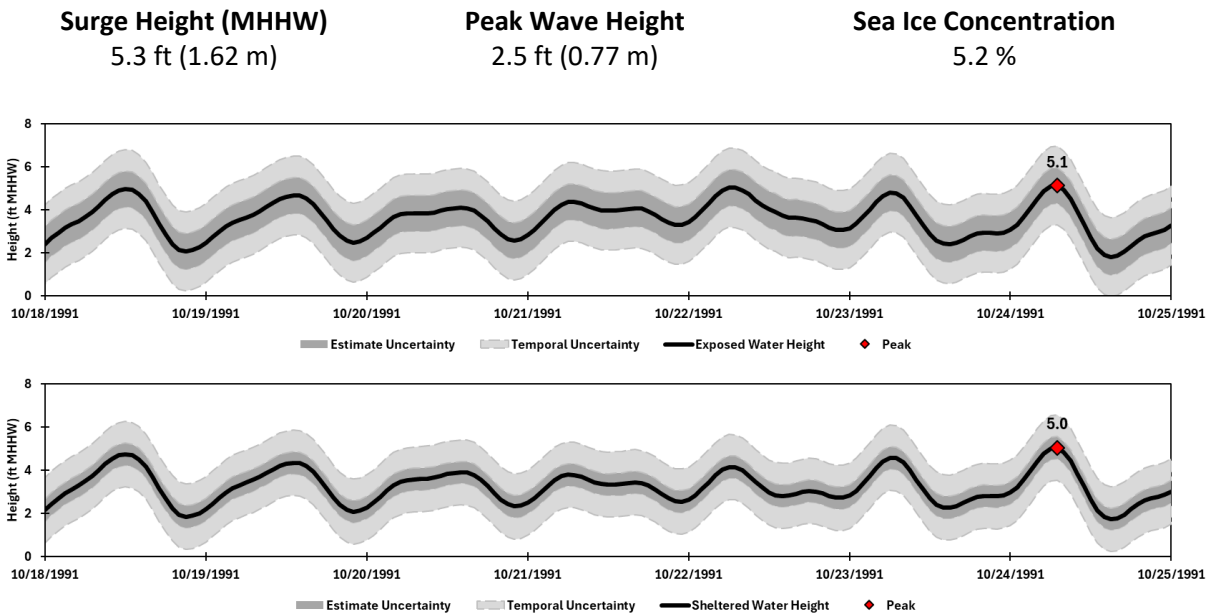
1991-OCT-24

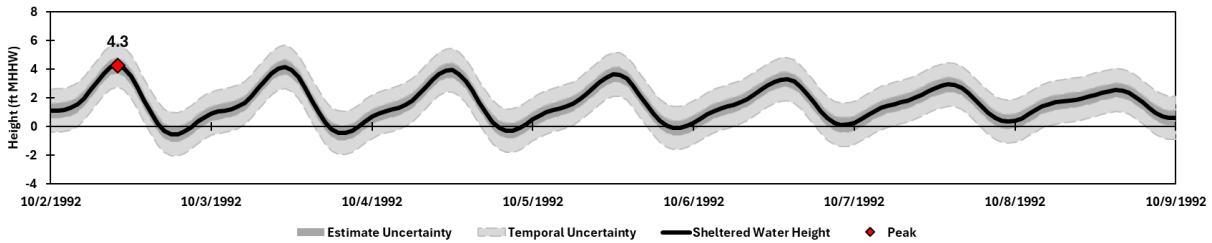
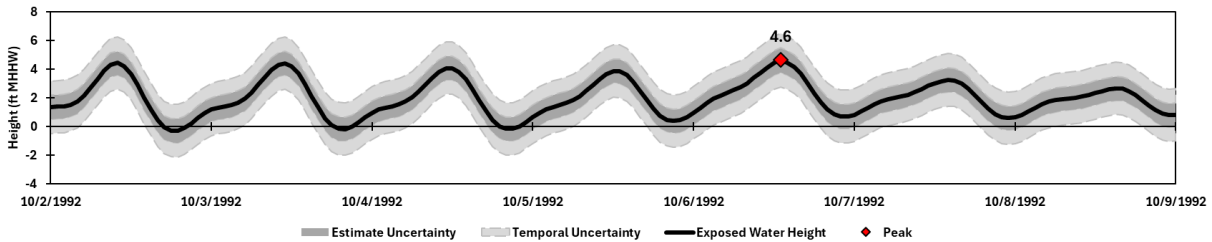
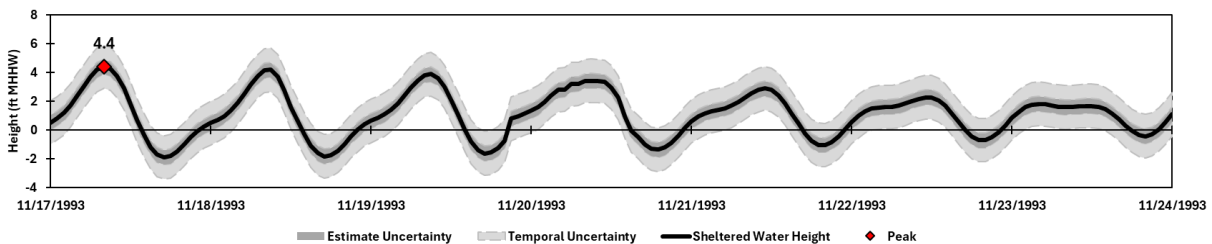
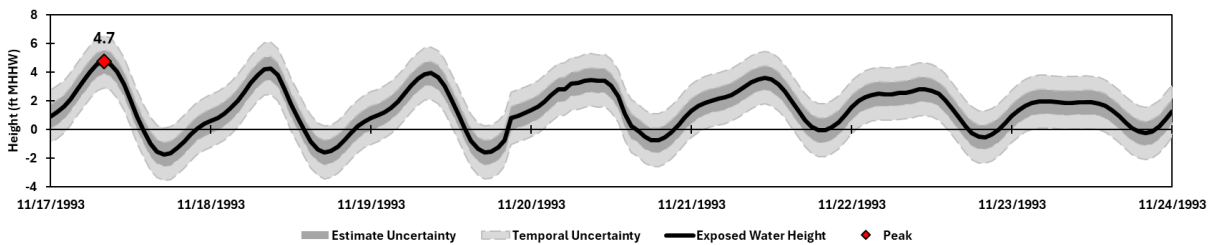
DSWL

SWL

5.1 ± 0.8 ft (1.56 ± 0.25 m) MHHW

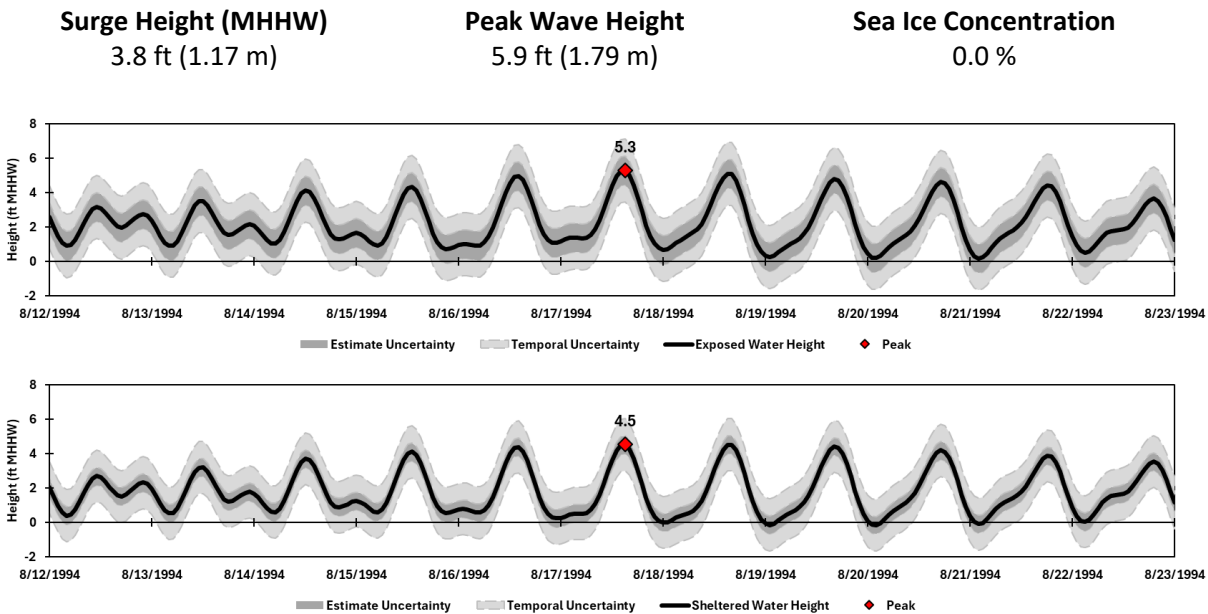
5.0 ± 0.5 ft (1.54 ± 0.16 m) MHHW



1992-OCT-06**DSWL** **4.6 ± 0.9 ft (1.41 ± 0.26 m) MHHW****1992-OCT-02****SWL** **4.3 ± 0.5 ft (1.30 ± 0.16 m) MHHW****Surge Height (MHHW)****3.7 ft (1.12 m)****Peak Wave Height****7.7 ft (2.36 m)****Sea Ice Concentration****0.0 % / 0.4 %****1993-NOV-17****DSWL** **4.7 ± 0.8 ft (1.45 ± 0.25 m) MHHW****SWL** **4.4 ± 0.5 ft (1.34 ± 0.16 m) MHHW****Surge Height (MHHW)****3.1 ft (0.94 m)****Peak Wave Height****5.7 ft (1.73 m)****Sea Ice Concentration****6.0 %**

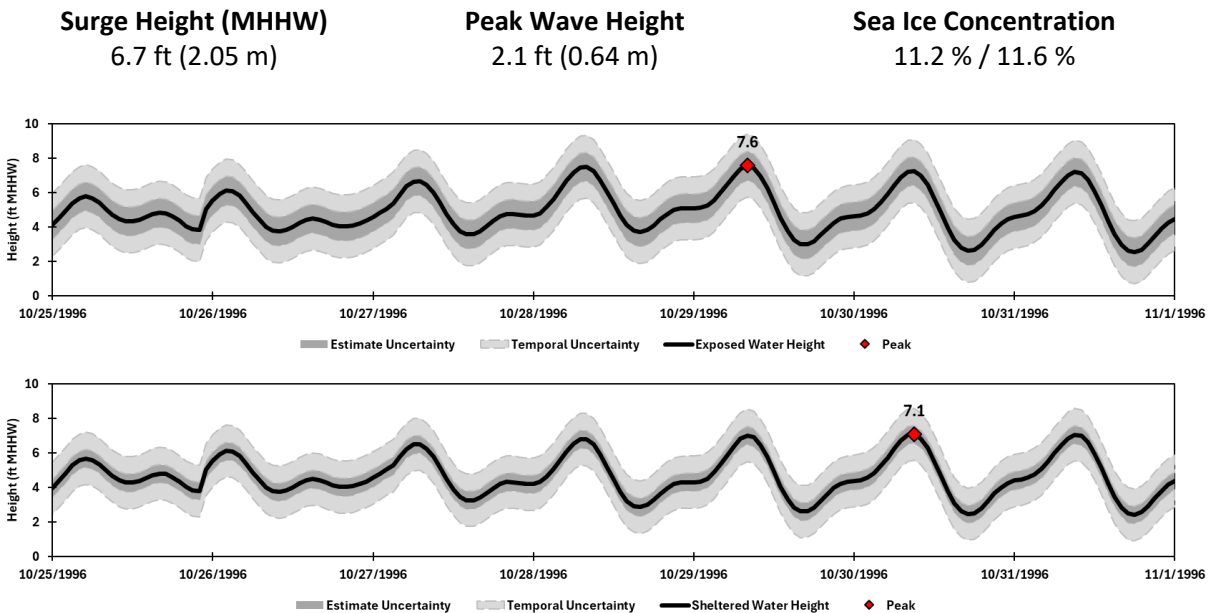
1994-AUG-17

DSWL 5.3 ± 0.8 ft (1.61 ± 0.26 m) MHHW
SWL 4.5 ± 0.5 ft (1.38 ± 0.16 m) MHHW



1996-OCT-29
1996-OCT-30

DSWL 7.6 ± 0.8 ft (2.31 ± 0.26 m) MHHW
SWL 7.1 ± 0.5 ft (2.16 ± 0.16 m) MHHW



1996-NOV-15
1996-NOV-16

DSWL **4.9 ± 0.8 ft (1.50 ± 0.26 m) MHHW**
SWL **4.3 ± 0.5 ft (1.30 ± 0.16 m) MHHW**

Surge Height (MHHW)

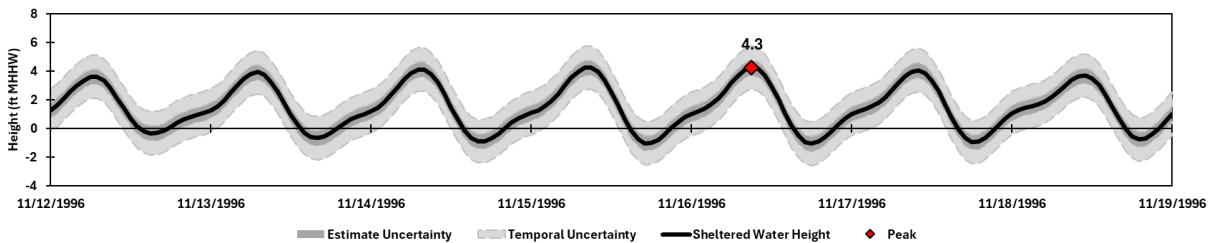
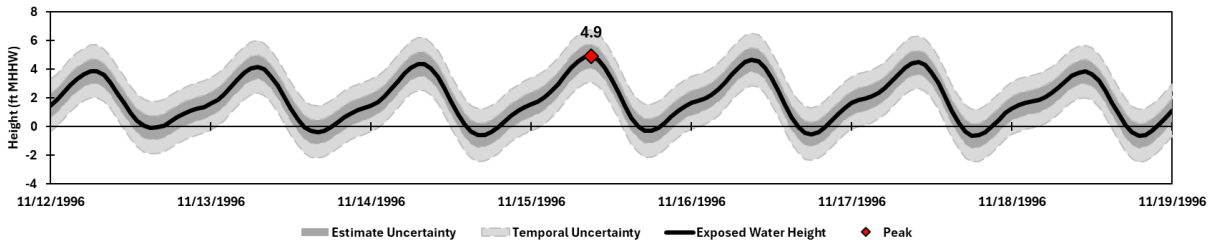
3.5 ft (1.08 m)

Peak Wave Height

6.8 ft (2.07 m)

Sea Ice Concentration

55.2 % / 48.0 %



1997-AUG-03
1997-AUG-01

DSWL **4.1 ± 0.8 ft (1.26 ± 0.25 m) MHHW**
SWL **3.9 ± 0.5 ft (1.20 ± 0.16 m) MHHW**

Surge Height (MHHW)

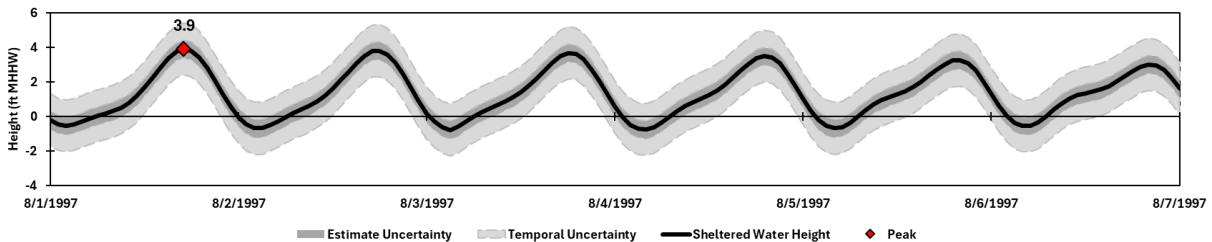
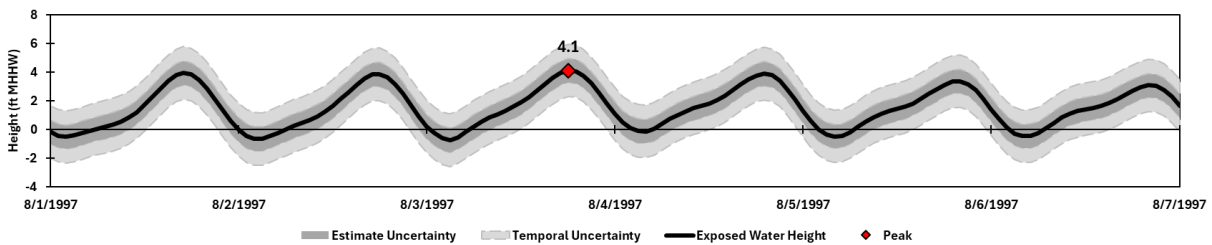
3.4 ft (1.03 m)

Peak Wave Height

4.1 ft (1.24 m)

Sea Ice Concentration

0.0 % / 0.0 %



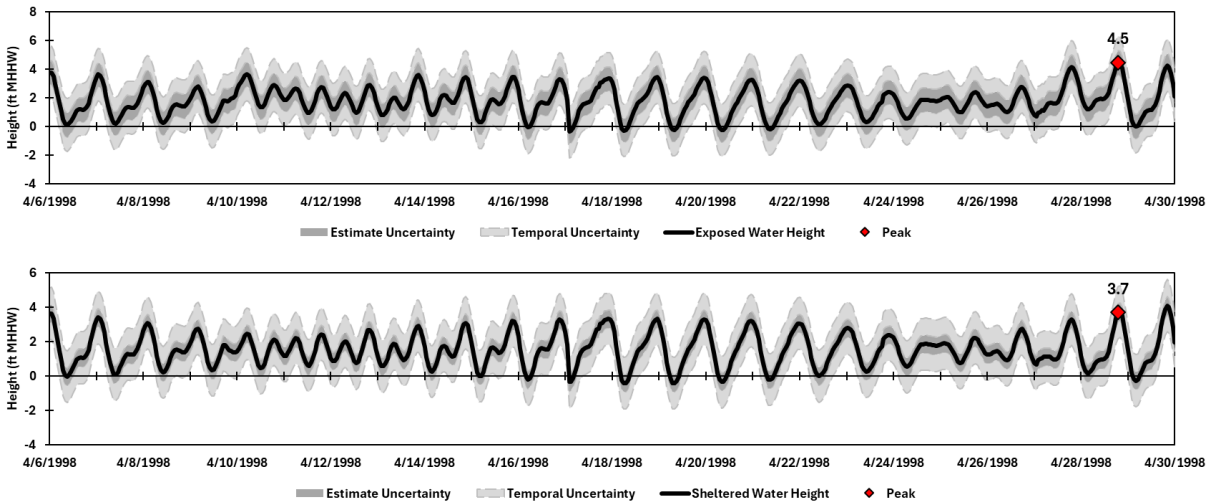
1998-APR-28

DSWL 4.5 ± 0.8 ft (1.36 ± 0.26 m) MHHW
SWL 4.1 ± 0.5 ft (1.25 ± 0.16 m) MHHW

Surge Height (MHHW)
3.6 ft (1.09 m)

Peak Wave Height
7.4 ft (2.25 m)

Sea Ice Concentration
29.6 %



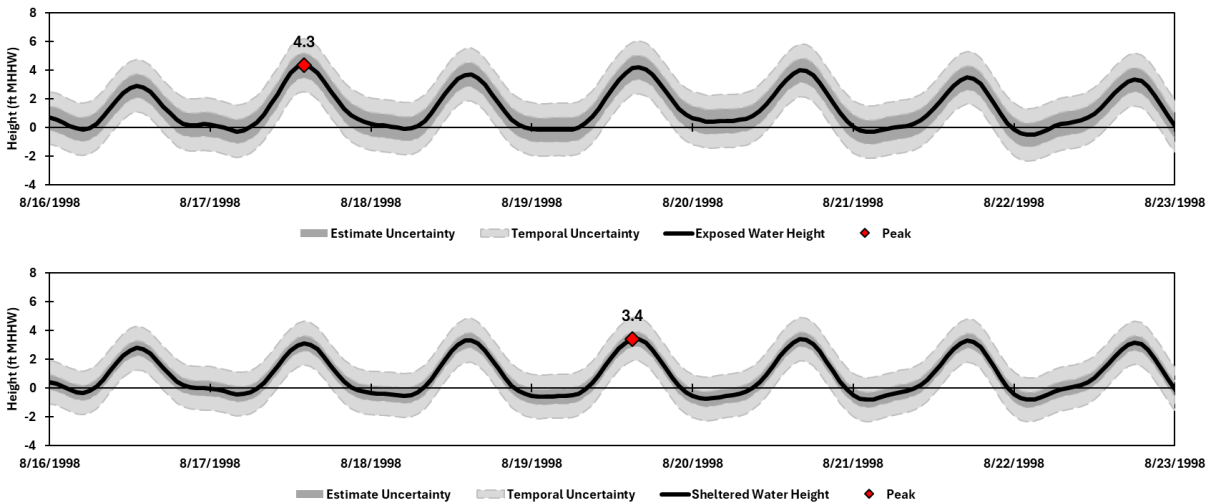
1998-AUG-17
1998-AUG-19

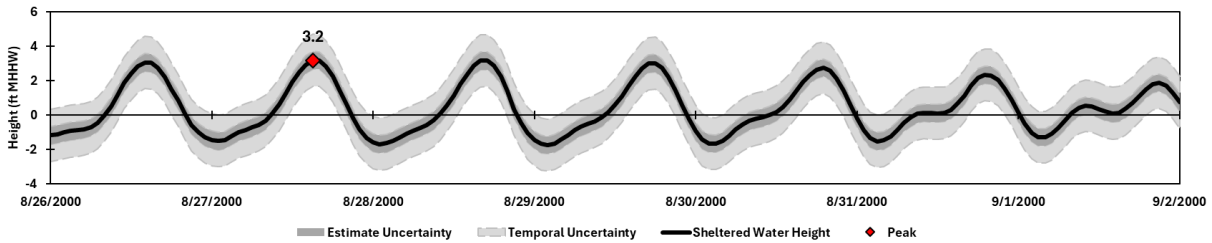
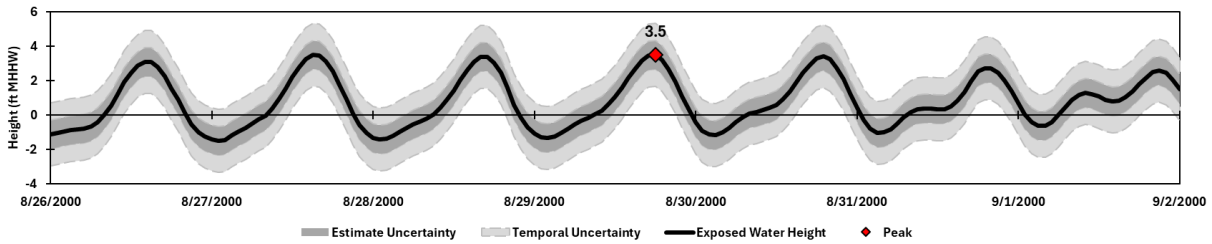
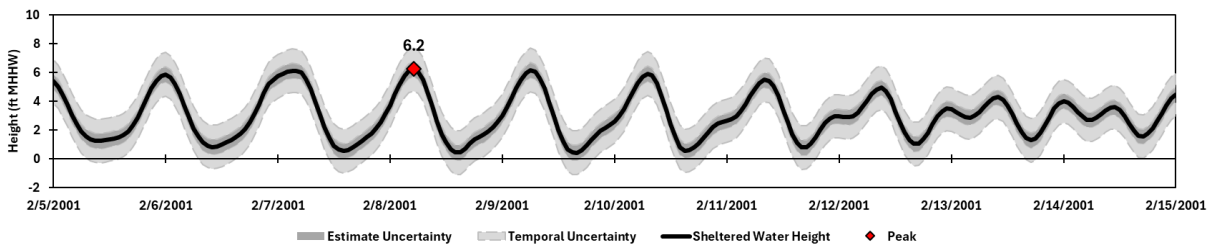
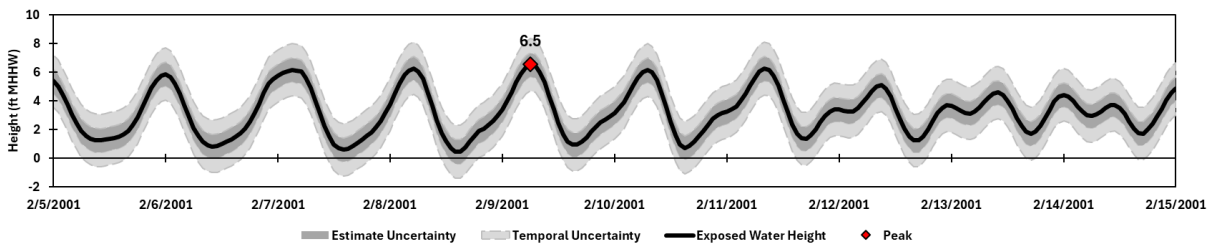
DSWL 4.3 ± 0.9 ft (1.33 ± 0.26 m) MHHW
SWL 3.4 ± 0.5 ft (1.04 ± 0.16 m) MHHW

Surge Height (MHHW)
2.9 ft (0.89 m)

Peak Wave Height
7.2 ft (2.20 m)

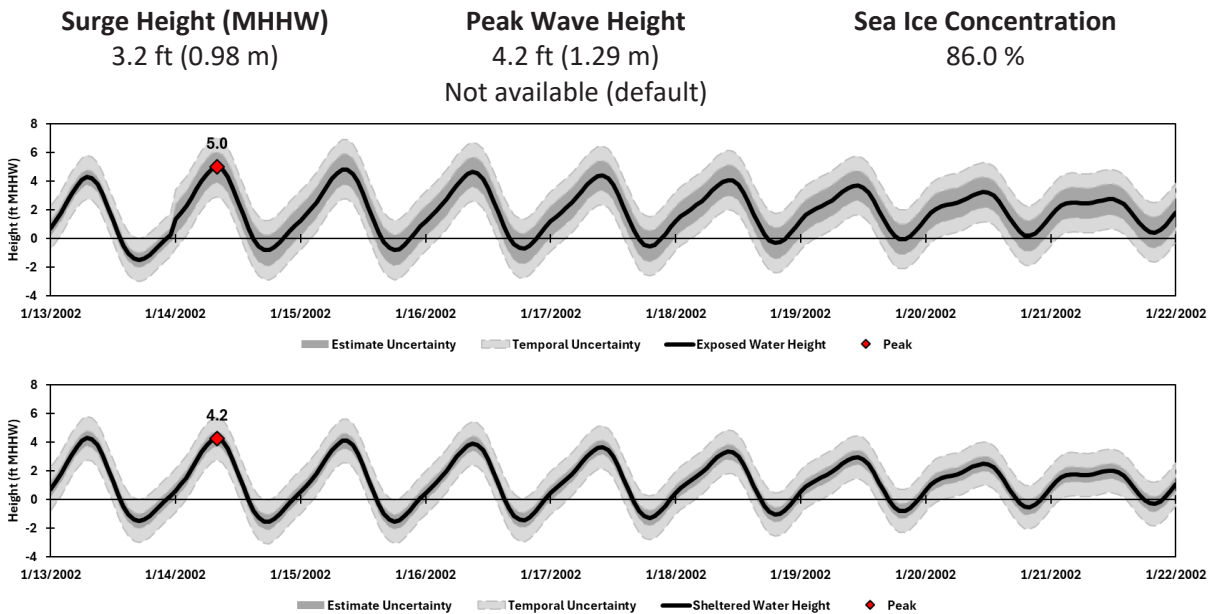
Sea Ice Concentration
0.0 % / 0.0 %



2000-AUG-29**DSWL** **3.5 ± 0.8 ft (1.07 ± 0.26 m) MHHW****2000-AUG-27****SWL** **3.2 ± 0.5 ft (0.97 ± 0.16 m) MHHW****Surge Height (MHHW)****2.4 ft (0.74 m)****Peak Wave Height****4.6 ft (1.40 m)****Sea Ice Concentration****0.0 % / 0.0 %****2001-FEB-09****DSWL** **6.5 ± 0.8 ft (2.00 ± 0.25 m) MHHW****2001-FEB-08****SWL** **6.2 ± 0.5 ft (1.90 ± 0.16 m) MHHW****Surge Height (MHHW)****5.0 ft (1.53 m)****Peak Wave Height****5.5 ft (1.68 m)****Sea Ice Concentration****72.0 % / 76.0 %**

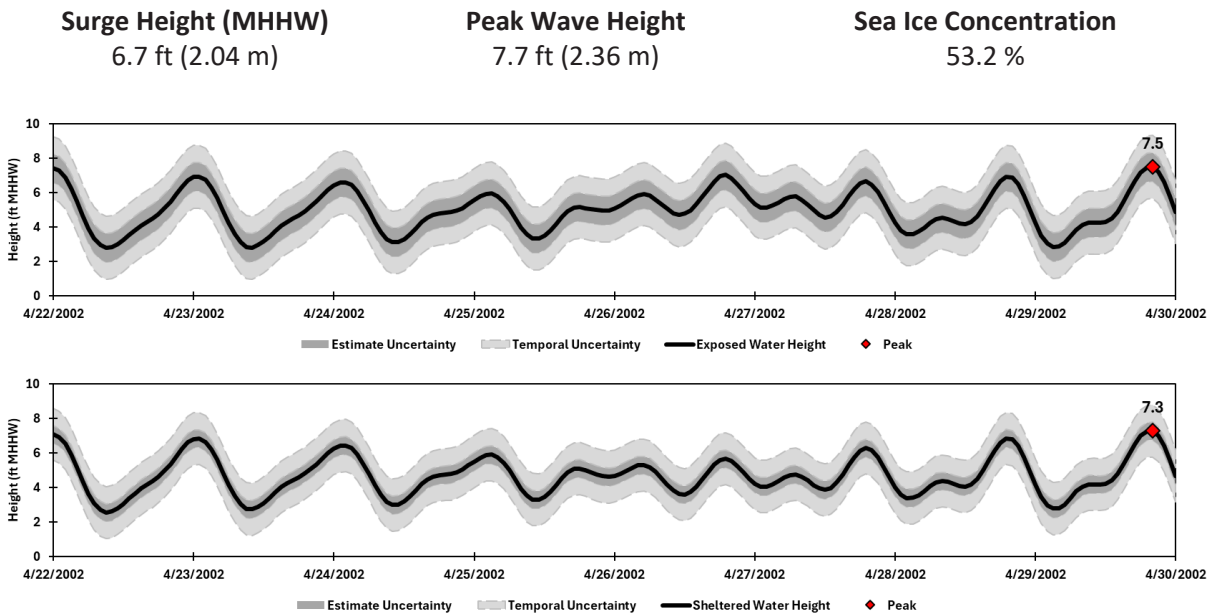
2002-JAN-14

DSWL 5.0 ± 1.1 ft (1.52 ± 0.32 m) MHHW
SWL 4.2 ± 0.5 ft (1.29 ± 0.16 m) MHHW



2002-APR-29

DSWL 7.5 ± 0.8 ft (2.28 ± 0.25 m) MHHW
SWL 7.3 ± 0.5 ft (2.22 ± 0.16 m) MHHW



2003-NOV-26

DSWL 6.7 ± 0.8 ft (2.05 ± 0.25 m) MHHW
SWL 6.4 ± 0.5 ft (1.96 ± 0.16 m) MHHW

Surge Height (MHHW)

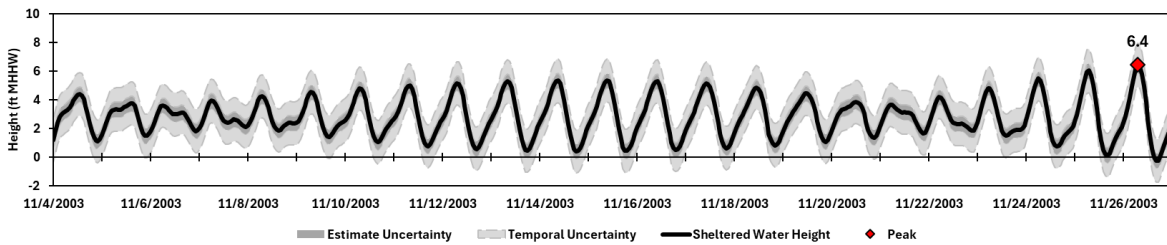
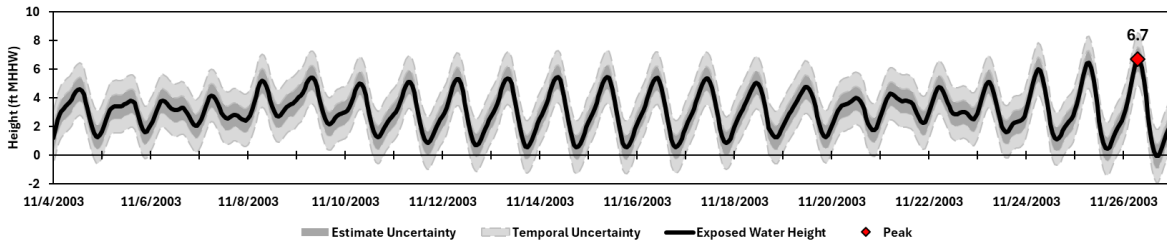
4.9 ft (1.49 m)

Peak Wave Height

8.8 ft (2.68 m)

Sea Ice Concentration

61.6 %

**2003-DEC-22****DSWL** 6.2 ± 0.8 ft (1.89 ± 0.26 m) MHHW**2003-DEC-25****SWL** 6.2 ± 0.5 ft (1.89 ± 0.16 m) MHHW**Surge Height (MHHW)**

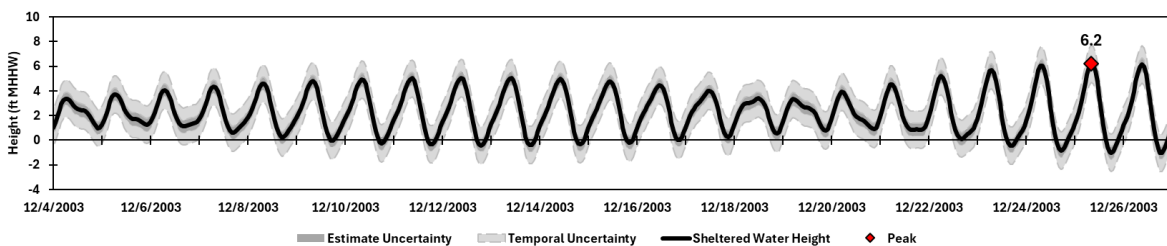
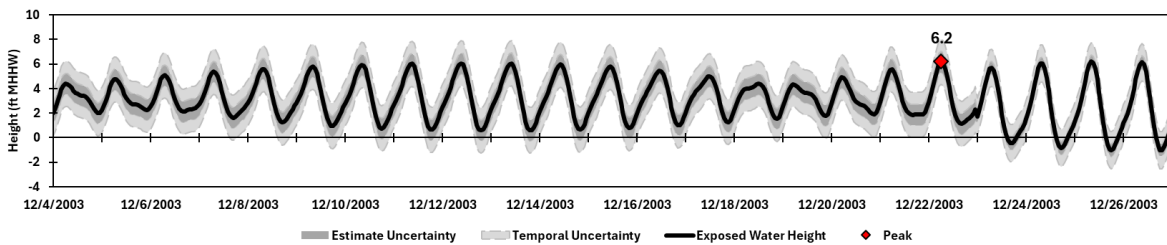
4.3 ft (1.32 m)

Peak Wave Height

5.7 ft (1.75 m)

Sea Ice Concentration

86.4 % / 95.6 %



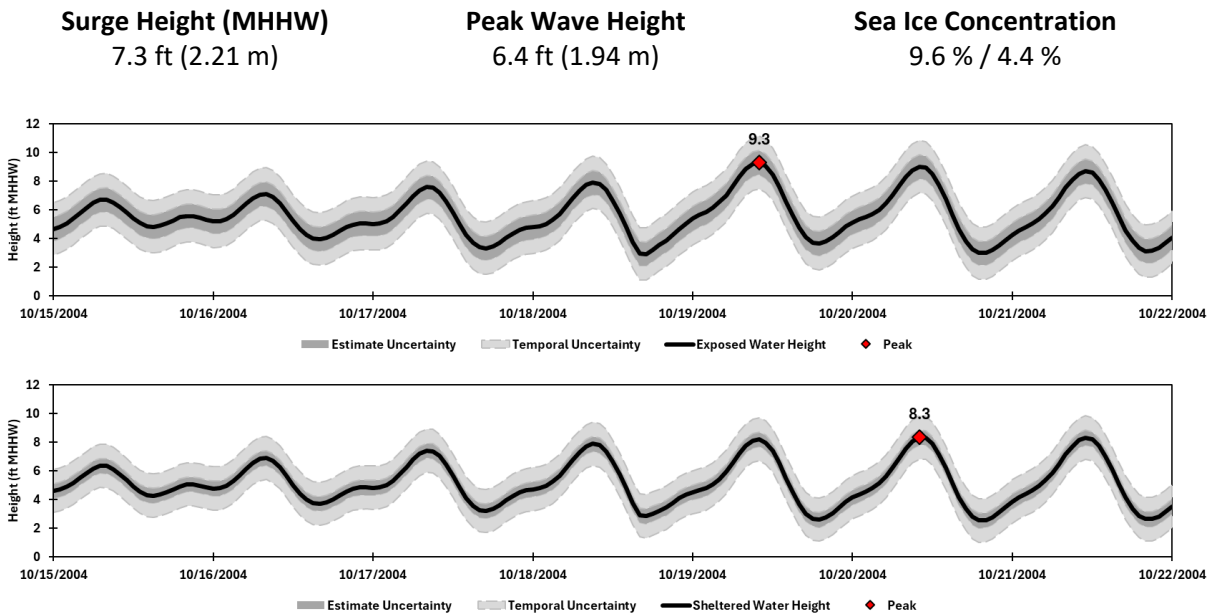
2004-OCT-19
2004-OCT-20

DSWL

SWL

9.3 ± 0.8 ft (2.83 ± 0.26 m) MHHW

8.3 ± 0.5 ft (2.54 ± 0.16 m) MHHW



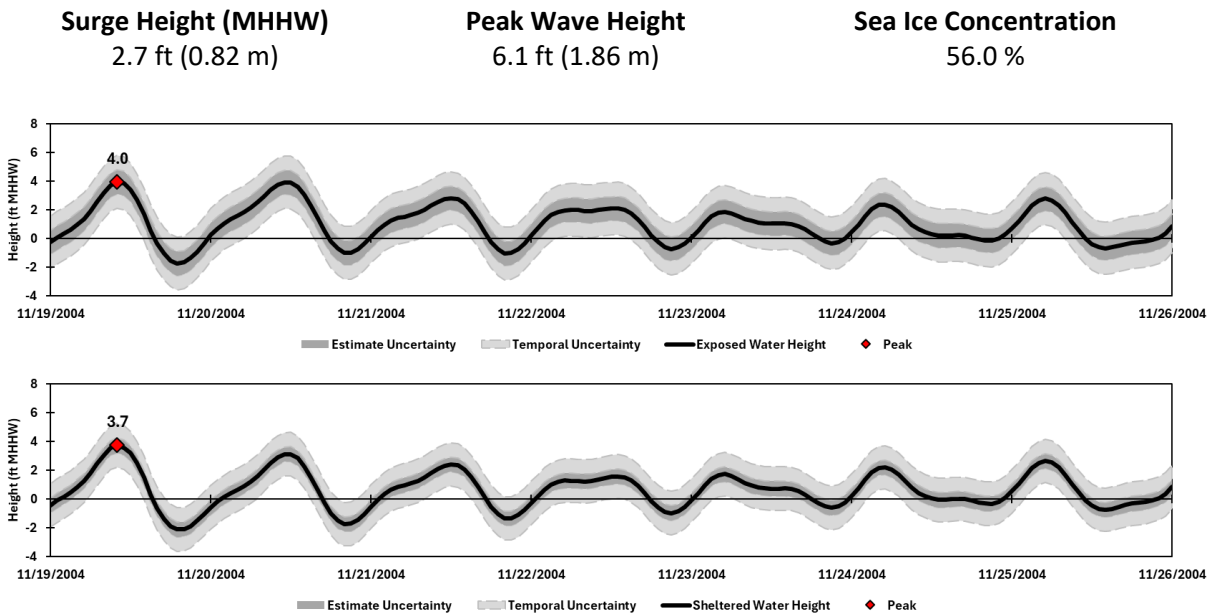
2004-NOV-19

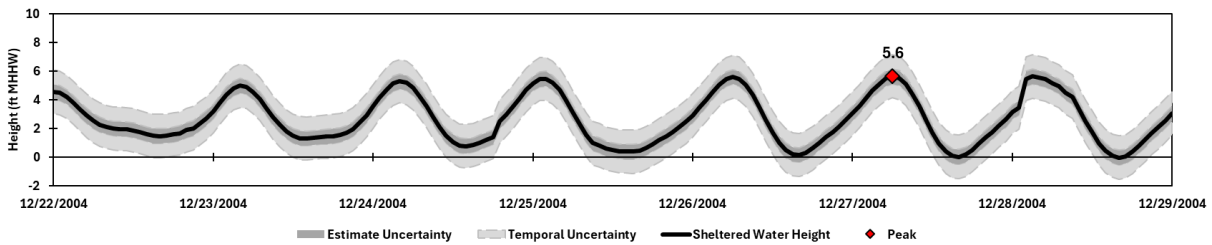
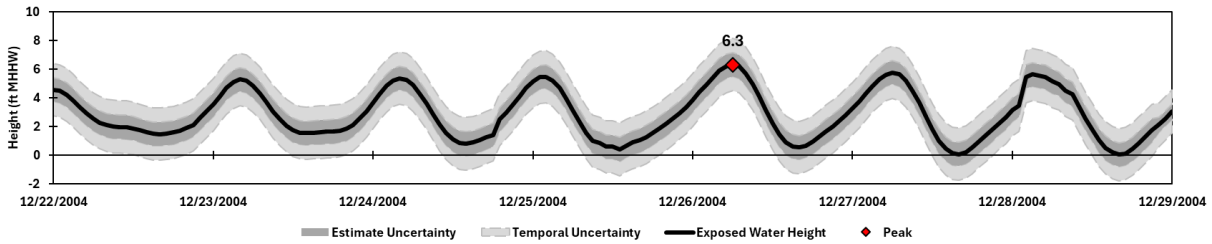
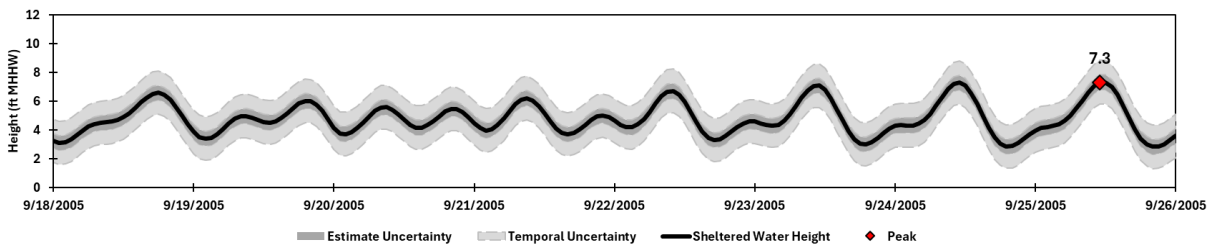
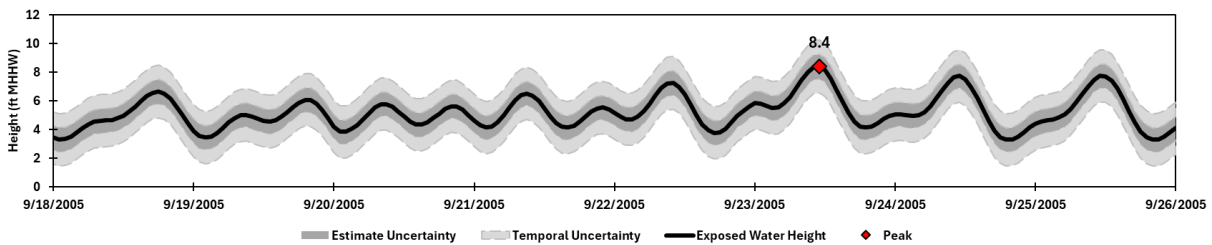
DSWL

SWL

4.0 ± 0.8 ft (1.21 ± 0.25 m) MHHW

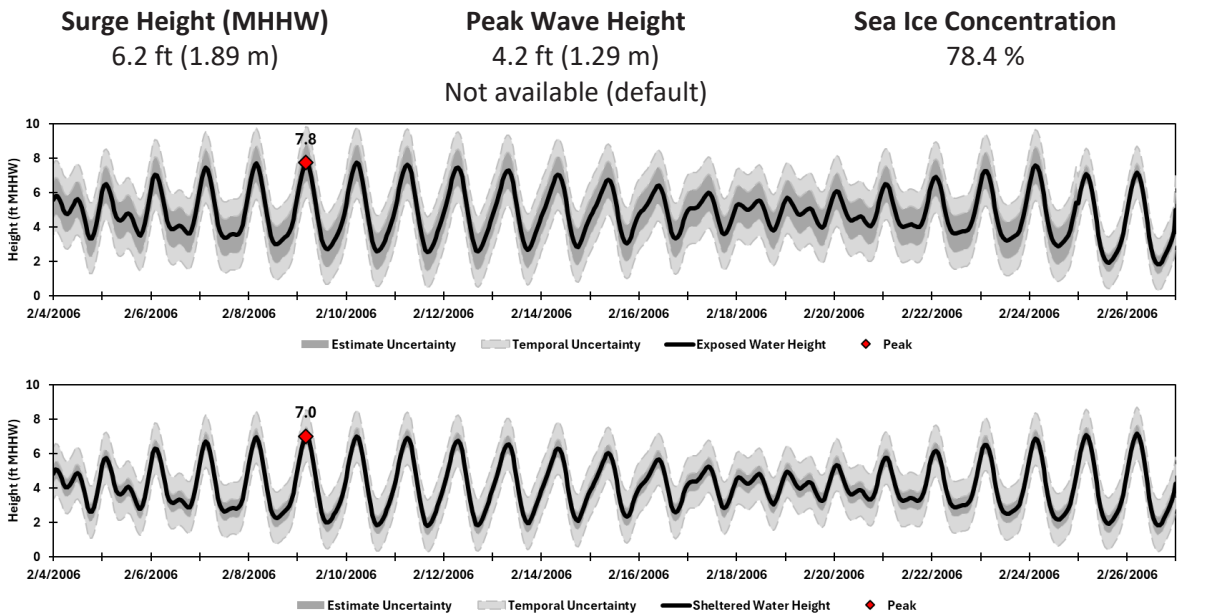
3.7 ± 0.5 ft (1.14 ± 0.16 m) MHHW



2004-DEC-26**DSWL** **6.3 ± 0.8 ft (1.93 ± 0.26 m) MHHW****2004-DEC-27****SWL** **5.6 ± 0.5 ft (1.72 ± 0.16 m) MHHW****Surge Height (MHHW)****4.8 ft (1.46 m)****Peak Wave Height****5.4 ft (1.66 m)****Sea Ice Concentration****73.2 % / 83.6 %****2005-SEP-23****DSWL** **8.4 ± 0.9 ft (2.57 ± 0.26 m) MHHW****2005-SEP-25****SWL** **7.3 ± 0.5 ft (2.23 ± 0.16 m) MHHW****Surge Height (MHHW)****6.9 ft (2.10 m)****Peak Wave Height****7.9 ft (2.40 m)****Sea Ice Concentration****38.8 % / 19.2 %**

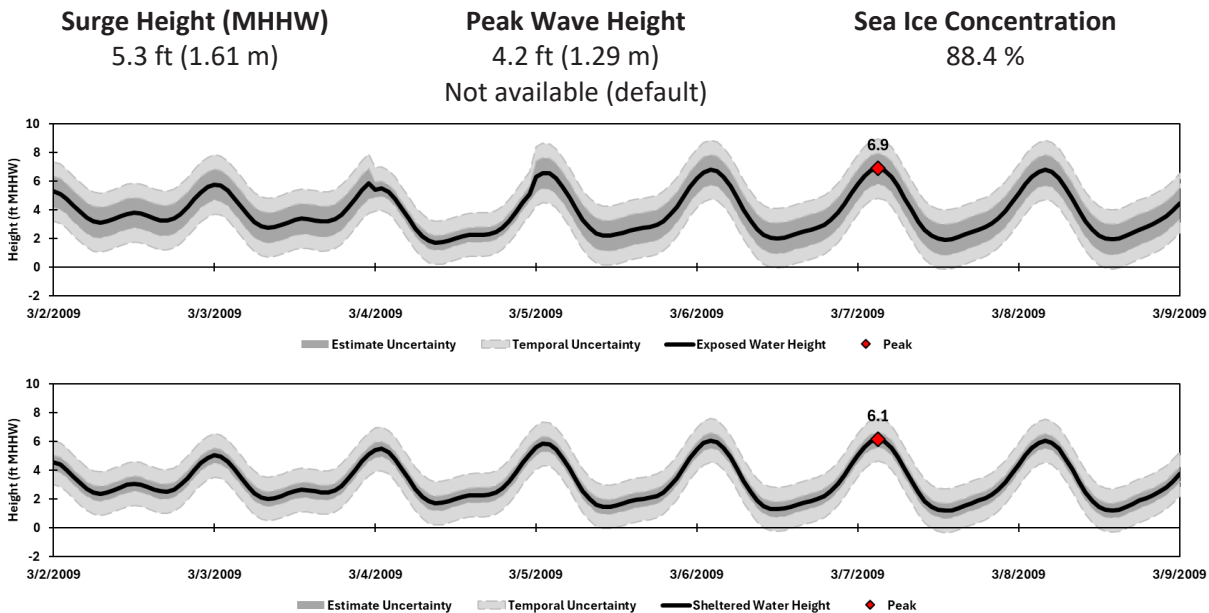
2006-FEB-09

DSWL 7.8 ± 1.1 ft (2.36 ± 0.32 m) MHHW
SWL 7.0 ± 0.5 ft (2.14 ± 0.16 m) MHHW



2009-MAR-07

DSWL 6.9 ± 1.1 ft (2.10 ± 0.32 m) MHHW
SWL 6.1 ± 0.5 ft (1.87 ± 0.16 m) MHHW



2009-NOV-08**DSWL** **4.8 ± 0.8 ft (1.47 ± 0.25 m) MHHW****SWL** **4.8 ± 0.5 ft (1.46 ± 0.16 m) MHHW****Surge Height (MHHW)**

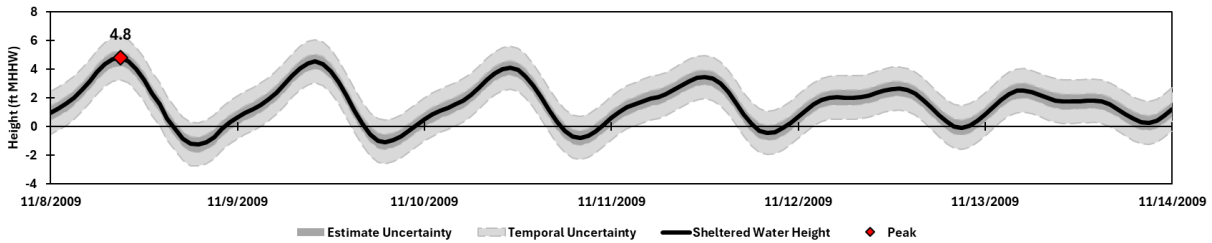
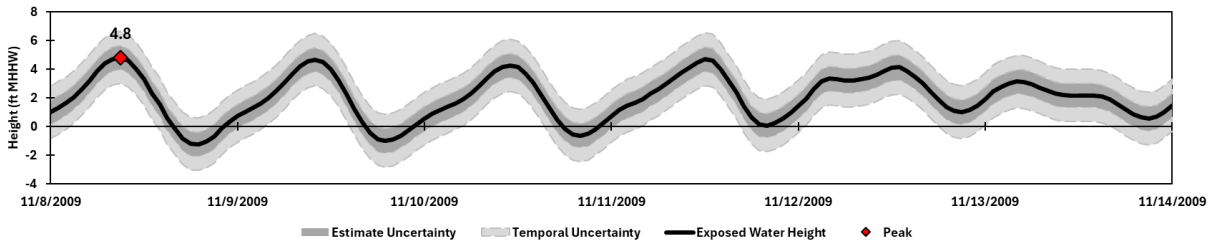
3.6 ft (1.10 m)

Peak Wave Height

8.5 ft (2.58 m)

Sea Ice Concentration

27.6 %

**2009-DEC-05****DSWL** **6.0 ± 1.1 ft (1.81 ± 0.32 m) MHHW****SWL** **5.2 ± 0.5 ft (1.59 ± 0.16 m) MHHW****Surge Height (MHHW)**

3.6 ft (1.11 m)

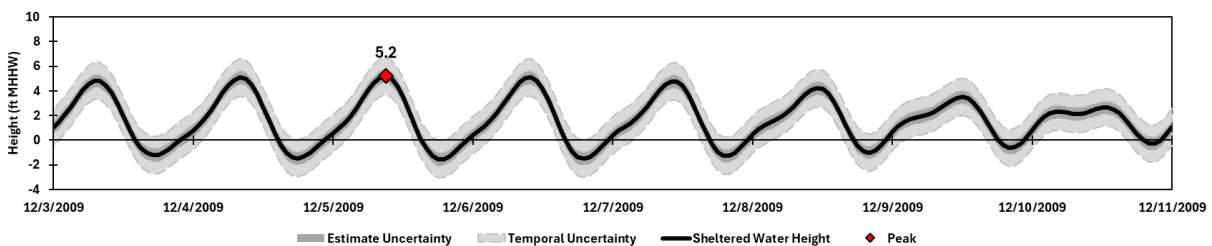
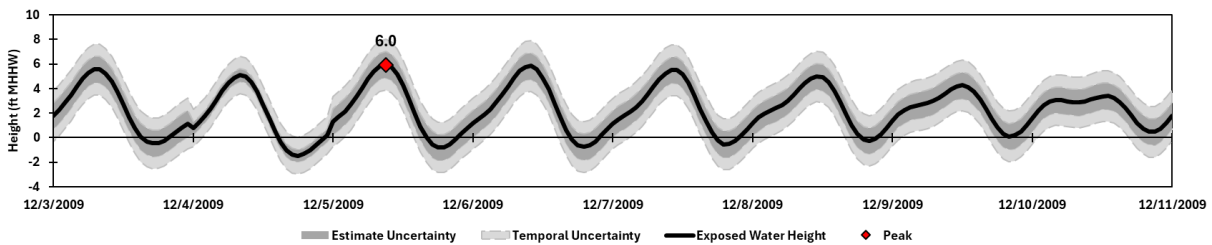
Peak Wave Height

4.2 ft (1.29 m)

Not available (default)

Sea Ice Concentration

78.4 %



REFERENCES

- Chapman, R.S., Kim, Sung-Chan, and Mark, D.J., 2009, Storm-induced water level prediction study for the western coast of Alaska: United States Army Corps of Engineers, 102 p.
- Erikson, L.H., McCall, R.T., van Rooijen, Arnold, and Norris, Benjamin, 2015: Hindcast storm events in the Bering Sea for the St. Lawrence Island and Unalakleet regions, Alaska: United States Geological Survey Open-File Report 2015-1193, 57 p. <https://pubs.usgs.gov/of/2015/1193/ofr20151193.pdf>
- Fetterer, F., Knowles, K., Meier, W.N., Savoie, M., and Windnagel, A. K., 2017, Sea Ice Index (G02135, Version 3): National Snow and Ice Data Center, accessed April 3, 2025. <https://doi.org/10.7265/N5K072F8>
- Golder Associates Ltd., 2020, Climate Change Vulnerability and Risk Assessment - Shaktoolik, Alaska: Golder Associates Ltd., 134 p.
- Iowa Environmental Mesonet (IEM), 2024, ASOS-AWOS-METAR data download: Iowa State University, retrieved from https://mesonet.agron.iastate.edu/request/download.phtml?network=AK_ASOS
- Kohout, A.L., Williams, M.J.M., Dean, S.M., and Meylan, M.H., 2014, Storm-induced sea-ice breakup and implications for ice extent: *Nature*, vol. 509, pp. 604-607. <https://doi.org/10.1038/nature13262>
- Kriebel, D.L., 2019, Review of the USACE report on Shaktoolik water levels: Coastal Analytics, LLC, 17 p.
- 1994, Swash zone wave characteristics from SUPERTANK, 24th International Conference on Coastal Engineering, Kobe, Japan, pp. 2207-2221.
- Liu, A.K., Vachon, P.W., Peng, C.Y., and Bhogal, A.S., 1992, Wave attenuation in the marginal ice zone during LIMEX: *Atmosphere-Ocean*, vol. 30, no. 2, pp. 192-206. <https://doi.org/10.1080/07055900.1992.9649437>
- Montiel, F., Squire, V.A., Doble, M., Thomson, J., and Wadhams, P., 2018, Attenuation and directional spreading of ocean waves during a storm event in the autumn Beaufort Sea marginal ice zone: *Journal of Geophysical Research: Oceans*, vol. 123, pp. 5912-5932. <https://doi.org/10.1029/2018JC013763>
- Moritz, Heidi, White, Kathleen, and Gouldby, Ben, 2016, An updated USACE approach to the evaluation of coastal total water levels for present and future flood risk analysis: United States Army Corps of Engineers, 9 p. <https://doi.org/10.1051/e3sconf/20160701012>
- National Centers for Environmental Information (NCEI), 2024, Bathymetric Data Viewer—NOS Hydrographic Survey: H02479, retrieved from <https://www.ngdc.noaa.gov/nos/H02001-H04000/H02479.html>
- National Oceanic and Atmospheric Administration (NOAA), 2004, Nautical chart for Norton Sound to Bering Strait, Chart No. 16200, Ed. 14, retrieved from <https://www.historicalcharts.noaa.gov/image.php?filename=16200-10-2004>
- Office of Coastal Management (OCM) Partners, 2024, 2021 USACE NCMP Topobathy Lidar DEM: Alaska. <https://www.fisheries.noaa.gov/inport/item/73829/>
- Schureman, Paul, 2001, Manual of harmonic analysis and prediction of tides: U.S. Department of Commerce, Coast and Geodetic Survey Special Publication No. 98
- Sorensen, R.M., 2006, Basic Coastal Engineering, 3rd ed.: Springer Science+Business Media, Inc., New York, NY.
- United States Army Corps of Engineers (USACE), 2011, Shaktoolik coastal flooding analysis, 73 p.
- 2024, Wave Information Study Data Portal, retrieved from <https://wisportal.erdc.dren.mil/>
- Walsh, J.E., Chapman, W.L., Fetterer, F., Stewart, S., 2019, Gridded monthly sea ice extent and concentration, 1850 onward, version 2: National Snow and Ice Data Center. <https://dx.doi.org/10.7265/jj4s-tq79>
- Walsh, J.E., and Johnson, C.M., 1979, Analysis of Arctic sea ice fluctuations 1953-77: *Journal of Physical Oceanography*, vol. 9, no. 3, pp. 580-591.
- Zetler, B.D., 1982, Computer applications to tides in the National Ocean Survey: U.S. Department of Commerce, National Oceanic and Atmospheric Administration, National Ocean Survey Supplement to Special Publication No. 98